AD-A093 485 INSTITUTE OF ENVIRONMENTAL MEDICINE AND PHYSIOLOGY S--ETC F/G 6/19
THE PATHOPHYSIOLOGY OF DECOMPRESSION SICKNESS AND THE EFFECTS O--ETC(U)
DEC 80 M R POWELL, M P SPENCER N00014-73-C-0094

UNCLASSIFIED NL

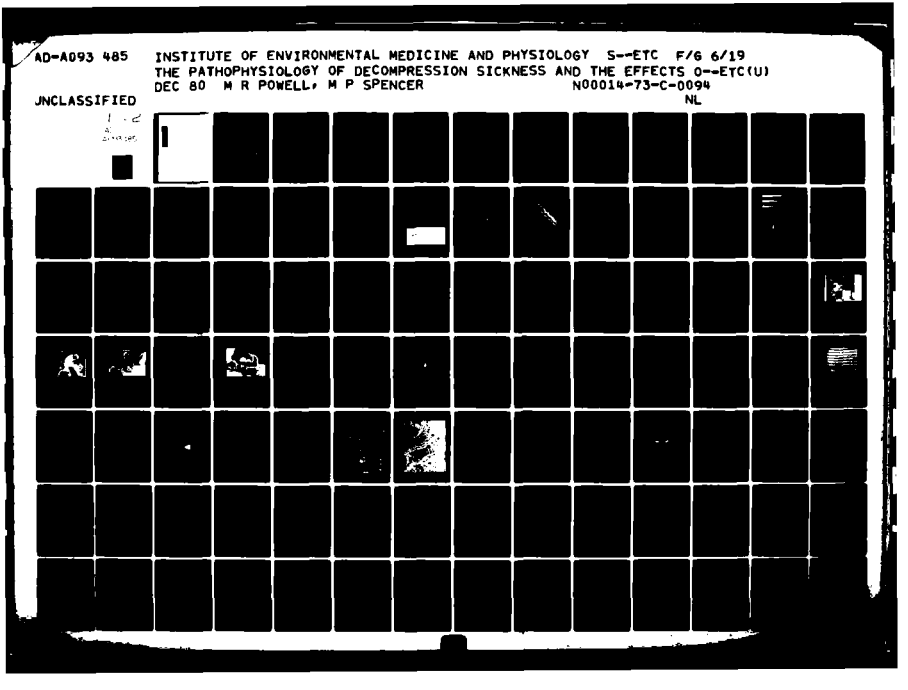

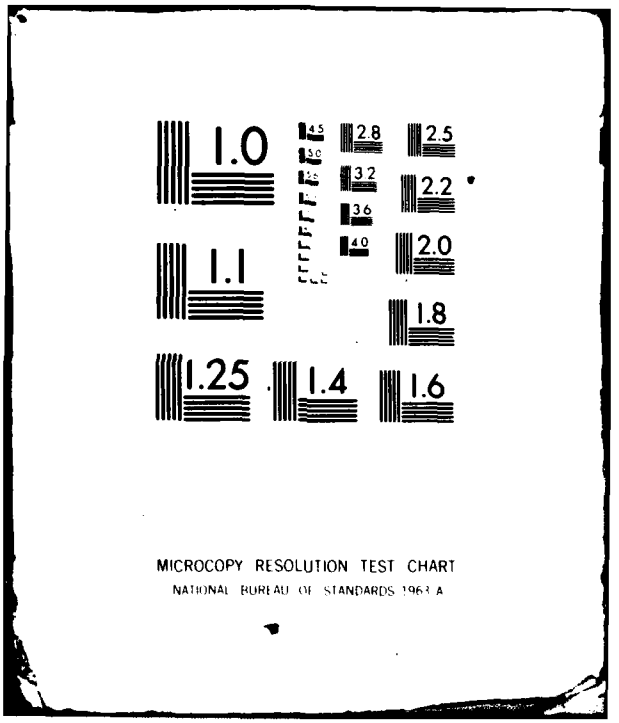
1.0
1.1
1.25
1.4
1.6
1.8
2.0
2.2
2.5
2.8
3.2
3.6
4.0
MICROCOPY RESOLUTION TEST CHART
NATIONAL BUREAU OF STANDARDS 1963 A

THE PATHOPHYSIOLOGY OF DECOMPRESSION SICKNESS AND THE EFFECTS OF DOPPLER DETECTABLE BUBBLES

BY

Michael R. Powell, Ph.D.
and
Merrill P. Spencer, M.D.

Technical Report O.N.R. Contract
N00014-73-C-0094

Institute of Applied Physiology and Medicine
701 - 16th Avenue
Seattle, WA 98122

TABLE OF CONTENTS

PREFACE

This, the final report for Office of Naval Research Contract N00014-73-C-0094, is a continuation of the first report of Spencer and Johanson of July, 1974. That first report dealt primarily with the development of the Doppler ultrasonic precordial bubble detector and its use in manned diving. This second report concerns itself mainly with the pathophysiology of Doppler-detectable bubbles.

The report covers work conducted at the Institute from 1975 to 1978. During the intervening year, the data were analysed, interpreted and written in final form. It is the hope of the authors that this material will aid hyperbaric researchers in the interpretation of data received during the employment of Doppler bubble detectors in research with both human and animal subjects. Additionally, much background material has also been included which will be of interest to the more general reader.

While considerable progress in Doppler bubble detection has been made since the advent of the instruments in the late '60's, many questions of interpretation yet remain. It is our hope that the material here presented will elucidate some of these.

Michael R. Powell

Michael R. Powell, Ph.D.
Director, Hyperbaric Laboratory

Merrill P. Spencer

Merrill P. Spencer, M.D.
Director and President

18 December, 1980

Institute of Applied Physiology and Medicine
Seattle, Washington

SUMMARY

The optimal use of ultrasonic bubble detectors requires a knowledge of the various pathophysiological consequence of gas phase formation in the body following decompression. Our studies during the later portion of this contract have been focused primarily on an understanding of decompression sickness as illuminated by the Doppler ultrasonic bubble detector.

Studies of the amount of gas in the central venous system have shown that the Doppler bubble detectors are quite sensitive devices which are capable of detecting small quantities of dispersed gas. While gas bubbles with a very small radius may not be detectable in the precordial mode, the device can easily detect amounts smaller than 0.01 cc/kg/min.

Gas introduced into the central venous system by means of a catheter will elicit a rise in the right ventricular systolic pressure (RVSP) as the gas embolizes the pulmonary vasculature. The degree of rise is a function of the gas embolization rate. Following hyperbaric decompression, the RVSP is elevated by inert gas emboli. Assuming a steady state, the amount of gas needed for any RVSP can be deduced. For a precordial Grade IV (in sheep) this is 0.03 cc/kg/min.

Gas injected (per catheter) at this 0.03 rate produce neither signs of dyspnea nor can bubbles be detected in the systemic arteries (by a Doppler probe on the carotid artery). The smaller dysbarogenic bubbles (in contrast to catheter-produced) in concert with Grade IV or Grade V precordial bubbles, and the associated increase in RVSP, will often promote inert gas arterialization. Neurologic decompression sickness could result. For this reason, it is recommended that the carotid artery of divers be monitored (an easier procedure than precordial monitoring).

Except for the enhancement of arterialization, Class II bubbles (those which are Doppler detectable and in the venous system) appear to produce no deleterious effect. In fact, an amelioration of limb-bend decompression sickness has been detected in the three animal subjects (sheep) subjected to graded decompression profiles ("titration technique").

Brain tissue does not appear to produce a gas phase (which is Doppler detectable at the sagittal) except from the most violent of decompression. Thus, neurologic forms of decompression sickness are most likely to have gas embolism as their principal etiologic agent. Another highly perfused tissue, kidney, was also found to be resistant to gas phase formation. It is postulated that only tissues subjected to mechanical stress (muscle, and those connected with diarthrodial articulations) produce microgas nuclei; only these tissues would produce significant cavitation following pressure reduction.

If gas bubbles are detected in the systemic arterial circulation, recompression is appropriate. Pressure increases do not promote further arterialization.

In the development of saturation decompression schedules, Doppler ultrasonic bubble detectors are useful. They allow an assessment of tissue out-gassing with concomitant bubble formation. In some instances, it can be used on-line as a real time monitor of the decompression status of divers.

Chronic pulmonary oxygen toxicity is ameliorated by the addition of inert gas to the breathing mixture. The time to reach an LD_{50} in mice is a function of the inert gas fraction (at a given fixed oxygen partial pressure).

I. INTRODUCTION

A. FUNDAMENTALS OF ULTRASOUND PHYSICS FOR HYPERBARIC PHYSIOLOGY

1. Nature of Ultrasound Waves

Sound waves, as distinct from electromagnetic waves, are matter waves and as such involve the rapid translocation of atoms or molecules in the transmitting medium. The frequency at which this motion takes place is in the range of 20 to 20,000 Hz for those sounds which are detectable by the normal human ear. Above the frequency of 20,000 Hz lies the region of "ultrasound", and the upper limits of this are traditionally placed at about 10^9 Hz. For medical diagnostic work, in which ultrasound is used for tissue visualization and hyperbaric physiology for bubble detection, the frequencies used are on the order of 10^6 Hz.

While the physical properties of audible (sonic) and ultrasound waves are the same, ultrasonic frequencies have some advantages in that:

(1) they are highly directional;
(2) they can be easily focused;
(3) their shorter wave lengths make them useful for examining small structures; and
(4) they show a large reflection at gas-liquid interfaces and are thus very good gas phase detectors; this specifically includes scattering of sound waves by bubbles.

All hyperbaric studies involve the use of low intensity ultrasound. This is contrasted with higher intensities as would be employed in ultrasonic heating of tissues or in ultrasound surgery.

Sound waves can be described in terms of their frequency and wavelength. As mentioned previously, the range of ultrasonic frequencies is from 2×10^4 to 10^9 Hz. The principal waves in fluid systems are of the type known as longitudinal waves. The source of the vibrations moves in a direction which is parallel to the direction of the travelling wave, and the particles themselves which carry the wave undergo motion which is parallel to the direction of the wave. A continuous pattern of compression and expansion is found. In systems with a high viscosity and in solids, transverse, or shear, waves are also found to occur. In this case, the direction of the wave travel is perpendicular to the direction of the particle motion. For biological systems, transverse waves are found to occur only in bone.

The wavelength is a particular dimension of the wave which helps to define many of its properties. Figure 1 shows a vibrating surface at the left in contact with a region of space which is represented by the rows of dots. These dots can be thought of as being the molecules in the region of space. As the source vibrates, it moves back and forth from left to right, pushing against and pulling apart the molecules. Each new push moves the compressed region to the right. This series of compressions is a wave and the distance between the compressed regions is the wavelength. The numerical

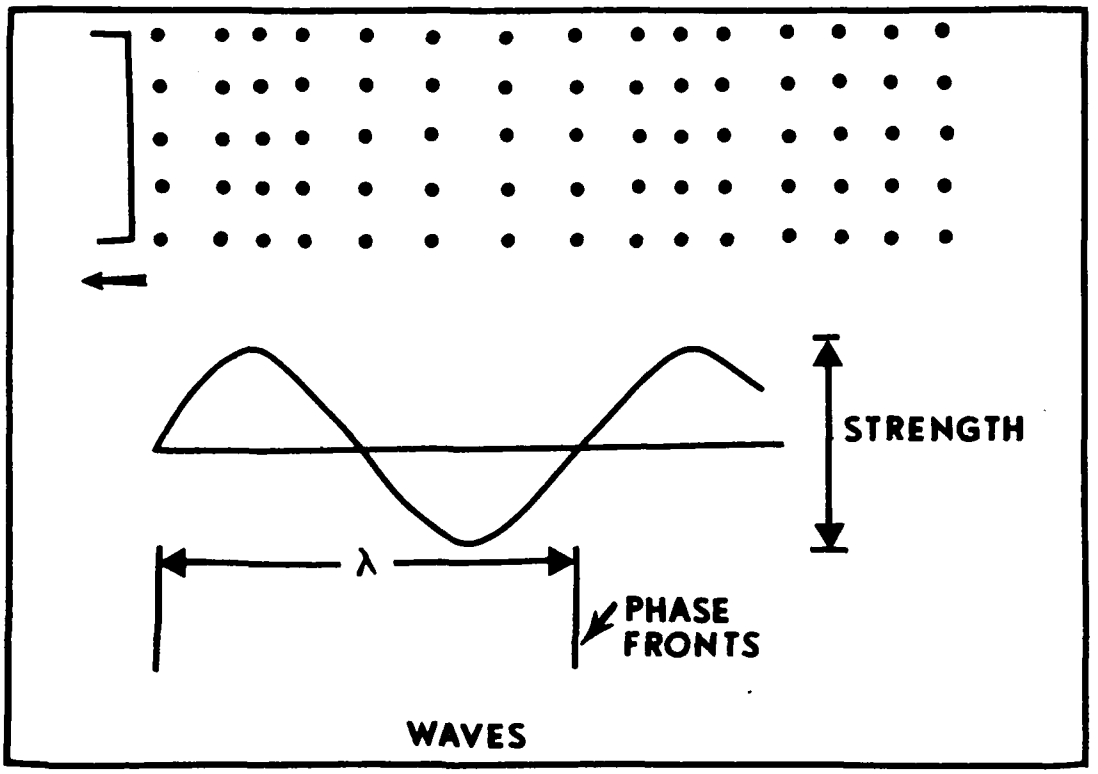

Figure 1. Definition of wavelengths. The wavelength is the physical distance between corresponding points of a repetitive wave form. At the upper left a transducer face is shown alternately compressing and spreading out the molecules of a medium. The wave is propagating from left to right.

value of the wavelength is found by dividing the velocity of the wave in a given medium by its frequency.

In equation form:

$$\lambda \text{ , wavelength } = \frac{\text{velocity in the medium}}{\text{frequency}} \qquad (1)$$

For blood and the average soft tissues in the body, we find:

$$\lambda \text{ (millimeters)} = \frac{1.5}{\text{frequency (MHz)}} \qquad (2)$$

2. Interactions of Sound Waves and Tissues

Ultrasonic waves travel in nearly straight lines in blood and in most soft tissues of the body. They are absorbed or gradually weakened by the tissues and can be reflected or scattered back to the surface of the body. The average soft tissue of the body is a tissue of very high water content. Sound travels in these tissues at the velocity characteristic of a saline solution containing proteins. When sound waves encounter tissues which are not liquid-like, most of the energy is reflected. Such tissues are the hard mineralized tissues such as bone and teeth, in which the elastic properties are more nearly those of a solid, and tissues containing appreciable quantities of air. The principal organ which contains air in its natural state is the lung. Acoustic properties of this tissue are sufficiently different than those of average soft tissue, to cause nearly complete reflection of the sound at the surface of the lung. Air is encountered in other regions of the body as well, primarily the bronchi, trachea and folds in the bowel; this will limit the use of ultrasound methods to investigate certain regions of the body for decompression bubbles because of the absence of beam penetration.

A sound wave passing through a medium - solid, liquid or gas - is reduced in intensity according to the formula

$$I = I_0 e^{-2\alpha x} \qquad (3)$$

where I is the intensity, x the distance traveled, and α is the amplitude absorption coefficient.

In average soft tissue sound is absorbed to a degree which is proportional to the frequency. In traveling into the body by 1 cm and back again, the power in the sound wave is reduced by 1/2 for every MHz of frequency. At a frequency of 5 MHz, sound waves which travel 1 cm into and 1 cm out of tissue will be reduced to 1/64 of the original power. Sound is absorbed by the same factor for each centimeter of depth. Therefore, lower frequencies are used for deep

penetration.

These absorption figures are about average for muscle. They are less for fat and considerably less for blood, about 1/10 that for muscle. Absorption is caused primarily by the conversion of sound energy into heat by a process which appears to be specific for the macromolecules involved, primarily proteins.

The reflection and scattering of sound is a much more pronounced and useful effect. These waves, which are sent back out to the examining probe from structures within the body, are used by a variety of medical ultrasonic diagnostic instruments. The strongest reflections arise from the greatest changes in the mechanical or elastic properties of tissue and hence are found at the boundary of soft tissue and bone or air-containing tissue such as the lung, as discussed above. Much smaller changes in elastic properties occur between and within many other organs of the body. Perhaps 1% of the incident energy can be reflected from smooth connective tissue sheets such as are found covering the kidney cortex, surrounding major muscle bundles, and in the walls of blood vessels. Smaller reflections, of the order of 1/10 to 1/100 of 1% occur between the muscle bundles in muscle and from smaller structures in kidney, liver, and other organized tissues. The distribution of the echoes appears to follow from the distribution of connective tissues in these tissues.

The intensity of sound waves passing through an interface is given by the transmission coefficient and is defined as the ratio of the intensity of the transmitted wave to the intensity of the incident wave. For a plane wave incident at right angles to a plane boundary separating media of acoustic impedances $\rho_1 c_1$ and $\rho_2 c_2$ where ρ is the density and c is the speed of sound in the medium, the transmission coefficient α_t is given by:

$$\alpha_t = \frac{4 \rho_1 c_1 \cdot \rho_2 c_2}{(\rho_1 c_1 + \rho_2 c_2)^2} \qquad (4)$$

Because of the large differences in acoustic impedance between liquids and gases, almost no transmission takes place at a liquid-gas interface, and hence gas "pockets" and bubbles will greatly reflect an ultrasound beam.

For the case where the sound interacts with small objects in a liquid medium, e.g. bubbles, an important factor is scattering. Scattering can be divided into three classes:

(1) when the body has dimensions which are much larger than a wavelength, specular reflection occurs and an "acoustic shadow" is produced;

(2) when the object is comparable in size to a wavelength of sound, scattering and diffraction phenomena both occur; and

(3) when the object is small with respect to a wavelength, scattering occurs but the attenuation of the beam is reduced greatly.

The equations for scattering have been developed for the case of the sphere and the cylinder (Gooberman, 1968). The intensity $I_{r\Phi}$ of the radiation scattered from a cylinder of radius r_o measured at an angle Φ with respect to the incident radiation and at a distance r is given by the equation:

$$I_{r\Phi} = I_o \frac{\pi r_o}{8 r} (\beta r_o)^3 (1 - 2 \cos\Phi)^2 \qquad (5)$$

when $\beta r_o << 1$

where I_o is the incident intensity, and $\beta = 2\pi/\lambda$, where λ represents wavelength. For the case of a spherical body, the scattered intensity is

$$I_{r\Phi} \approx 0.11 (\beta r_o)^4 (r_o / r)^2 (1-3 \cos\Phi)^2 \qquad (6)$$

when $\beta r << 1$

3. Pulsating Bubbles

The presence of a gas phase in a liquid causes a marked reflection of an ultrasound beam passing through it. Additionally, bubbles of a given size are found to pulsate under the influence of periodic oscillations of the surrounding medium. The idea of a "resonant frequency" in a gas bubble suspended in a liquid phase was first used by Minnaert (1933) to explain the sound generated by running water in streams. He developed an equation relating the bubble size to the sound frequency; this frequency f is given by

$$f = \frac{1}{2\pi R_o} \left(\frac{3 \gamma P_a}{\rho} \right)^{1/2} \qquad (7)$$

where P_a is the ambient pressure, R_o is the radius, ρ is the

liquid density, and γ is the ratio of specific heats for the gas in the bubble ($\frac{C_p}{C_v}$). In an attempt to explain cavitation damage, Smith (1935) developed a similar equation for bubbles oscillating in a sound field. His equation took into account the effect surface tension would have on very small bubbles. The "resonant frequency" is thus given by:

$$f = \frac{1}{2\pi R_o} \left[\frac{3\gamma (P_a + 2S/R_o)}{\rho} \right]^{\frac{1}{2}} \qquad (8)$$

where S is the surface tension. The resonant frequency for air bubbles in water at 1 atm as a function of their diameter is shown in Figure 2.

The modes by which pulsating bubbles dissipate acoustic energy was first studied theoretically by Devin (1959); he lists these modes as thermal, radiation, and viscous. The acoustic amplitude absorption coefficient is dependent upon these three modes (Fry and Dunn, 1962; Dunn, et al., 1969) and the relative importance of each mode will depend on the characteristics of the total system.

The acoustic amplitude absorption coefficient is given by the equation

$$\alpha = \frac{bN_v}{4} \left[\frac{\frac{3\gamma P_a}{R_o^2} + W^2\rho}{\left[\frac{1}{4\pi R_o} \left(W^2\rho - \frac{3g\gamma Pa}{\varepsilon R_o^2} \right) \right]^2 + b^2W^2} \right] \qquad (9)$$

Meanings and numerical values of the terms are given in Table I. Calculations show that, for the bubble size dealt with here, i.e., on the order of microns, the numerical values of g and ε are approximately equal to 1. In addition, the thermal dissipation parameter is small with respect to the radiation and viscous dissipation parameters.

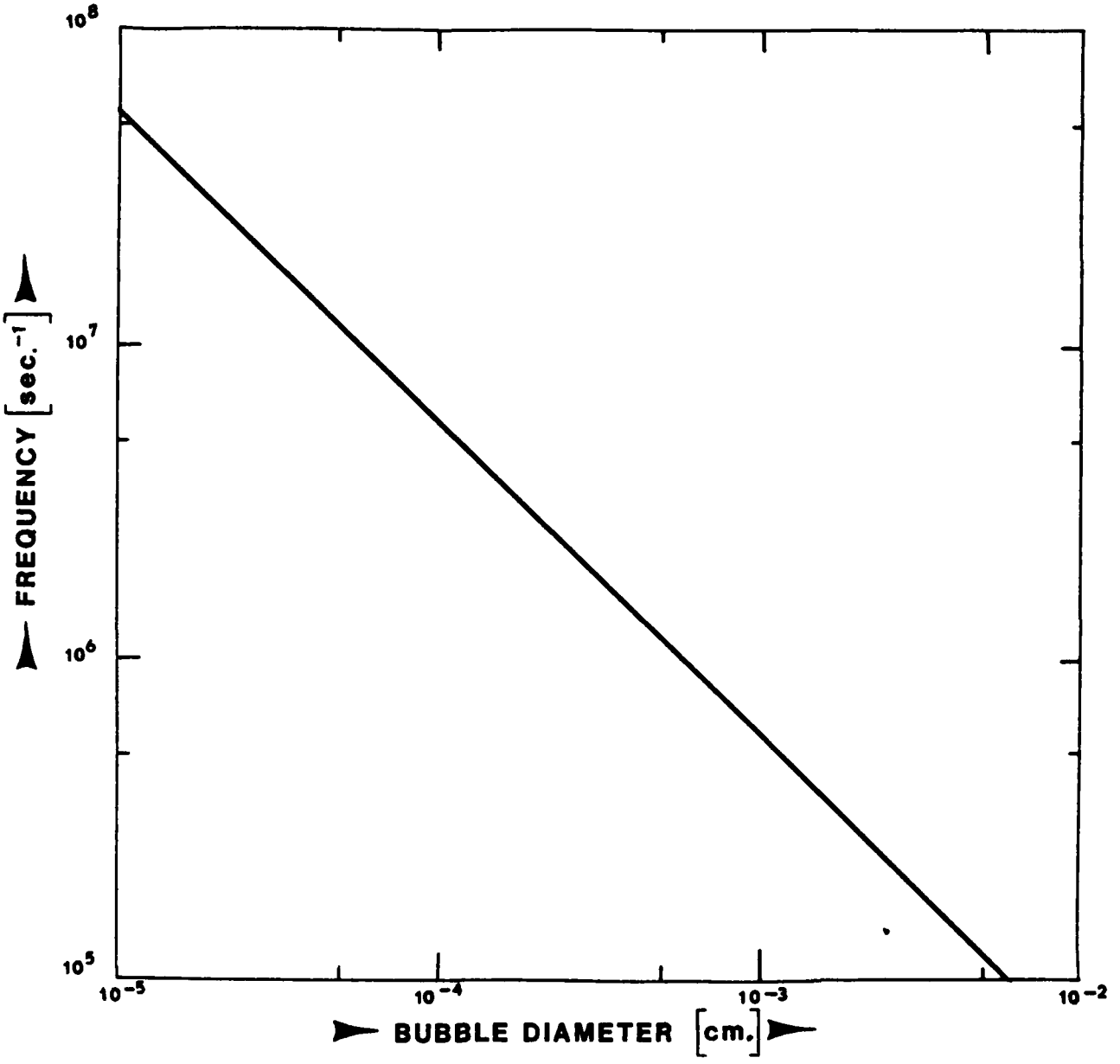

Figure 2. Theoretical bubble diameter at resonance vs. frequency. Calculated for air bubbles in water at 1 ATA.

TABLE I

Acoustic Amplitude Absorption Coefficient

$$\alpha = \frac{b N v}{4} \left\{ \frac{\omega_o^2 \rho + \omega^2 \rho}{\left[\frac{1}{4\pi R_o}\left(\omega^2 \rho - \omega_o^2 \rho\right)\right]^2 + b^2 \omega^2} \right\}$$

Quantity	Definition	Numerical Value
ω_o	$\frac{1}{R_o}\left\{\left(\frac{3\gamma P_o}{\rho}\right)\left(\frac{g}{\epsilon}\right)\right\}$ angular resonant frequency of bubble	e.g. 10 micron diameter is 10^5 sec.$^{-1}$
g	$1+\frac{2\sigma}{P_o R_o}\left(1-\frac{1}{3h}\right)$	approximately = 1
ϵ	$1+\frac{3(\gamma-1)}{2\Phi R_o}\left\{1+\frac{3(\gamma-1)}{2\Phi R_o}\right\}$	approximately = 1
Φ	$\left(\frac{\omega_o \rho_g C_p}{2K}\right)$	
v	acoustic velocity in water	1.5×10^5 cm/sec
γ	ratio of specific heats of air	1.4
p_o	static pressure	10^6 dyne/cm^2
ρ	density of plasma	1.0 g/cm^3
ρ_g	density of air	1.29×10^{-3} g/cm^3
σ	surface tension of water	75 dyne/cm
h	γ/ϵ	$1<h<\gamma$
C_p	heat capacity at constant pressure of air	0.24 cal/g
K	thermal conductivity coefficient of air	5.6×10^{-6} cal/cm sec°C
η	viscosity of plasma	3.2×10^{-2} poise
N	number of bubbles per unit volume	
b	total dissipation parameter, $b_t + b_r + b_v$	
b_t	thermal dissipation parameter	very small
b_r	radiation dissipation parameter, $\frac{\rho\omega^2}{4\pi v}$	6.9×10^8 g/cm^4-sec
b_v	viscous dissipation parameter, $\frac{\eta}{\pi R_o^3}$	
R_o	radius of gas bubble	
ω	angular frequency of sound field, $2\pi f$	3.58×10^7 radians/sec (at 5.7 MHz)

At its resonant frequency, the scattering cross-section of bubble increases by approximately one order of magnitude (Devin, 1959; Nishi, 1972, 1975). This is illustrated in Figure 3 where absorption of sound is plotted against bubble radius for f = 5.7 MHz (from Powell, 1971). This property of resonance tends to increase the ability of Doppler bubble detectors to detect small bubbles though resonance is reduced in blood because of increased viscosity and damping (Nishi, 1972, 1975). An experimental comparison between the equation of Nishi and scattering cross-section has been made by Moulinier and Masurel (1977).

In vitro measurements by Nishi (1972) indicated that from measurements of amplitude alone, it would not be possible to determine bubble size in vivo without an internal reference.

He indicated that bubbles should be detectable as long as they are above their resonant size. Other measurements by Hills and Grulke (1975) in vitro indicated that the minimum detectable bubble size was a function of the blood velocity. A bubble of 20 micron radius could be detected if the mean fluid velocity carrying it was 55 cm;sec while the minimum detectable size was a 90 micron radius if the velocity was only 20 cm/sec. For the velocities encountered in the heart and larger arteries, they predicted that the smallest bubble detectable by reflection alone would be 20 to 25 microns in radius when background noise is taken into account. This may then be the limit of detectability as even at resonance the scattering intensity for a smaller bubble would be an order of magnitude less than that of the 25 micron radius bubble (Nishi, 1975). It is our experience that bubbles can be easily detected in peripheral veins, and not detected with precordial detection.

In addition to gas bubbles, large blood emboli can strongly scatter ultrasound. A 30 micron particle will have a scattering intensity that is 4×10^3 greater than a single erythrocyte (Nishi and Livingstone, 1973). Even when bubbles were no longer detected 24 hours post-dive, Nishi and Livingstone detected changes in the waveform of the Doppler signal which they interpreted as being the result of hematological changes, i.e., larger scattering sites.

4. Generation and Detection

Ultrasonic diagnostic equipment consists of transmitters to generate the ultrasonic frequency, transducers to convert the ultrasonic waves to electrical energy and vice versa, receivers to amplify the weak scattered wave, and display devices to present them to the human operator. The basic characteristics of these devices are determined by the interactions between tissues and sound waves mentioned above. The frequencies of ultrasound are very high and require electronic apparatus for generation and amplification. One MHz, for example, is a frequency found in the middle of the broadcast band when it is in the form of radio frequency energy. Higher frequencies up to 10 MHz are in the shortwave bands used by the military and a variety of land and mobile services. The basic arrangement is shown in Figure 4. The transmitter, thus, is an electronic oscillator producing electrical waves. These waves are

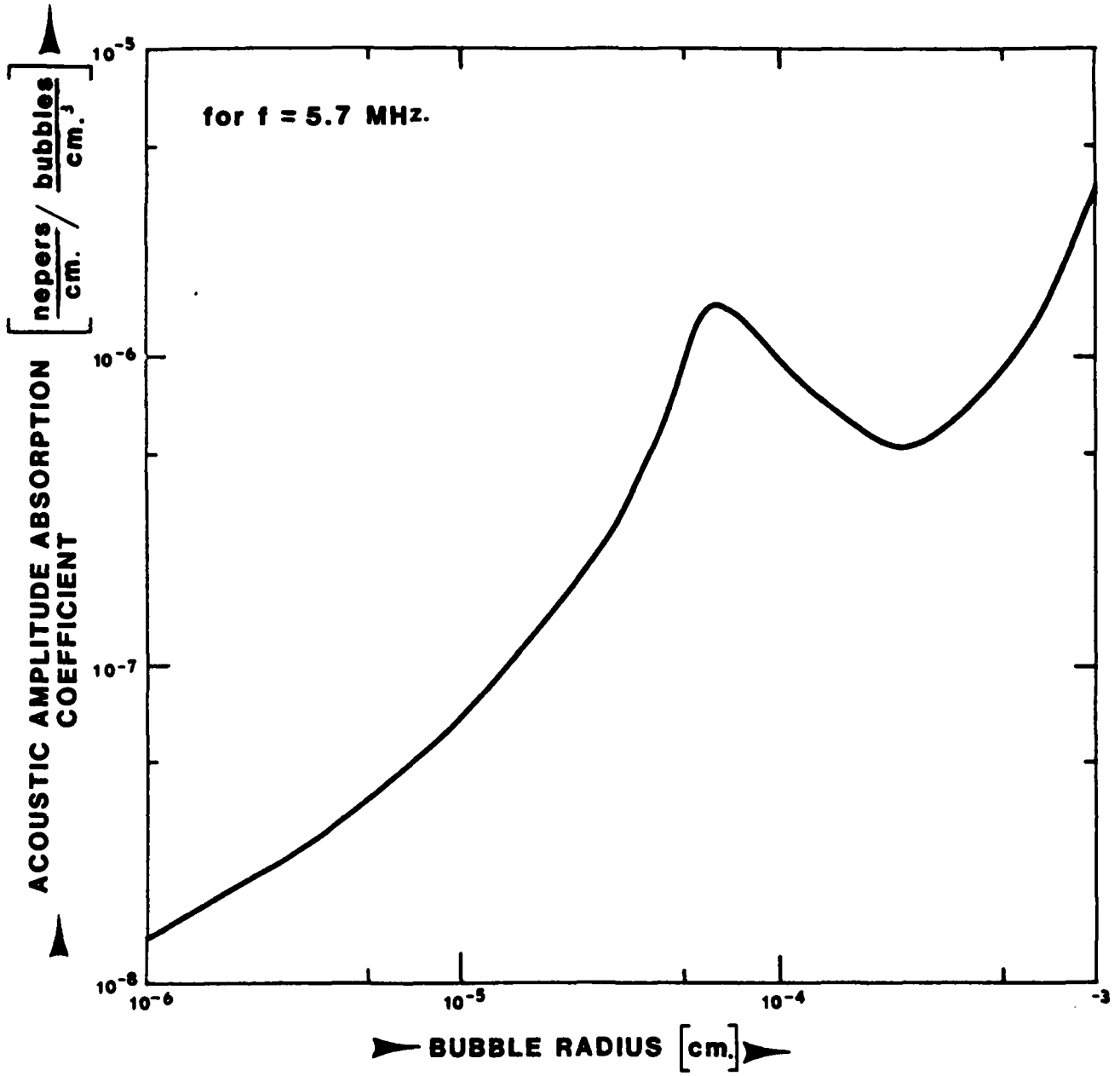

Figure 3. Attentuation coefficient vs. bubble radius for a frequency of 5.7 MHz. Calculated for air bubbles in plasma at 1 atm. The peak occurs at a bubble radius of about 0.6 microns.

converted into mechanical form by a transducer. The word "transducer" means to lead between, and refers to converting the energy from electrical form to acoustic form. The types of transducers commonly used in biomedical application are reciprocal and function equally well in converting reflected waves into electrical energy. The voltages from these reflected waves are usually very small and require amplification to the level required to affect display apparatus. Display apparatus usually consists of cathode ray tubes similar to those used in a television set for displaying dimensions and coordinates, loudspeakers for listening to Doppler sounds, and various types of spectrum analyzers and strip chart recorders for reproducing flow waveforms and motion curves. These will all be discussed further in the next chapter.

The transducer is the most critical element in the entire Doppler flowmeter system. The choice of transducer determines the operating frequency, depth of penetration, size of the ultrasonic beam, and the frequency of the Doppler shift which is recorded from a blood vessel. In multiple crystal transducers, which are commonly used with Doppler flowmeters, separation of the transmitting and receiving elements can further localize the regions from which flow can be recorded.

The "heart" of a transducer is a material which will change its dimensions when an electric field is applied to it or which will generate an electrical field when it is deformed by a vibration as sketched in Figure 5 . This element, termed the crystal, is usually a single or a poly-crystalline material in which the crystal structure is aligned suitably with the field produced by electrodes applied to the surfaces of the material. Practically all medical transducers use a poly-crystalline ceramic which has the property of being electrostrictive. That is, it will change its shape in response to an electrical field. These ceramics are a poly-crystalline lead zirconate titanate.

The components of the transducer (see Fig. 6), besides the ceramic, are the protective case, the lead wires connecting it to the electronic apparatus, and internal connections. Optional elements are backing materials used to provide isolation, greater strength, or to widen the bandwidth of the transducer for pulse operation; and a lens which may be used to focus the sound beam. The shape of the sound field depends on the operating frequency and size of the elements.

The most sensitive frequency for operation of a transducer is the fundamental resonance frequency of the ceramic crystal element. The frequency at which the electronics operate is usually adjusted to coincide with the resonant frequency of the transducer. Although low frequencies penetrate more deeply into tissues, they also result in low Doppler shift frequencies, in longer wavelengths, and hence, wider beamwidths. Too high a frequency cannot be used, since the penetration will be too small or the Doppler frequency too high to hear. A compromise frequency is usually used. Most Doppler systems use frequencies between three and ten MHz. A chart of the frequency giving the theoretically best echo strength is shown in Figure 7 .

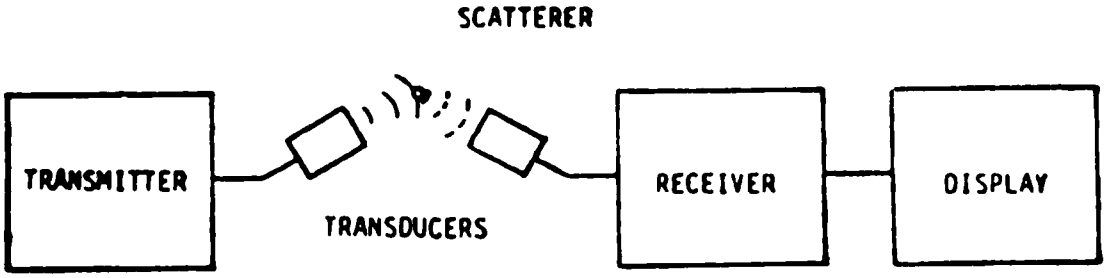

Figure 4. Block diagram of basic ultrasound system showing electronic components connected to transducer.

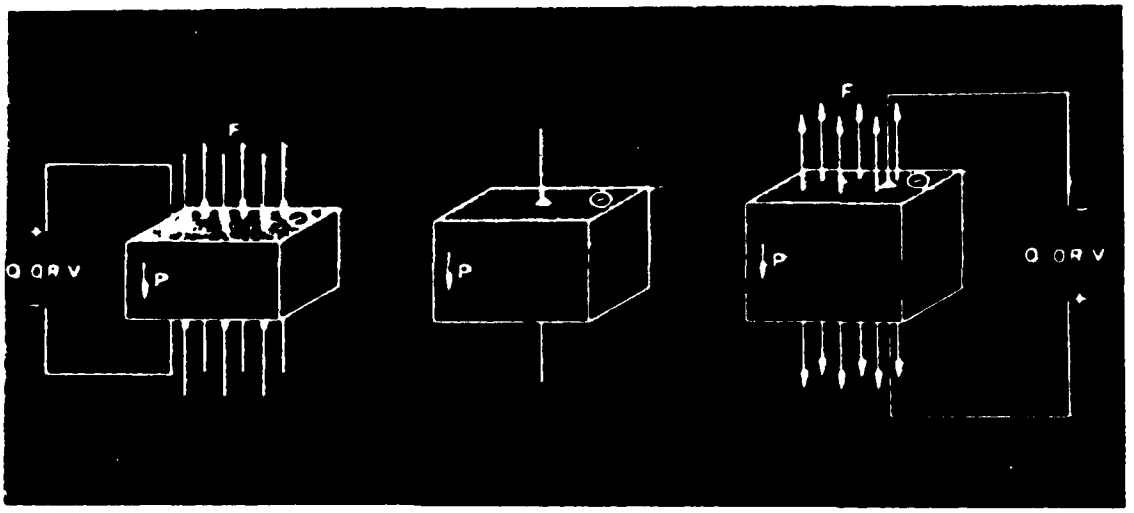

Figure 5. The center shows a biased ceramic material with electrodes on the major faces. Application of a voltage results in a change in thickness depending on the polarity. Application of pressure results in generation of a charge on the surfaces.

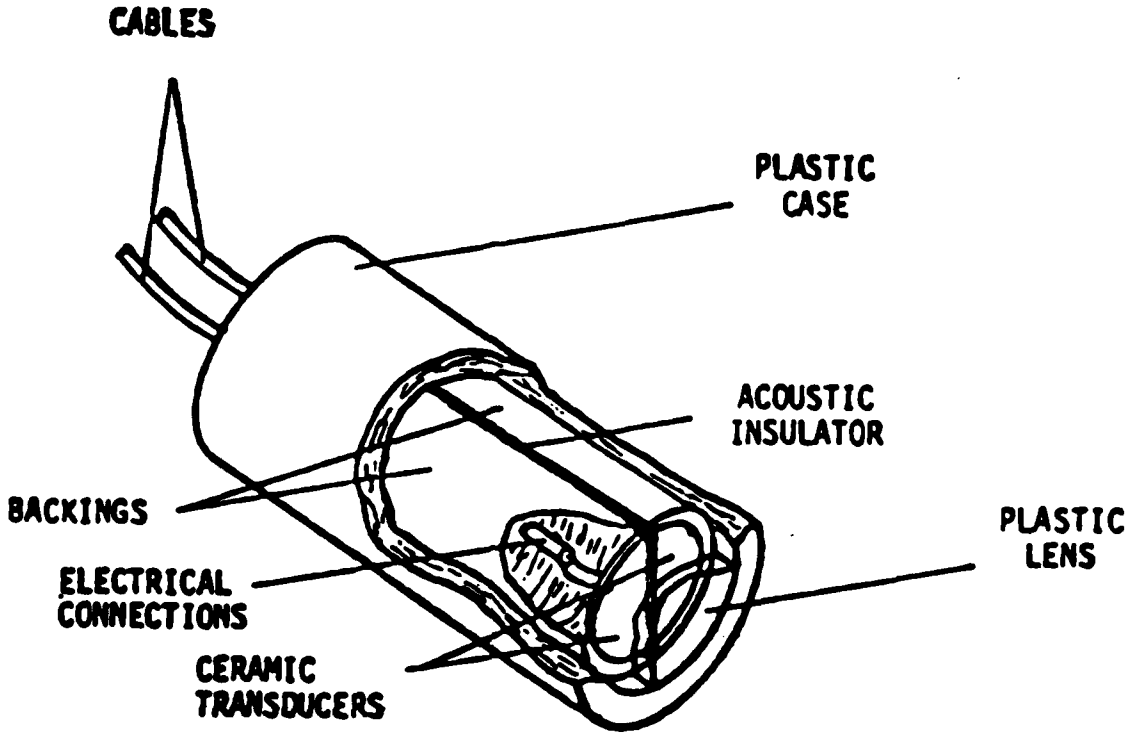

Figure 6. Cut-away view of ultrasound transducer. Two elements are shown for Doppler operation, although only one is used for pulse-echo operation. Backing material adjusts pulse length of transducer, the lens focuses the field to produce narrow beams. (See Figures 8 and 9.)

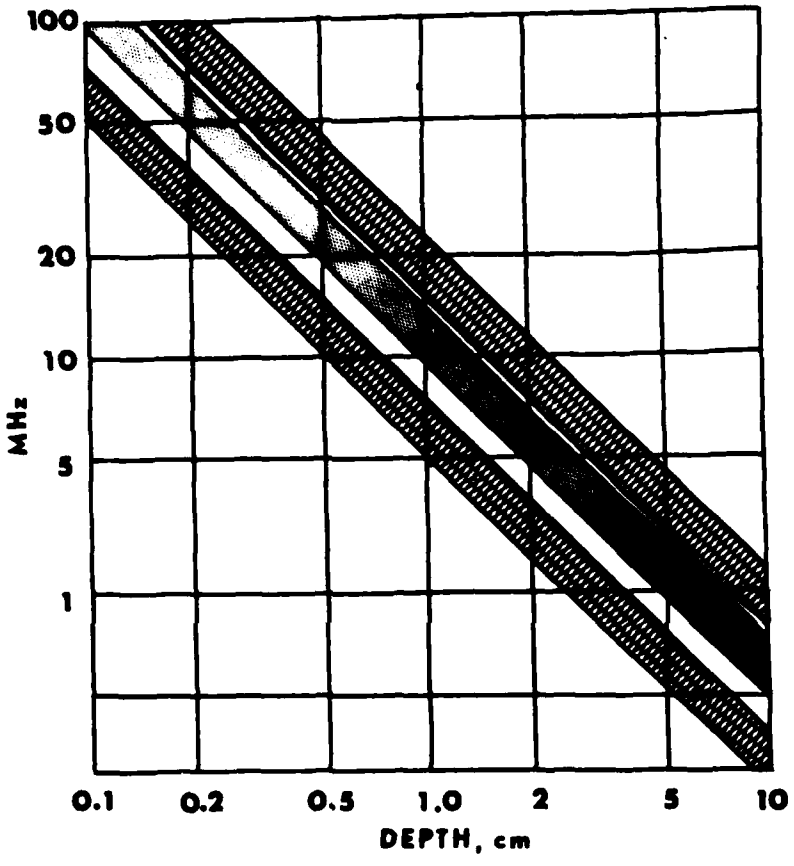

Figure 7. Chart of ultrasound frequency giving maximum echo strength from small scatterers (red cells). Theoretically determined frequency for depths of three intervening tissues, based on measured attenuation.

The low frequencies are preferred for penetration into the heart and the higher frequencies for vessels in the extremities.

The outlines of the width of the field for two sizes of unfocused transducers shown in Figure 8 illustrate three major points.

1. The field consists of two different regions. The near-field, close to the transducer, is approximately cylindrical. The far-field, at greater ranges, diverges.

2. The minimum field width occurs at the range where the near-field changes to the far-field, and this minimum width is approximately equal to the radius of the transducer. (The distance between the transducer and this narrow point in the field is found by dividing the square of the radius by the wavelength.)

3. In the near-field, the width of the beam is directly proportional to the size of the transducer and in the far-field the width is inversely proportional to the size of the transducer.

The approximate appearance of the fields from focused transducers are shown at C and D, Figure 8. The four major points for focused fields are:

1. The width of the field is determined by the same divergence angle that governs the far-field region of the unfocused transducer.

2. A narrow field is produced only at distances that were previously within the wide near-field of the unfocused transducer. The far-field is not affected by focusing.

3. The width of the field at and beyond the focus is inversely proportional to the diameter of the transducer.

4. The intensity of the field drops off quite rapidly after the focal region is reached, so that the length of the focused field is limited.

Focusing is accomplished by using plastic lenses (see Fig. 6) or phased-array elements. Plastic lenses are relatively inexpensive and produce excellent results. Photographs of actual focused acoustic fields are shown in Fig. 9. These were taken with a Schlieren optical system which makes the waves visible. For very strong focusing, bottom Fig. 9, the field is concentrated at the focus and does not reach to long ranges.

In many Doppler transducers (blood-bubble detectors, for example), the sending and receiving elements are separated. The region of space from which Doppler-shifted signals can be received is that region which is common to the ultrasonic field sent out by the transmitting transducer and the sensitive area of the receiving transducer. Since the receiving transducer has a sensitive area

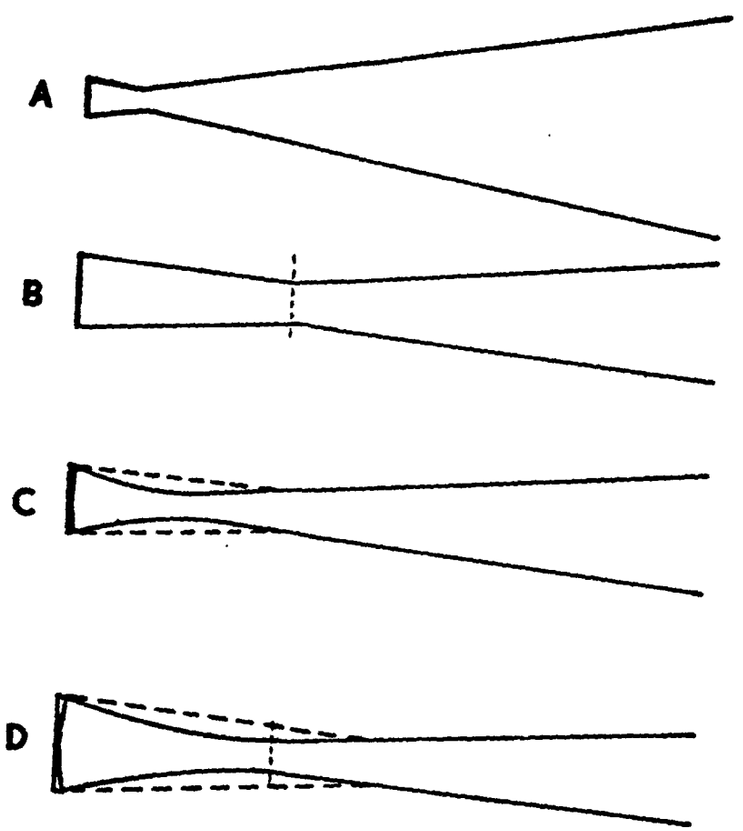

FIGURE 8

Outline of approximate field shape from focused and unfocused transducers.

A - Small unfocused transducer.
B - Larger unfocused transducer having a smaller field width at the range shown by the dotted line.
C - Effect of focusing transducer shown at "B." Field can be narrowed only at the near-field region.
D - Effect of increasing the size of the focused transducer at "C." A smaller field is obtained at the range shown by the dotted line.

which is indentical in shape to its beam pattern as a transmitter, it is possible to sketch the approximate location of the sensitive region. Such a construction is illustrated in Figure 10, which assumes that the near-field region of both elements extends across the entire sketch.

Usually the transmitter and receiver elements are placed closely together so that the sensitive region will cover as great a range in tissue as possible. In other cases, it is desirable to separate them to localize the sensitive region. An extreme example of such a transducer is the precordial probe developed by this Institute for its bubble detector. This probe is designed to be placed on the chest and receive signals scattered from blood and air emboli in the pulmonary artery only.

It is possible to use the same ceramic element for simultaneous transmission and reception in a continuous-wave system. Such a system has been developed by the Institute for use with its catheter flowmeter. These catheter flowmeter probes are about 1 mm in diameter and do not provide sufficient room for separate sending and receiving elements. This technique can be used with larger probes with the advantage that the sensitive region extends from the transducer face to a depth which is set by absorption in the tissues.

5. Doppler Effect

The Doppler effect exists for ultrasonic waves. This effect is a change in the frequency of an ultrasonic wave when the transmitter, the receiver, or the scatterer are moving with respect to each other. Therefore, reflections from moving red cells and gas bubbles have a different ultrasonic frequency from the transmitted frequency. Ultrasonic Doppler flowmeters respond only to reflections which have experienced a Doppler shift (bubbles in blood, for example) and not at all to the reflections from stationary structures which have no Doppler shift (stationary, tissue gas phases).

The amount of the Doppler shift, when the scatterer is moving with a particular velocity, can be calculated from the rate of change of phase experienced by the wave as it travels from the transmitter to the scatterer and back to the receiver. The result is:

$$f_\partial \text{ (Doppler shift in } H_3 \text{)} = 2 \frac{\left[\begin{array}{l}\text{velocity of} \\ \text{scatterer with} \\ \text{respect to probe}\end{array}\right] \left[\begin{array}{l}\text{ultrasonic} \\ \text{frequency} \\ \text{in Hertz}\end{array}\right]}{\text{[velocity of ultrasound in medium]}} \quad (10)$$

When the flowmeter probe makes an angle to the vessel, as shown in Figure 11, this equation can be modified. If we put in the actual value of the velocity and straighten out the units, we obtain:

$$f_\partial \text{ (Hertz)} = 130 \left(\frac{\text{cm}}{\text{sec}}\right) \quad f \text{ (MH}_3\text{)} \quad \cos \theta$$

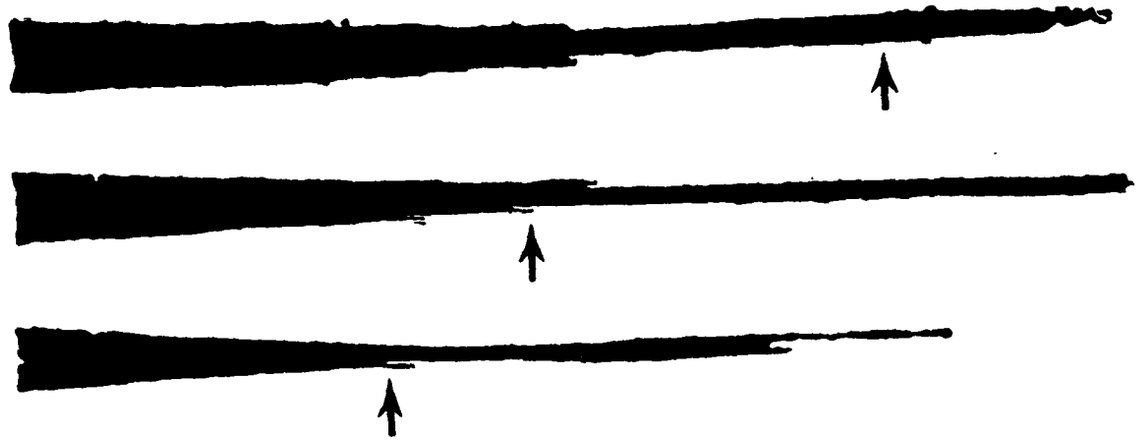

Figure 9. Schlieren photograph of actual sound field shapes for three different lenses applied to the same diameter transducer. Arrow marks focal length.

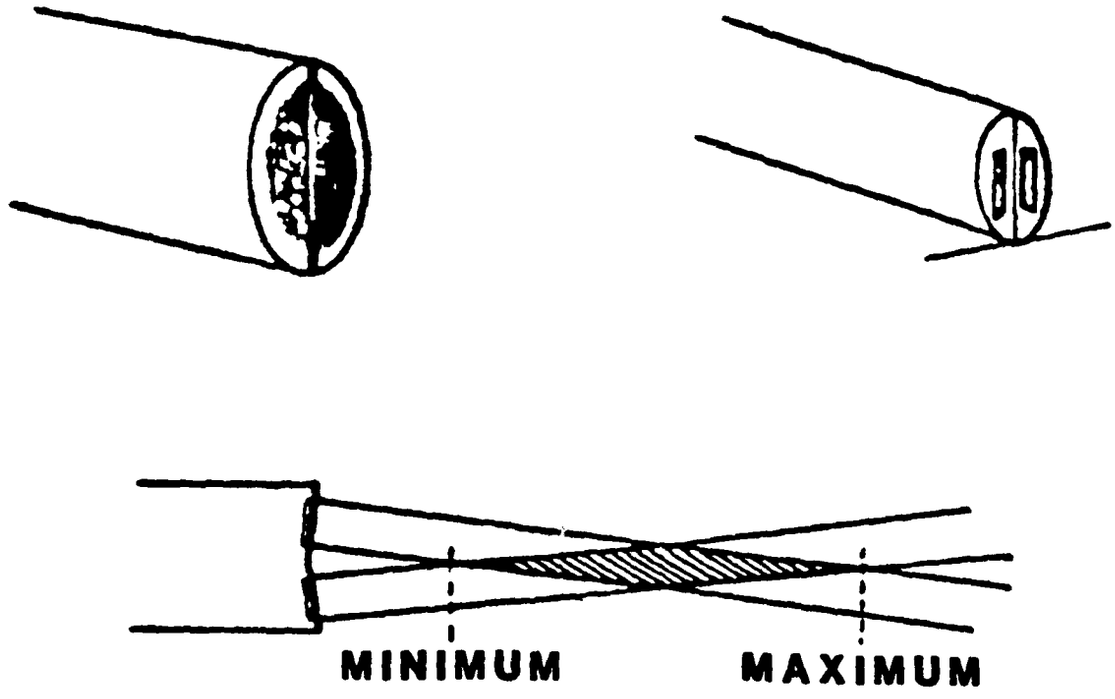

Figure 10. Top cross-hatched areas show radiating faces for typical Doppler transducers. Bottom, the transmitted field and receiving sensitive areas overlap to define the region in space from which flow can be detected.

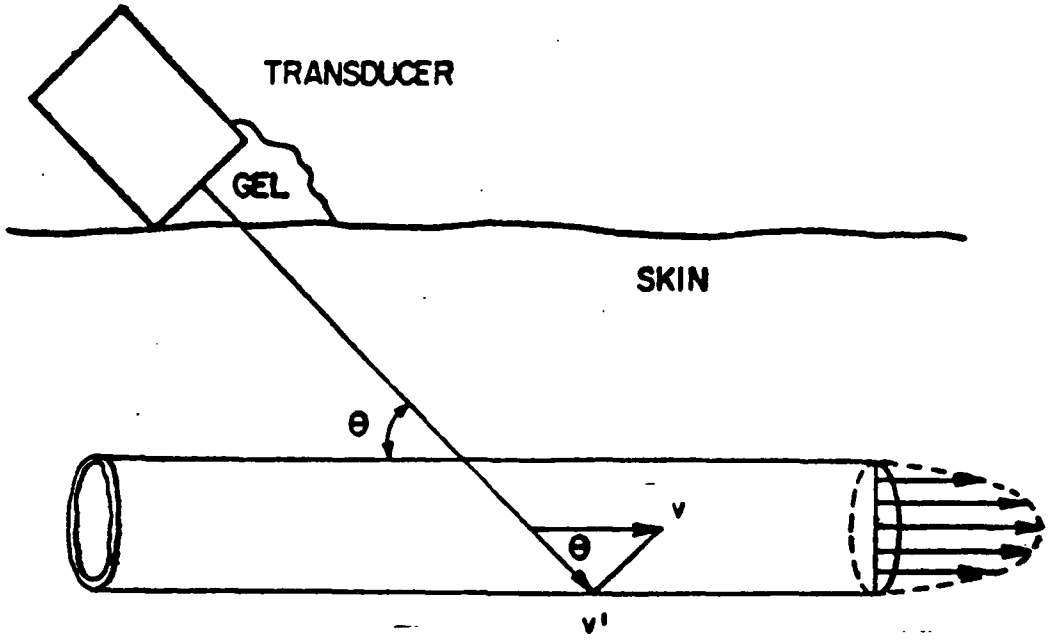

FIGURE 11

Sketch of transducer and soundbeam determining Doppler shift from a blood vessel.

θ = angle between soundbeam and blood vessel
v = velocity of a red cell within the blood vessel

Arrows to the right show distribution of velocities within the vessel at an instant of time.

In a practical case with an ultrasonic frequency of 5 MHz and an angle, θ, of 60°, the result is:

$$f_d = 32.5v \text{ (Hertz per cm per sec.)}$$

A fortunate result of these numbers is that the Doppler shift frequency is usually within the range of human hearing. A velocity of 16 cm per second gives rise to a note about one octave in pitch above middle-C on the piano. Higher velocities give higher frequencies. Simply listening to the Doppler frequencies and using the discriminating abilities of the human ear and brain is a useful technique for interpreting many points both in the dynamics of flow and the detection of gas bubbles. Another important point which is sometimes overlooked is that the Doppler shift is proportional to the ultrasonic frequency. The pitch from a 10 MHz flowmeter is, thus, twice that from a 5 MHz flowmeter. If the velocity is very high, for example, in an artery the resulting pitch may be too high for faithful reproduction or recording, or for some persons to hear.

A block diagram of the basic Doppler system is shown in Figure 12. The functions shown in this diagram are carried out for either continuous-wave or pulse-Doppler systems. The transmitter excites a transducer to send out ultrasonic waves of a particular frequency. Another, or the same transducer can receive these waves which are fed to a receiver. A special property of Doppler systems is that the receiver has two inputs, the received wave, and the frequency of the transmitted wave. The output frequency of the receiver is the difference between the two inputs. This means that there is an output only for the reflections from moving structures. The low-frequency amplifier response covers the range of frequencies between roughly 200 Hz and 20,000 Hz or more. The choice of these pass-band frequencies for the Doppler receiver is extremely important in managing interference or artifact signals. A further step can be taken with the Doppler frequency signals coming from the receiver. If these are to be displayed in the form of flow velocity waveforms, the Doppler frequencies must be converted to a voltage. This is done by a readout, or analysis circuit which is a part of the Doppler flowmeter as shown in Figure 12. The signals can also be further analyzed and recorded.

6. Safety Considerations

High-power sound waves can affect tissues by several mechanisms. No observable effects have been demonstrated on intact mammalian tissues from the amounts of power used with medical diagnostic and bubble detection apparatus.

To discuss the damage question, we must define the units of exposure. For historical reasons, the rate of power transfer in watts has been used. A watt is a measurement of power and the warming or heating effect of ultrasound is proportional to the power density, expressed usually as watts per square cm. This power

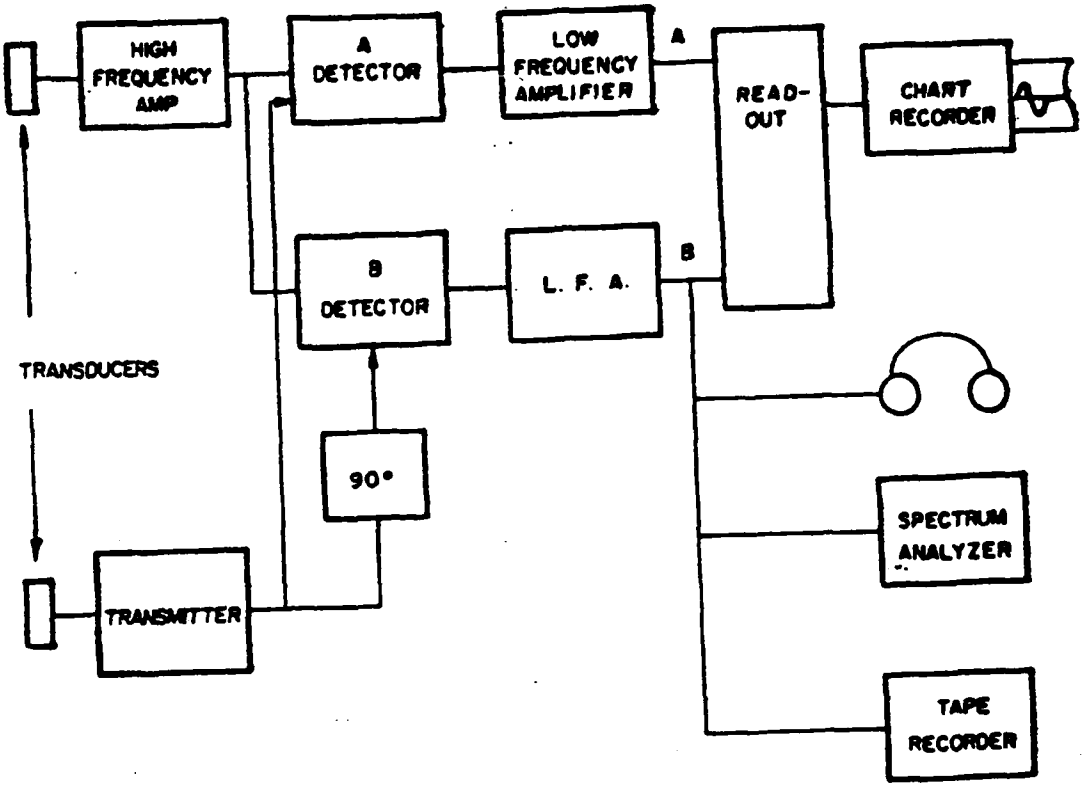

Figure 12. Block diagram of directional Doppler flowmeter system. Functions are described in text.

density figure is termed the "intensity" of sound waves.

The intensity of most diagnostic and bubble detection ultrasonic equipment ranges between 10 and 100 milliwatts per square cm. As a standard of comparison, the average power output of heat due to metabolic processes of the human body is about 10 milliwatts per square cm. At intensity levels of 1-3 watts per square cm, the conversion of ultrasonic energy to heat by absorption of the tissues becomes noticeable. The heat flow is greater than that due to metabolism and a distinct warming effect is noted. This effect has been used in physical medicine in ultrasonic therapy equipment. It has become very useful in athletics because the sound waves are absorbed more by muscle and tissues of high protein content than by fat, whereas for microwave diathermy the reverse is true.

At higher intensity levels, ranging from 1 watt per square cm to thousands of watts per square cm, damage can be obtained in liquid solutions. This damage results from the low-pressure areas in the sound wave tearing the liquid apart. This phenomenon, called "cavitation," results in the production of small cavities in the fluid. This is a high-energy process and results in free radical formation and a variety of chemical and biological effects. Cavitation has not been demonstrated in highly viscous materials, nor at frequencies much over 5 MHz. The effect may be of some importance because the peak power of pulse ultrasonic apparatus, such as conventional pulse-echo clinical diagnostic machines and pulse-Doppler flowmeters, may reach into the 10 to 100 watts per square cm range. Operation at high frequencies, where higher power levels are required to cause cavitation, and in bursts of extremely short time duration, one to five-millionths of a second, apparently prevents cavitation from occurring even in lower viscosity materials, such as blood.

Considerable interest in these tissue-altering effects of ultrasound has been maintained for many years. Currently investigations are under way on the use of ultrasonic heating for potentiating the effects of radiotherapy in tumors. These studies, and several studies directed specifically toward the possible hazards of diagnostic equipment, have not to this date been able to verify that any hazard exists from the use of ultrasonic diagnostic equipment at current power levels.

(M.R. Powell)
(J.M. Reid)

B. A BRIEF HISTORY OF GAS PHASE SEPARATION, DECOMPRESSION SICKNESS, AND ULTRASOUND

The pathophysiology of decompression sickness has been obscure since Robert Boyle (1670) first noted the signs in small animals which he had subjected to a reduced pressure. Bibliographical sourcebooks of Hoff (1948, 1954) and Greenbaum and Hoff (1966) provide a good historical picture of the development of ideas of the etiology of decompression sickness to the recent past. Before the work of the French physiologist Paul Bert in 1893, it was generally believed that decompression sickness or "Caisson Workers' Disease" was the result of rheumatism produced by the cold, damp working conditions. Bert (translation 1943) developed the "bubble hypothesis" at a time when the other theories were more prevalent. However, the inability of Bert's early hypothesis to explain all the known problems of the malady, especially the latent manifestations of the disease, eventually led to the proposal of other (and possible more excessively complicated) mechanisms. End (1938) suggested that the agglutination of blood cells was the primary factor with bubbles being only a secondary and complicating factor; platelet clumping has also recently been implicated (Philp, 1974). Hemoconcentration has also been suggested as an important factor in altitude decompression sickness by Malette, et al. (1962). Heparin has been utilized by many as an adjunct to treating decompression sickness perhaps by reducing lipid emboli (Barthelemy, 1963; Philp, et al., 1967; Crockett, et al., 1968).

In spite of the other hypotheses proposed, the "bubble hypothesis" is believed by the majority of workers in the field of hyperbaric physiology to be essentially correct despite the lack of specific facts concerning the origin of bubbles and their site of action. Gersch and Catchpole (1951) provided evidence for intravascular bubbles as the primary agent in both altitude and hyperbaric decompression sickness. The action of the bubbles was postulated to produce stagnation anoxia. Gersch, Hawkinson and Jenny (1945), in experiments in which guinea pigs were decompressed from atmospheres consisting of either helium, argon, nitrogen or oxygen, demonstrated that intravascular gas bubbles were present in all tissues and organs but were more numerous in those rich in lipid. Extravascular bubbles were found in lipid tissues such as adipose, adrenal cortex and myelin sheath or nerve fibers, but were absent from fat-poor tissues such as liver, skeletal muscle or tendon.

Nims (1951) proposed a physical theory wherein nerve endings were deformed by growing gas bubbles such that when a given distortion pressure was reached, pain would result. The location of these bubbles was thought to be extravascular. This later theory was expounded upon by Hills (1966) who introduced the idea that the gas phase need not be a spherical bubble, but would rather conform to the confining area in which it was growing.

The mechanism for bubble formation in animals subjected to reduced pressures is still not known with any degree of certainty. The early study of Harvey and co-workers (Harvey, 1951a and 1951b) and Blinks, Twitty and Whiteker (1951) show that muscular activity was a

predisposing factor to the formation of visible bubbles in animals. Harvey postulated that micro-gas nuclei, stabilized in hydrophobic crevices, were the sites for bubble growth. The rapid diffusion of carbon dioxide and later other more slowly diffusing inert gases of the breathing mixture into the stabilized cracks would result in the bubbles responsible for decompression problems. While this hypothesis is attractive, solid evidence for the existence of gas micro-nuclei is lacking. Work by Evans and Walder (1969) has lent credence to the possibility that gas micro-nuclei do exist in living systems. In more recent studies (Powell, 1975) it was demonstrated that extensive gas phase formation occurs intravascularly following hyperbaric decompression. This occurs even in subjects killed at pressure where the circulatory system has been arrested demonstrating that hemodynamic forces are, therefore, not necessary during pressure reduction. It was found that as phase formation did not occur outside of the vascular system, and this suggests that the gas phase may grow on small micro-nuclei which are possibly injected into the blood in passage through the pulmonary circulation or generated by hemodynamic mechanisms, possibly in the heart itself.

The hypothesis that bubbles are primarily responsible for limb-bend decompression sickness leads directly to questions of the exact role of these bubbles in the pathophysiology. In those theories specifying bubbles in an extravascular locus (Nims, 1951; Ferris and Engal, 1951; Hills, 1966), the mechanism of action is somewhat specific (neural distension); but for those theories utilizing circulation and/or intravascular bubbles, the mechanism is more vague. Intravascular bubble theories propose that bubbles form in the capillaries and block a venous or arterial channel causing stagnation anoxia.

Of crucial importance to bubble formation is the hypothesis of a metastable limit for bubble formation. This was first proposed by Haldane (Boycott, et al., 1908), and the "Haldane Method" of rapid ascent with shallow decompression stops resulted from it. This hypothesis states that blood can tolerate a considerable degree of super-saturation without the formation of a separated gas phase. Furthermore, this super-saturation limit is a fixed constant; and below the postulated limit bubbles will not form, while above it gas phase separation will definitely occur. In contemporary decompression models, this metastable limit is proposed to be different for each tissue and to depend upon the tissue half-time (Workman, 1969). Whether a true metastable limit exists has been a difficult question to answer. Early attempts to detect gas in the body made use of x-rays; however, the method was not very sensitive and was successful only for the detection of large pockets of gas. If, indeed, small bubbles were involved, they could not easily be detected by the insensitive method.

Following the analysis of certain dive profiles, Hills (1966) concluded that gas phase separation always occurs during decompression with commonly employed tables; for example, the U. S. Navy Diving Tables. He proposed that these tables merely controlled the size of bubbles; this concept has yet to be cogently proven. The existence of the sub-clinical gas phase or "silent bubble" has been

proposed earlier by Behnke (1951). Following the demonstration with ultrasonic techniques by Spencer and Campbell (1968) and Gillis, et al. (1968a, b) that "silent bubbles" do exist following asymptomatic decompressions, work has been done to determine what implications, if any, exist because of this sub-clinical gas phase. Hempleman (1963) earlier had proposed that a tissue-bubble "complex" occurred; it could retard gas release even in asymptomatic decompressions because blood flow was impeded by gas bubbles in capillaries.

The concept of an absolute metastable limit has been questioned in recent years because of the question of a lag period for the development of decompression sickness symptoms. If, indeed, bubbles do form when this limit has been exceeded, to a first approximation, the symptoms should follow immediately or very shortly thereafter. However, in man a lag period of many minutes or even hours after decompression begins has been noted (Nims, 1951) and, indeed, for the case of altitude decompression sickness, the symptoms are not noted often until the fliers are descending to the ground.

A major problem has thus been to determine: (1) the presence or absence of bubbles in decompressed subjects, and (2) the relationship of these bubbles to the signs and symptoms which may later develop. Before ultrasonic techniques, the observation of bubbles was largely confined to those visible in major vessels upon autopsy. Dissection techniques can be contradictory, however, in that bubbles were not always found if autopsy was delayed. Furthermore, if the problem was caused by small bubbles in the microcirculatory system, gross dissection techniques would not reveal them.

A voice was given to "silent bubbles" with the advent of the Doppler ultrasound flowmeter. First proposed and demonstrated by Satomura (1957) and by Franklin, Schlagel and Rushmer (1961), the Doppler technique involves radiating blood with an ultrasound beam in the 2-10 MHz range and detecting the reflected signal. Early flowmeter workers noted that small air bubbles in the calibrating liquids such as milk or blood produced very large signal artifacts as they passed through the transducer ultrasound beam. Exploiting this observation in 1967, Spencer subjected a Doppler-implanted sheep to a simulated dive to 200 feet in a medical recompression chamber. During decompression, bubble signals consisting of sharp clicks, chirps and whistles were heard. Shortly thereafter the animal fell unconscious with convulsions and died. In the original experiments, Doppler probes were implanted on the abdominal aorta, but probes on the vena cava of other sheep also demonstrated that bubbles could be detected in this system and venous bubbles did not result in extreme symptoms such as convulsions and death. Similar experiments utilizing swine were also performed by Gillis and associates (1968).

Early experiments to demonstrate gas bubbles in human subjects were disappointing (Spencer, et al., 1969). Bubble signals could not be unequivocally detected in peripheral veins of the extremities or the neck using transcutaneous Doppler probes even in the presence of signs and symptoms of decompression sickness. Spencer observed that the monitoring of individual peripheral veins was difficult, and a better system might be devised by detecting all peripheral tissue

bubbles as they appeared in the pulmonary artery. Spencer and Clark (1972) constructed a large, crystal, blood bubble transducer which could be used over the precordial region.

Running in a parallel course to the Doppler bubble detection systems, other groups have been employing ultrasonic absorption methods. A program using the absorption technique was initiated in 1962 by Surgeon Lieutenant Commander Kidd at the Canadian Forces Institute of Aviation Medicine. Initial work was conducted on a contract to the Research and Development Division of Huntec Limited in 1963 to investigate the application of ultrasonics to the study of decompression sickness (Hutchins, 1964 a,b). Their basic method was to employ ultrasound to detect bubbles in living tissue and determine their number by noting the decrease in the beam strength as it passed through a bubble-containing medium. In later tests (Hutchins, 1965), conducted in the hyperbaric chamber at Toronto General Hospital, changes in the structure of the received signal were observed which were noted to be different from those observed previously ascribed solely to mechanical changes. These changes seemed to be related to the time-pressure history of the subject. Further testing of this system could not continue as financial support for the project was terminated, although a system of improved design was tested in vitro (Hutchins, 1966).

Mackay (1963) also made an early suggestion to use ultrasound to detect decompression bubbles. The early work by Mackay and Rubissow (1971) and Rubissow and Mackay (1971) showed that separated gas can be detected and imaged by pulse-echo techniques. Tucker and Welsby (1968) suggest detecting the harmonics generated by an oscillating bubble in an ultrasound beam to determine the early appearance of a gas phase. An application of this non-linear approach was made by Martin, et al. (1973) to detect decompression bubbles in human divers following a hyperbaric exposure.

Pulsed ultrasound techniques were tested in vitro by Sutphen (1968) and Manley (1969) to determine the feasibility of using ultrasound to determine the presence of in vivo tissue gas bubbles. Buckles and Knox (1969) employed acoustic optical imaging for bubble detection; however, the system suffered from problems in resolution. Walder, et al. (1968) monitored the strength of ultrasound beam reflected from tissue to determine the presence of a gas phase in a guinea pig leg following rapid decompression.

Through-transmission ultrasound (Powell, 1971) was employed to detect in vivo bubbles in rats. The time course for sound attenuation was correlated with the time course of decompression sickness signs to conclude that in vivo tissue bubbles appeared and disappeared with the same time course as the appearance and disappearance of limb-bend decompression sickness signs in rats. From measurements of ultrasound attenuation, visual studies of bubbles in the venous and arterial system of rats, and observations of gait disturbances as rats walked a treadmill, a general theory was hypothesized (Powell; 1971; 1972) for the pathological effects of bubbles appearing in different regions of the body. The best correlation between the time course for the appearance of bubbles in one group of anesthetized

subjects and the time course for the appearance of signs and symptoms of limb-bend decompression sickness in one group of active subjects was noted with through-transmission ultrasound devices. It is not possible to put these probes upon the proper anatomical areas of moving subjects, so correlations between the two groups of subjects exposed to the same decompression conditions was used. It was noted that small muscle movements would produce signal artifacts an order of magnitude larger than that produced by the presence of the gas phase; thus, at present, the through-pass system is confined to laboratory studies only. Because attenuation is a function of both bubble size and number, only qualitative measurements are possible at the present time.

Most efforts in producing an operationally useful, diver-monitoring device have been directed towards the more easily operable Doppler ultrasound bubble detectors. One practical difficulty lies in the poor understanding of the temporal relationship between gas phase formation in tissues and the later appearance of bubbles in the larger veins draining these tissues. The problem is compounded when one uses the ultimate confluence of all of the veins and monitors the pulmonary artery, as is done in diving today where Doppler devices have been employed with limited success. As decompression procedures become longer and Doppler monitoring becomes more extensively employed, it is absolutely necessary that the temporal relationships between the tissue gas phase and Doppler-detected bubbles be known. This is to ensure that therapy not be instituted too late nor adequate decompression procedures changed too early following the appearance of Doppler-detected bubbles. Additionally, we require information concerning the number of precordial bubbles and the probability of decompression sickness.

Attempts to employ Doppler detection methods to aid decompression in human divers have been sporadic, and the scattered results have been difficult to analyze. It is the general observation, however, that decompression gas bubbles are always detected before the symptoms of decompression sickness (Smith and Johanson, 1970; Smith and Spencer, 1970; Spencer and Clark, 1972). There have been numerous observations that gas emboli are frequently produced in hyperbaric chamber exposures on U. S. Navy tables, and there are few researchers today who would seriously consider that venous gas bubbles are found only in bends-producing dives. Both Spencer and Johanson (1974) and Pilmanis (1974) found there was a great variability in divers to produce bubbles, and those divers with a greater propensity to bubble formation had a greater tendency to get decompression sickness. Limited predictive success in large animal diving experiments so far has come from calculating probabilities of decompression sickness outcome to bubble frequency detected precordially. In studies utilizing miniature swine dived on nitrogen-, helium-, or neon-oxygen mixtures (Powell, 1974), or humans dived on neon- or helium-oxygen mixtures (Powell and Johanson, 1978), there was a definite tendency for a bends outcome to result following a high degree of bubbles detected over the precordial region. This will be covered in greater detail in a later section.

Following the analysis of certain dive profiles, Hills (1966) concluded that gas phase separation always occurs during decompression with commonly employed tables; for example, the U. S. Navy Diving Tables. He proposed that these tables merely controlled the size of bubbles; this concept has yet to be cogently proven. The existence of the sub-clinical gas phase or "silent bubble" has been proposed earlier by Behnke (1951). Following the demonstration with ultrasonic techniques by Spencer and Campbell (1968) and Gillis, et al. (1968a, b) that "silent bubbles" do exist following asymptomatic decompressions, work has been done to determine what implications, if any, exist because of this sub-clinical gas phase. Hempleman (1963) earlier had proposed that a tissue-bubble "complex" occurred; it could retard gas release even in asymptomatic decompressions because blood flow was impeded by gas bubbles in capillaries.

The concept of an absolute metastable limit has been questioned in recent years because of the question of a lag period for the development of decompression sickness symptoms. If, indeed, bubbles do form when this limit has been exceeded, to a first approximation, the symptoms should follow immediately or very shortly thereafter. However, in man a lag period of many minutes or even hours after decompression begins has been noted (Nims, 1951) and, indeed, for the case of altitude decompression sickness, the symptoms are not noted often until the fliers are descending to the ground.

A major problem has thus been to determine: (1) the presence or absence of bubbles in decompressed subjects, and (2) the relationship of these bubbles to the signs and symptoms which may later develop. Before ultrasonic techniques, the observation of bubbles was largely confined to those visible in major vessels upon autopsy. Dissection techniques can be contradictory, however, in that bubbles were not always found if autopsy was delayed. Furthermore, if the problem was caused by small bubbles in the microcirculatory system, gross dissection techniques would not reveal them.

A voice was given to "silent bubbles" with the advent of the Doppler ultrasound flowmeter. First proposed and demonstrated by Satomura (1957) and by Franklin, Schlagel and Rushmer (1961), the Doppler technique involves radiating blood with an ultrasound beam in the 2-10 MHz range and detecting the reflected signal. Early flowmeter workers noted that small air bubbles in the calibrating liquids such as milk or blood produced very large signal artifacts as they passed through the transducer ultrasound beam. Exploiting this observation in 1967, Spencer subjected a Doppler-implanted sheep to a simulated dive to 200 feet in a medical recompression chamber. During decompression, bubble signals consisting of sharp clicks, chirps and whistles were heard. Shortly thereafter the animal fell unconscious with convulsions and died. In the original experiments, Doppler probes were implanted on the abdominal aorta, but probes on the vena cava of other sheep also demonstrated that bubbles could be detected in this system and venous bubbles did not result in extreme symptoms such as convulsions and death. Similar experiments utilizing swine were also performed by Gillis and associates (1968).

Early experiments to demonstrate gas bubbles in human subjects were disappointing (Spencer, et al., 1969). Bubble signals could not be unequivocally detected in peripheral veins of the extremities or the neck using transcutaneous Doppler probes even in the presence of signs and symptoms of decompression sickness. Spencer observed that the monitoring of individual peripheral veins was difficult, and a better system might be devised by detecting all peripheral tissue bubbles as they appeared in the pulmonary artery. Spencer and Clark (1972) constructed a large, crystal, blood bubble transducer which could be used over the precordial region.

Running in a parallel course to the Doppler bubble detection systems, other groups have been employing ultrasonic absorption methods. A program using the absorption technique was initiated in 1962 by Surgeon Lieutenant Commander Kidd at the Canadian Forces Institute of Aviation Medicine. Initial work was conducted on a contract to the Research and Development Division of Huntec Limited in 1963 to investigate the application of ultrasonics to the study of decompression sickness (Hutchins, 1964 a,b). Their basic method was to employ ultrasound to detect bubbles in living tissue and determine their number by noting the decrease in the beam strength as it passed through a bubble-containing medium. In later tests (Hutchins, 1965), conducted in the hyperbaric chamber at Toronto General Hospital, changes in the structure of the received signal were observed which were noted to be different from those observed previously ascribed solely to mechanical changes. These changes seemed to be related to the time-pressure history of the subject. Further testing of this system could not continue as financial support for the project was terminated, although a system of improved design was tested in vitro (Hutchins, 1966).

Mackay (1963) also made an early suggestion to use ultrasound to detect decompression bubbles. The early work by Mackay and Rubissow (1971) and Rubissow and Mackay (1971) showed that separated gas can be detected and imaged by pulse-echo techniques. Tucker and Welsby (1968) suggest detecting the harmonics generated by an oscillating bubble in an ultrasound beam to determine the early appearance of a gas phase. An application of this non-linear approach was made by Martin, et al. (1973) to detect decompression bubbles in human divers following a hyperbaric exposure.

Pulsed ultrasound techniques were tested in vitro by Sutphen (1968) and Manley (1969) to determine the feasibility of using ultrasound to determine the presence of in vivo tissue gas bubbles. Buckles and Knox (1969) employed acoustic optical imaging for bubble detection; however, the system suffered from problems in resolution. Walder, et al. (1968) monitored the strength of ultrasound beam reflected from tissue to determine the presence of a gas phase in a guinea pig leg following rapid decompression.

Through-transmission ultrasound (Powell, 1971) was employed to detect in vivo bubbles in rats. The time course for sound attenuation was correlated with the time course of decompression sickness signs to conclude that in vivo tissue bubbles appeared and disappeared with the same time course as the appearance and disappearance of limb-bend

decompression sickness signs in rats. From measurements of ultrasound attenuation, visual studies of bubbles in the venous and arterial system of rats, and observations of gait disturbances as rats walked a treadmill, a general theory was hypothesized (Powell; 1971; 1972) for the pathological effects of bubbles appearing in different regions of the body. The best correlation between the time course for the appearance of bubbles in one group of anesthetized subjects and the time course for the appearance of signs and symptoms of limb-bend decompression sickness in one group of active subjects was noted with through-transmission ultrasound devices. It is not possible to put these probes upon the proper anatomical areas of moving subjects, so correlations between the two groups of subjects exposed to the same decompression conditions was used. It was noted that small muscle movements would produce signal artifacts an order of magnitude larger than that produced by the presence of the gas phase; thus, at present, the through-pass system is confined to laboratory studies only. Because attenuation is a function of both bubble size and number, only qualitative measurements are possible at the present time.

Most efforts in producing an operationally useful, diver-monitoring device have been directed towards the more easily operable Doppler ultrasound bubble detectors. One practical difficulty lies in the poor understanding of the temporal relationship between gas phase formation in tissues and the later appearance of bubbles in the larger veins draining these tissues. The problem is compounded when one uses the ultimate confluence of all of the veins and monitors the pulmonary artery, as is done in diving today where Doppler devices have been employed with limited success. As decompression procedures become longer and Doppler monitoring becomes more extensively employed, it is absolutely necessary that the temporal relationships between the tissue gas phase and Doppler-detected bubbles be known. This is to ensure that therapy not be instituted too late nor adequate decompression procedures changed too early following the appearance of Doppler-detected bubbles. Additionally, we require information concerning the number of precordial bubbles and the probability of decompression sickness.

Attempts to employ Doppler detection methods to aid decompression in human divers have been sporadic, and the scattered results have been difficult to analyze. It is the general observation, however, that decompression gas bubbles are always detected before the symptoms of decompression sickness (Smith and Johanson, 1970; Smith and Spencer, 1970; Spencer and Clark, 1972). There have been numerous observations that gas emboli are frequently produced in hyperbaric chamber exposures on U. S. Navy tables, and there are few researchers today who would seriously consider that venous gas bubbles are found only in bends-producing dives. Both Spencer and Johanson (1974) and Pilmanis (1974) found there was a great variability in divers to produce bubbles, and those divers with a greater propensity to bubble formation had a greater tendency to get decompression sickness. Limited predictive success in large animal diving experiments so far has come from calculating probabilities of decompression sickness outcome to bubble frequency detected precordially. In studies utilizing miniature swine dived on nitrogen-, helium-, or neon-oxygen

mixtures (Powell, 1974), or humans dived on neon- or helium-oxygen mixtures (Powell and Johanson, 1978), there was a definite tendency for a bends outcome to result following a high degree of bubbles detected over the precordial region. This will be covered in greater detail in a later section.

(M.R. Powell)

C. HISTORY OF DOPPLER ULTRASONIC BLOOD BUBBLE DETECTION

The early diagnosis and prevention of decompression sickness requires objective evidence of impending danger before clinical symptoms and signs develop. The modified Doppler ultrasonic flowmeter meets many of the requirements of the ideal diagnostic instrument. It detects venous gas emboli (VGE) of evolving gas during decompression before symptoms of decompression sickness develop, and it is both non-invasive and small in size. Improvements in the automatic recognition of bubble signals will bring it into more widespread use and thereby lower its cost. It was in 1967 that research technician Norman Simmons first called out during experimental decompression of a sheep in the medical chamber of the Seattle Lake City Tunnel Project, "Funny signals on Doppler" (Figure 13). With presently available equipment, hyperbaric investigators and physicians have a tool with extensive research and clinical capabilities.

1. Doppler Ultrasonics in Hyperbaric Research and Medicine

Behnke (1942) first proposed the presence of "silent" bubble formation in rapid ascent to altitudes of 20,000 to 25,000 feet and that, within this range, silent bubbles were those which did not produce pain. The possibility of "giving audibility" to Behnke's silent bubbles began with the work of Satomura (1957) who provided the first medical applications of Doppler ultrasonic detection of the motions of the heart and blood. Franklin, Schlegal and Rushmer (1961) further developed the Doppler ultrasonic flowmeter in the United States and popularized its world-wide use. Spencer and Campbell (1968) first detected decompression gas emboli in the arterial and venous blood of sheep following decompression from a 200 foot, 60-minute exposure in air, and VGE were shown to occur before the first stop recommended by the U.S. Navy Tables of Exceptional Exposure. Arterial bubbles occurred immediately upon surfacing to 1 ATA and produced the collapse and convulsion of the animals. Gillis, Peterson and Karagianes (1968), confirmed our result for swine and dogs and also demonstrated the capabilities of the external Doppler sensor, while Evans and Walder (1970) demonstrated the same phenomenon in the guinea pig utilizing the Doppler fetal heart rate detector.

It was at first difficult to demonstrate the decompression VGE in human subjects because the peripheral-type external detectors, utilized to monitor the peripheral veins, allowed only local portions of the venous return in the extremities to be monitored. The first VGE signals, in retrospect, were present at that time in subject SC who sustained a painful hand as a result of the exposure, but were not recognized because they produced such large amplitude signals that the typical chirping quality was destroyed by overload of then available electronics. Those first signals were elicited in the basilic vein upon squeezing of the fist (Figure 14).

Figure 15 represents the extreme limits to which we extended ourselves at that time. A catheter-tipped Doppler ultrasonic flowmeter was devised, constructed and tested before insertion under sterile conditions in a human subject in the belief that human

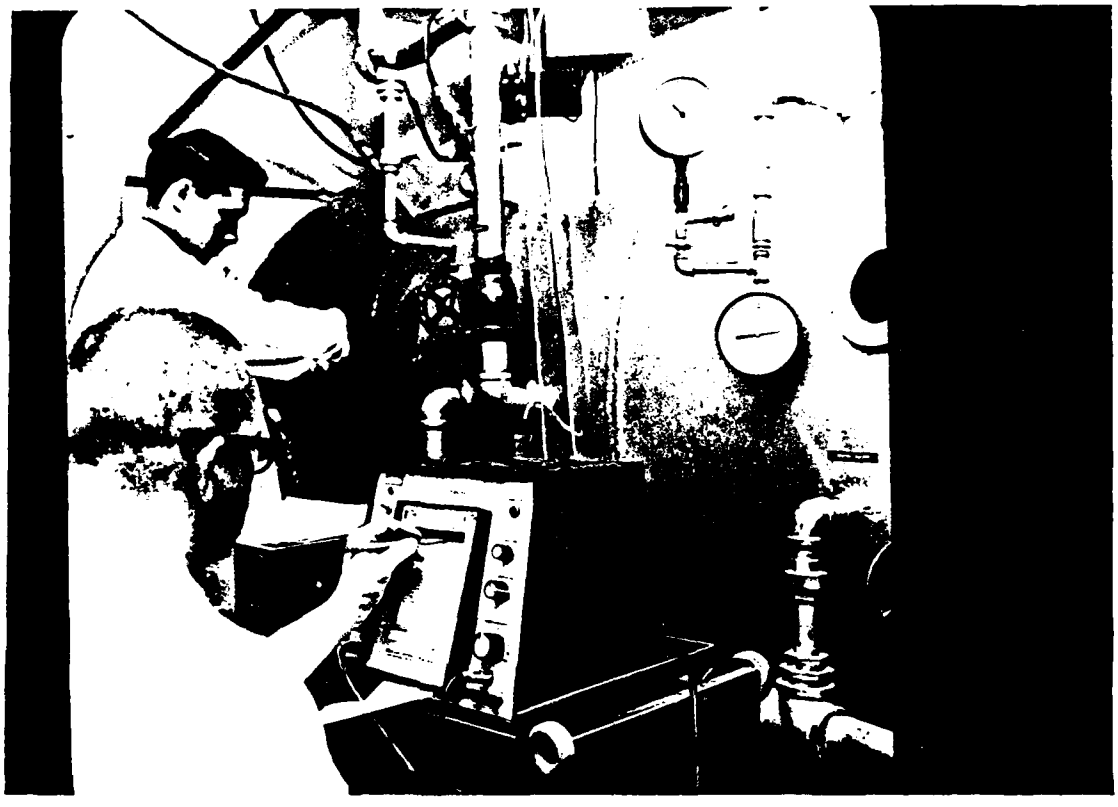

Figure 13. Seattle Lake City Medical Hyperbaric Treatment Lock at the first time of Doppler-detected venous gas emboli, 1967. (Courtesy of Dr. Leon Sealey.)

Figure 14. First attempt at detection of decompression VGE in human subjects. Jon Lindbergh and Spence Campbell after surfacing from a 200 for 30 minute exposure examine the veins in the upper extremities for Doppler-detectable venous gas emboli.

Figure 15. Experimental subject with catheter tip in place through the femoral vein at the time of surfacing from 200 for 30-minute exposure. Doppler blood flow signals are clear, but no VGE were detected. July 24, 1968.

decompression bubbles would be produced during stressful human exposures represented by U.S. Navy Exceptional Exposure Tables. After a 200-foot exposure for 60 minutes and decompression on U.S. Navy tables, Doppler bubble signals were not detected in the vena cava, even though good quality venous flow signals were detected with the catheter. The first unequivocal VGE (Spencer, et al., 1969) occurred in a hyperbaric technician following an equipment test exposure consisting of 15 minutes at 300 fswp air and decompressed according to U.S. Navy tables. Pain developed in the upper arm with skin bends over the right biceps, and monitoring over the right brachial vein elicited typical chirping quality bubble signals both at rest and enhanced by local tissue manipulation. These signals disappeared upon recompression. This finding established the probability that the Doppler VGE detection offered a diagnostic method for human decompression sickness. At that time it was also recognized that Doppler detection could be used during recompression treatment to determine both the necessary extent of recompression and subsequent decompression schedule on the basis of the frequency of incidence of VGE.

At this point it was realized that improved detection of VGE from any portion of the body would be available if a detector could be constructed to monitor the blood flowing through the right ventricle and pulmonary artery with an external sensor placed over the precordium. Meanwhile, Maroon, et al. (1968 and 1969) had reported the detection of air embolism in dogs utilizing the fetal heart rate detector applied over the heart. Spencer, Lawrence, Thomas and Sauvage (1969) reported the usefulness of the Doppler in detecting arterial aeroembolism during open heart surgery.

The first precordial blood bubble detector was constructed by Spencer, Clarke and Simmons in 1971. This device proved superior to the fetal heart rate detector because the unique crystal separation focusing technique eliminated many of the cardiac clutter signals which still, however, hamper the audio recognition of VGE. The transducer, by focusing more deeply, eliminated confusion from the possibility of gas emboli in the blood vessels of the chest wall itself. The electronics were improved to meet the requirements of a wide dynamic range and unusually low empedence of the large crystals needed (Spencer and Clarke, 1972). The present equipment is a compact, battery-operated system (Figure 16).

Early laboratory experiments in sheep by Smith and Spencer (1970) demonstrated that the precordial Doppler detector was an accurate means of detecting impending decompression sickness prior to the development of symptoms or signs. Further experiments established that the Doppler did not itself precipitate gas phase separation in the venous blood during decompression. Asymptomatic Doppler bubble signals were also reported to continue for more than 72 hours after recompression treatment of one animal.

VGE were first detected in scuba divers by Spencer and Campbell (1972) while Spencer and Okino (1972) detected VGE in a Japanese breath-holding Funado Ama after a 51-minute period of 30 successive open ocean dives to 15 meters, with ascent and descent averaging 12

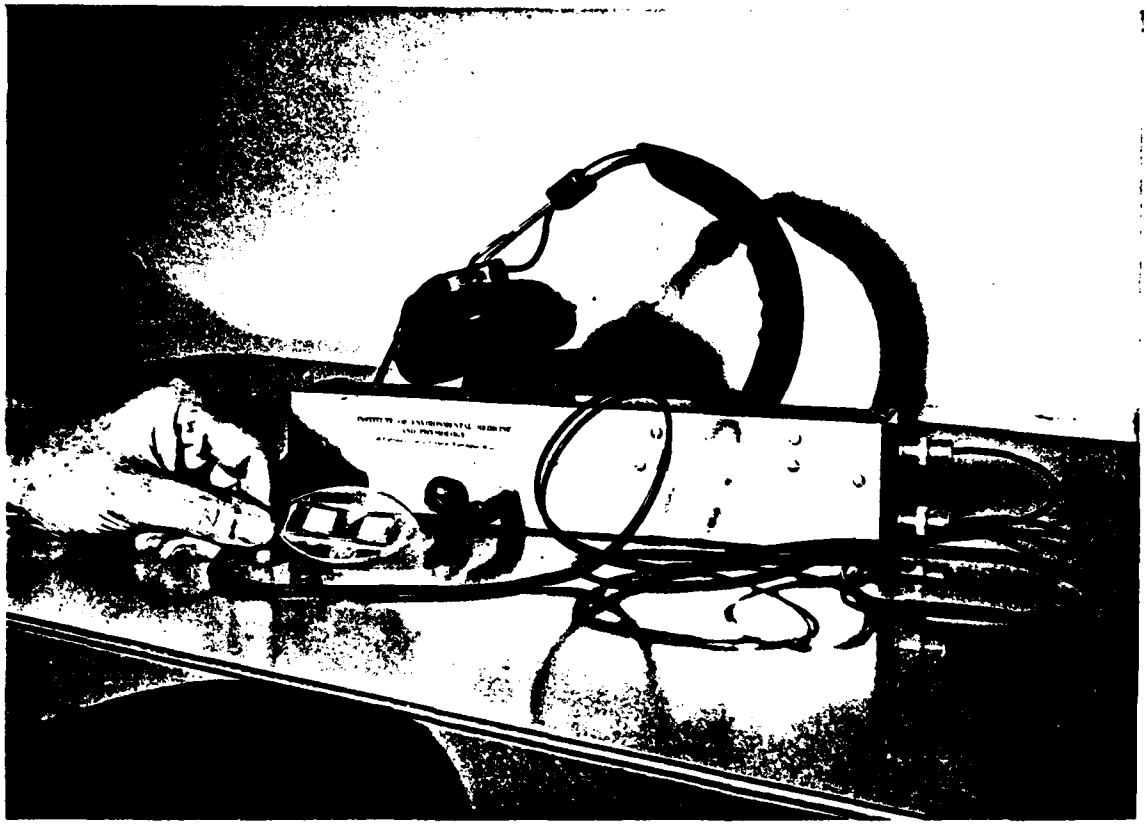

Figure 16. Present portable battery-operated Doppler ultrasonic blood bubble detector with a precordial probe and headphones attached.

seconds and with an average dive length of 53.3 seconds. Fine bubble chirps and clicks were heard, enhanced by movements of the limbs and lasted for one hour without symptoms. Spencer, Hong and Strauss (1974) reported venous gas embolism in Hawaiian seafood divers and black coral divers; similarly, VGE have been detected in Japanese Caisson workers (Nashimoto and Gotoh, 1978).

Evans, Barnard and Walder (1972) detected VGE in men following decompression after breathing oxy/helium mixtures in chamber-simulated dives. They also concluded that bubbles appear to be a precursor of decompression sickness and, therefore, can be used as an indicator end-point rather than relying on pain or other systemic disturbances for assessing the efficacy of decompression procedures. Gas bubbles of helium or neon were found in pigs (Powell, 1974) and man following decompression (Powell and Johanson, 1978).

The threshold for microembolus detection was examined by Gillis (1971) using graded microbeads and microballoons of glass injected via the femoral vein of anesthetized swine. Except for the smallest group (37 to 43μ m diameter), all produced individual Doppler chirps. Solid beads did not produce as large a Doppler signal as the hollow glass microballoons of the same size range. Microballoons of a diameter in the vicinity of 40μ m were virtually impossible to detect individually in the presence of blood flow. Nishi (1972) provided a careful review of the theoretical acoustic scattering properties of bubbles as applied to Doppler flow transducers. He concluded that in vivo sizing of bubbles was only crudely possible, and that absolute values of size cannot be obtained without an in vivo reference. Hills and Grulke (1975) examining two types of Doppler flowmeters, reported that 150μ m bubbles could be detected singly and as small as 50 μ m clouds of bubbles may be detected. Monjaret, Guillerm and Masurel (1975) reported that bubble size versus amplitude of the Doppler-shifted signal followed the proportionalities predicted by Nishi and made some progress towards gas volume quantification. They reported that the amplitude of the Doppler signal was nearly proportional to the radius of the bubble. Spencer and Johanson (1974) devised a grading system for quantities of VGE.

Clinical use of blood bubble detection in diagnosis, prevention and treatment of decompression sickness was reported by Spencer, Johanson, Campbell and Postles (1974). They reported that dry chamber experimental results are predictive of what can be expected in actual open water dives, though the incidence of VGE on the same pressure exposures is less in the chamber than in open water. These authors reported that decompression sickness never developed, in their six-year experience, before detectable VGE and that certain divers are prone to develop VGE and bends while others on the same schedules are relatively immune. For the earliest possible detection of VGE, they recommended combined use of precordial and peripheral monitoring probes and limb manipulation to promote the dislodging of gas bubbles sequestered in the peripheral veins. VGE, without bends, were cleared by respiration of 100% oxygen at 1 ATA and recompression to 30 fswp on 100% oxygen cleared VGE and bends formed by much deeper initial exposures (Spencer, Johanson, Campbell and Postles, 1974). VGE signals served as a practical clinical guide to prevent bends by

indicating specific preventive and treatment measures, including deferred repetitive dives and indicating when it is safe to proceed with decompression during recompression treatment.

Powell and Spencer (1976b) reported VGE following saturation diving with and without decompression sickness. Guillerm, Masurel, LePechon and Guillaud (1977) reported the existence of asymptomatic VGE during decompression from helium saturation dive with men from 300 meters; VGE continued asymptomatic for 20 hours after surfacing. Spencer, Johanson and Campbell (1972) demonstrated VGE and bends produced by direct decompressions after saturation on air at 30 fswp and later demonstrated 25 feet saturation also produced VGE and bends pain in experienced divers.

Spencer and Powell (1977) found gas bubbles in the renal vein but not in the sagittal sinus unless arterial gas emboli (AGE) occur. These locations are in addition to the earlier reports of their occurrence in the jugular and femoral veins, as well as the inferior and superior vena cava and pulmonary artery.

2. Hyperbaric Contributions of the Doppler Bubble Detector

(a) Research in the Etiology of Decompression Sickness and Inert Gas Exchange

The principal contribution of Doppler detection of decompression VGE is the confirmation of previous theories that gas phase separation precedes and is the initiating occurrence for the development of decompression sickness. VGE occurs prior to clinical signs or symptoms, both during and after, decompression from oxy/helium and air exposures, including non-saturation and saturation dives. Many investigators have optically visualized bubbles in the arterial circulation of animals, but only when death supervened (Emerson, Hempleman and Lentle, 1967; and Buckles, 1968). The combined work of Spencer and Campbell (1968) and Powell (1971, 1972) has shown that decompression bubbles form first in the capillaries, are released into the veins, and reach the arterial channels after overload of the pulmonary filtering and elimination mechanism.

The etiological relationship of gas phase separation to the pathophysiology of decompression sickness, as modified from Powell (1971), is summarized in Figure 17. During decompression from hyperbaric exposures, the earliest bubbles appear to form in the peripheral capillaries from which they are readily dislodged into the venous circulation, pass to the pulmonary artery and are harmlessly eliminated at the alveoli. Should the local tissue super-saturation be so great as to produce Grade III to IV VGE, clinical signs of decompression sickness may develop through several mechanisms. Stationary bubbles at the local tissue-producing VGE may produce limb bends if occurring in the periarticular tissues, skin bends if in the cutaneous tissues, in the eighth nerve, symptoms of vertigo and hearing defects, or osteonecrosis if occurring within the bone marrow.

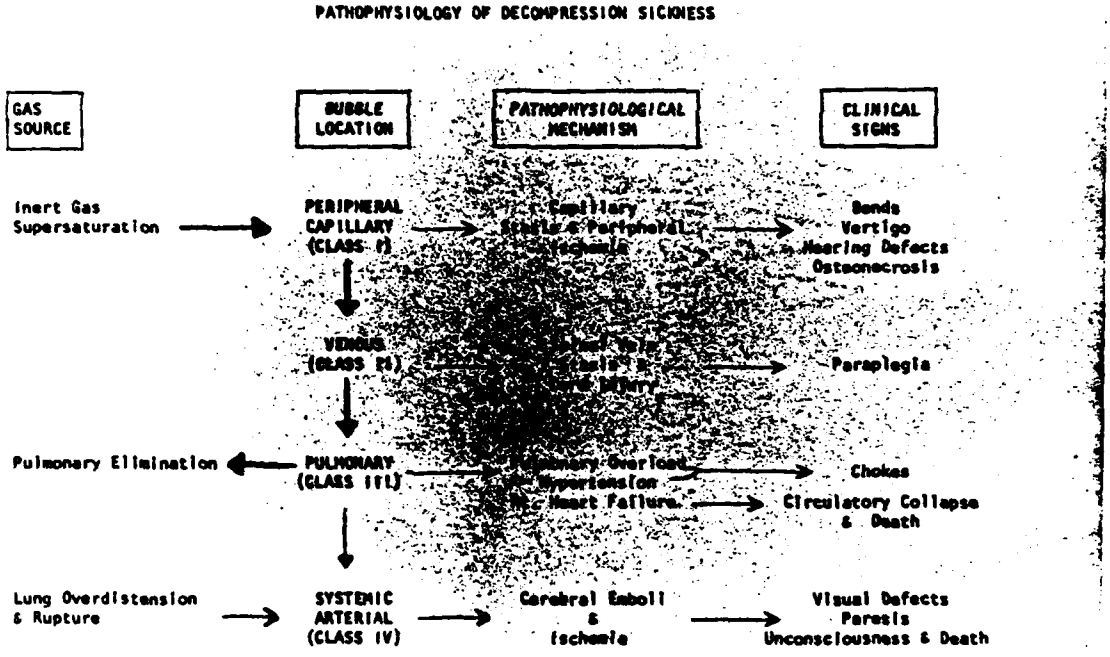

Figure 17. Relationship between the gas source, bubble location, pathophysiological mechanism and clinical signs of decompression sickness. Heavy arrows indicate the pathway of formation of supersaturation bubbles with normal elimination through the lungs. Smaller arrows indicate the pathological consequences.

Spinal cord paraplegia may result from stasis produced by gross accumulation of venous bubbles in the spinal plexis (Bove, Hollenbeck and Elliott, 1974). Stationary extravascular bubbles may contribute to stasis by compression of the local blood vessels. Chokes, right ventricular failure and circulatory collapse may develop when great quantities (Grade IV) VGE persist and overload the pulmonary filter producing pulmonary hypertension.

Arterial gas emboli (AGE) may result from Grade IV VGE overloading the pulmonary filter mechanism and may be squeezed through by recompression treatment or by rapid lung overdistention and rupture when the diver holds his breath during ascent or when pulmonary pathology blocks the bronchiols. Although there is some cerebral tolerance to AGE without producing symptoms, visual defects, paresis, unconsciousness and death may result from considerable quantities of AGE (Spencer and Campbell, 1968; Spencer and Oyama, 1971; Guillerm, Masurel, Guillaud and Monjaret, 1975; Powell, 1971). The brain apparently does not produce Doppler detectable VGE, presumably because of the high perfusion rate of even its slowest tissue, the white matter (Spencer and Powell, 1976, 1977).

Powell (1977) has shown that decompression-generated VGE can pass the pulmonary vasculature producing AGE when the pulmonary artery pressure exceeds 120% of its control value and have determined that less than 6% of absorbed gas is eliminated in the gas phase through the lung.

It has been shown during laboratory chamber simulated dives, as well as open ocean dives, that certain individuals who form VGE readily are also bends prone. VGE prone individuals may be selected by chamber test exposures. Open ocean dives are shown to be more stressful than chamber dives, and bubbles-prone individuals will produce more bubbles in the ocean than in identical pressure exposures in the chamber. Pilmanis (1975) showed that exercise-induced changes in tissue perfusion can substantially affect N_2 uptake and the extent of VGE occurrence.

Coronary pathophysiological consequences of decompression gas phase formation have not been reported, and monitoring of the pulmonary flow during intramyocardial injection of air in experimental animals has shown that gas bubbles pass readily into the venous circulation. Cardiac surgeons have also reported ready passage of coronary artery gas emboli through the coronary circulation without apparent consequence. It may be that the high myocardial flow rate and the squeezing action of the myocardium acting on its own vasculature protects the heart from serious decompression sickness.

(b) Decompression Models and Table Testing

Direct decompression limits for hyperbaric air exposures have

been defined with VGE (Spencer, 1976) (Figure 18). The practical limits of VGE acceptability appear to be in the range of 10-20% incidence among the diving population which represents a less than 5% incidence of mild bends pain. The recommended bottom time for each work depth between 25 and 200 feet is

$$\text{Minutes} = (465/\text{feet})^2$$

These studies also disprove that direct decompression surfacing is safe after saturation lengths of time at a depth of 25 feet.

Guillerm, et al. (1977) found that a constant and feeble bubble output, during decompression from helium saturation dives, consitutes a good criteria for surveillance of decompression during a saturation dive. Neuman, Hall and Linaweaver (1976) confirmed the findings of others that U.S. Navy Exceptional Exposure Tables consistently produce VGE, and they indicate that taking an extra, deeper stop considerably reduces the incidence and severity of VGE and bends.

3. Diagnosis, Prevention and Treatment of Decompression Sickness

The principal value of VGE detection is to alert the diver and his supervisors of the possibility of bends or to eliminate such possibility if the suject is "clean". It has been found that Grade I-II VGE are infrequently associated with bends and that higher grades, III-IV, are associated with a high incidence of bends. Experience with divers at Cobb Sea Mount diving to 130 feet for 15-20 minutes illustrates the usefulness of the precordial detector in preventing state I and II decompression sickness. Monitoring on the deck immediately after the dive led to clinical guidlines for prevention and treatment of decompression sickness.

The observer should be carefully qualified by training and experience in recognizing Doppler VGE signals. The diver should be monitored during and after decompression and not at the working level unless making a large upward excursion. Both the precordial and the peripheral vein detectors should be utilized. Positioning of the precordial probe should be by anatomical and cardiac signal criteria. Causing the subject to hold the breath in expiration while leaning forward brings the heart closer to the chest wall and increases the cardiac and VGE signals. The subject should be breathing quietly and otherwise motionless in a sitting or supine position. If VGE are detected in a peripheral vein but not detectable in the precordial signal, the precordial grade should be considered Grade I. Precordial signals are graded on a Zero to IV scale by estimating the bubbling rate.

Grade Zero is taken to indicate the complete lack of bubble signals.

Grade I indicates an occasional bubble signal

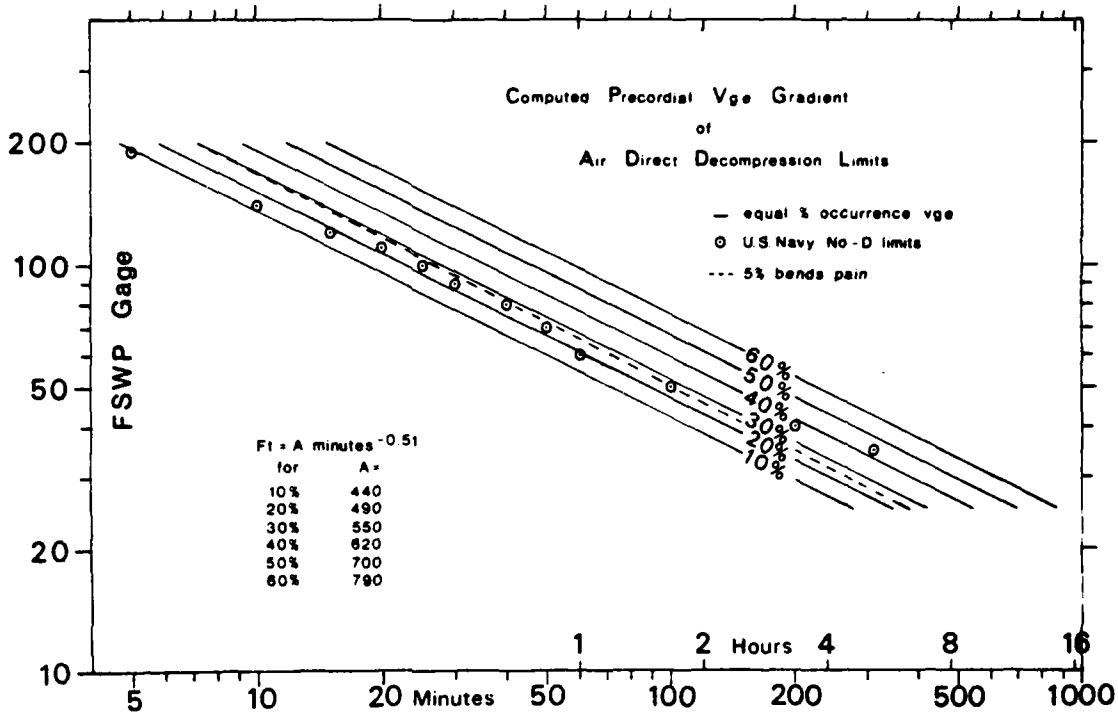

Figure 18. Venous gas embolism isopleths determined with Doppler blood bubble detection in a group of regular scuba divers exposed in the hyperbaric chamber with direct decompressions to the surface. Circles represent U.S. Navy recommendations which appear conservative in the deeper, shorter-term devices but insufficiently conservative in the shallow, longer exposures.

discernable within the cardiac motion signal but with the great majority of cardiac periods free of bubbles.

Grade II is designated when many but less than half of the cardiac periods contain bubble signals either single or in groups.

Grade III is designated when all of the cardiac periods contain showers or single bubble signals but not dominating or over-riding the cardiac motion signals.

Grade IV is the maximum detectable bubble signal sounding continuously throughout systole and diastole with every heart cycle and over-riding the amplitude of the normal cardiac signal.

When in doubt regarding Grades Zero or I, flexion and extension of an extremity, accentuated breathing motions or compression of the local tissues may be utilized to dislodge sequestered venous bubbles.

Peripheral monitoring is most useful for regional localization of VGE signals; monitoring of the femoral vein in the groin is of great value. The inferior vena cava may be interrogated with deeper focusing probes such as the large size (2 1/2 cm.) crystal transducer.

The following are recommended clinical actions to be taken based on the Doppler VGE findings (Spencer 1977):

A. Prevention of Decompression Sickness

1. During decompression

Grade Zero	Continue with decompression plan.
Grade I-II	Hold pressure until VGE disappear. OR Slow ascent (use O_2 if possible). Do not allow repeat dive for 24 hours.
Grade III-IV	Recompress in 1 ATA stages until VGE decrease. Hold (on O_2 if possible) until VGE disappear. Do not allow repeat dive.

2. On the surface

Grade Zero	Dismiss diver after 1 hour if short decompression dive. Dismiss diver after 5 hours if following saturation exposure.

Grade I-II	Administer O_2 until disappearance. No repeat dive.
Grade III-IV	Recompress to 1 ATA and place on O_2 until disapperance. No repeat dive.

B. Treatment of Decompression Sickness

Recompress according to accepted treatment tables and modify the tables according to prevention recommendations "A" for the asymptomatic diver. Extend time of disallowance of diving according to diver condition.

Recompression for Grade III-IV VGE should be accomplished carefully with monitoring of a peripheral artery to minimize and prevent VGE which may be produced by the passage of bubbles through the pulmonary vasculature.

Decompression by "bubble counting" was first proposed by Spencer and Campbell (1968). Because of the lag time between formation of capillary bubbles and their release as VGE, this technique is most applicable to staged decompression; but very slow ascent rates, used in saturation diving, may allow fine individual control to increase safety as well as speed of decompression.

4. Safety Considerations of Ultrasonic Monitoring

No untoward effects have been observed in the monitoring of animals or humans by application of the Doppler detector. Theorectical considerations by Hueter (1955) indicate that the utilization of clinical ultrasound energy levels cannot produce cavitation in the megahertz frequency range. It is particularly noteworthy that no cutaneous cavitation has been identified immediately beneath the area of application of the transducer. Attenuation of the ultrasonic energy as it penetrates deeper could be expected to provide an additional margin of safety (Spencer and Johanson, 1974). Conservative estimates of power delivered to the surface of the heart with the precordial transducer radiating 10 mW/cm^2 cannot exceed 30 $microW/cm^2$. The subambient pressure generated by 30 $microW/cm^2$ of 5 MHz of ultrasound is equivalent to approximately 3 inches of water. Even assuming a possible pumping effect due to the rapidity of the sonic oscillation, 3 inches of water pressure superimposed is considerably below the effects of supersaturation caused by the first steps of decompression which have been used safely for years in diving decompression practices.

While no one has yet defined a specific end-point for acceptable, safe tissue ultrasonic levels, Wells (1969) states the biological effects have not been observed at intensity levels below 100 mW/cm^2. Intensity levels varying from 0.05 W/cm^2 to 0.001

W/cm^2 for durations varying from 15 to 1,440 minutes at frequencies from 5-15 MHz have failed to demonstrate tissue damage in animals.

Animal experiments by Smith and Spencer (1970), and Spencer and Johanson (1974) have shown that delivering high energy levels of ultrasound to transducers applied to the vena cava do not produce VGE in venous blood of animals during decompression.

A definitive statement on the possibility that bubbles may be pumped up by ultrasonic oscillation would require the demonstration of the phenomonon at some power level and require that clinical sound levels be below that experimentally determined level. A reasonable approach to present practical and theoretical considerations results in the conclusion that the usefulness of the information obtained by the application of the Doppler ultrasonic bubble detector far outweighs any possibility that adverse effects might be encountered.

5. Characteristics of the Doppler Bubble Signal

The most singular characteristic of the Doppler blood bubble signal produced is that of their sinusodal character sounding to the ear like a chirp or whistle. If the velocity is extremely high, with consequent brief time under the transducer, the sinusodal chirp produces a clicking sound to the ear.

The work of Monjaret, Guillerm and Masurel (1975), demonstrates that the amplitude of the Doppler bubble signal is, as expected from the work of Nishi, nearly proportional to the radius of the bubble. Moulinier and Masurel (1977) have verified experimetally that the number of zero returns of the bubble Doppler signal is independent of the bubble speed and of its radius, i.e., the higher the speed of the bubble, the higher the frequency, but the period of time beneath the transducer is proportionally smaller. Because of their strong acoustical interface, bubbles in the blood and other liquids tend to backscatter ultrasound far more than solid or viscous particles of the same diameter. In a good signal-to-noise ratio situation, the amplitude of the Doppler signal rises more than 10 db above the blood flow signal itself and in its principal frequency band may rise 20 db above the Doppler signal within that band (Figure 19).

6. Progress in Signal Processing

In spite of the electronic signal processing presently utilized, the human hearing mechanism represents the most accurate processor for recognition of the presence or absence of bubble signals. This is apparently because the human hearing mechanism can recognize the sinusodal narrow band "chirping" quality signals at amplitudes less than the spectral signal of the Doppler blood flow itself. In the case of the precordial signal where the greatest recognition difficulty occurs, a skilled observer can recognize the sporadic nature of the chirping quality signals occurring as in a break in the pattern of normal cardiac signals. Before the Doppler blood bubble detector can become awidely used device for diving operations, it is

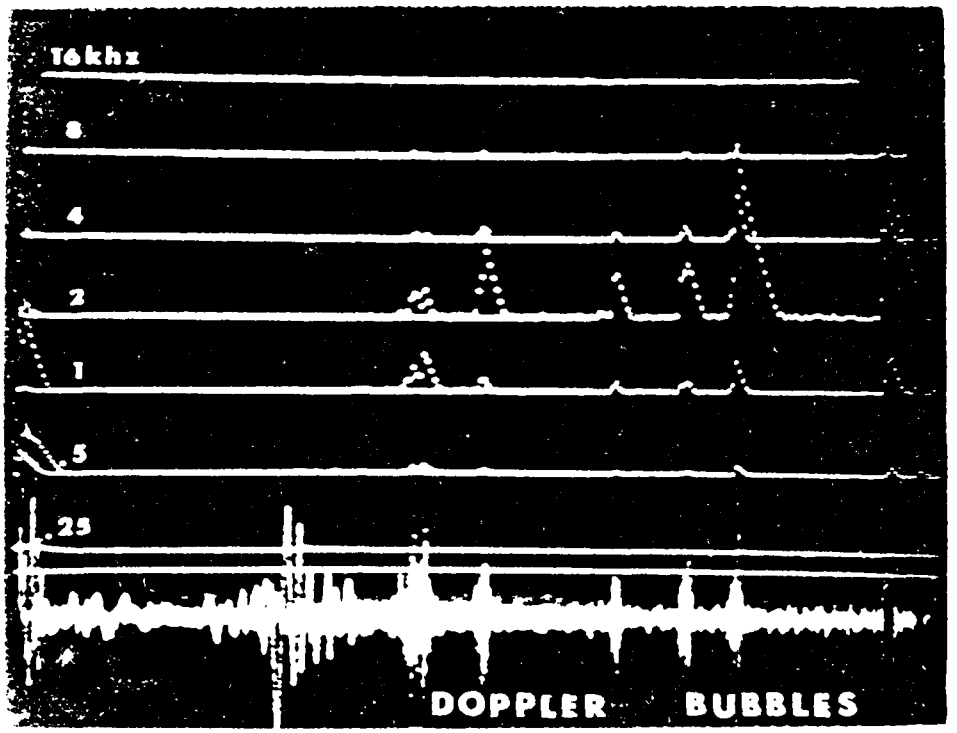

Figure 19. Lower tracing represents the raw Doppler ultrasonic combined flow and blood bubble signal. Upper tracings represent band pass analysis of the signals. The highest amplitude signals seem to represent artifacts on the Doppler signal and do not register in the band passes. Blood bubble signals rising above the Doppler flow signal register on the principal frequency bands.

desirable that an electronic method of signal processing be developed to provide a bubble signal which is not cluttered with cardiac signals or other artifacts.

(a) Band Pass Monitoring

Separation of the Doppler blood signal from VGE is possible by band pass filters. Each bubble signal tends to concentrate its principal frequency within a narrow band while the Doppler blood signal tends to be of broader frequency spectrum. This technique is used by all present investigators as one part of their automatic signal processing approach to VGE recognition and counting. Continuous spectral analysis represents an extension of the band pass filter approach. In this technique, both the conglomerate amplitude of the signal and the increasing irregularity of the cardiac pulse pattern are recognized to correlate with the increasing grade of VGE.

(b) Doppler Directional Readout Circuitry

The IAPM analogue readout circuitry for the directional Doppler flowmeter (Reid, et al., 1973) recognizes the direction of the moving target which, in the case of a bubble signal, is always in the same direction indicated by the blood flow direction(positive-going by most standards) while noise-producing artifacts such as vibration of cable and other microphonics produces a signal interpreted as bi-directional by the readout circuit. Incorporation of this logic into the signal processing circuitry will improve VGE signal separation.

(c) Phase-Locked Loop

The use of this technique takes advantage of the auto-correlation of the Doppler signal by virtue of its inherent sinusodal nature. This technique was first reported as applied to Doppler blood bubble counting by Spencer and Johanson (1974). It is accomplished when tracking filters are used to bring frequency modulated radio signals out of enveloping noise. Utilizing the oscilloscope and the audio signal in an eye and ear correlation technique, excursions of the tracking filter were found to correlate well with the audible bubble signals.

Of future interest would be an electronic circuit which would simulate the hearing mechanism by gradually blanking completely repetitive precordial signals and recognizing new sporadic events that do not occur with regular timing throughout the heartbeat.

(M.P. Spencer)

II. DOPPLER DETECTABLE DECOMPRESSION BUBBLES

A. PHYSIOLOGICAL SIGNIFICANCE OF DOPPLER-DETECTED BUBBLES IN DECOMPRESSION SICKNESS

1. Introduction

Considerable effort has been expended in the past decade toward developing methods to detect decompression sickness in its subliminal or pre-clinical state. The vast majority of these methods have utilized ultrasound be exploiting the large differences in acoustic impedance between a liquid and a gas-filled cavity. Early reports of doppler ultrasound work in the late 60's confirmed an early suspicion of Behnke's (1942, 1951) that so-called "silent bubbles" could be present following a hyperbaric decompression in which evidence of decompression sickness was absent.

This, of course, presented somewhat of a variance with the strict interpretation of the Haldanian principle that "clean" decompressions were free of a gas phase (Boycott, et al., 1908). For purposes of historical accuracy, and for equity towards Haldane, it should be remembered that he acknowledged the possibility of bubble formation with his procedure, proposing that the method kept them within manageable limits. Bubbles, regrettably, not only can lead to decompression sickness, but also change the gas elimination rates as contemporary decompression calculations assume all gas to be in the dissolved state.

Today, we have come to realize that some degree of gas phase formation can occur in the body following virtually any decompression as gas bubbles are detectable with Doppler ultrasonic flowmeters in all represented cases from short bounce dives to slow, saturation-dive decompressions, even in the absence of frank decompression sickness. Thus, while building on the foundation of Paul Bert that gas bubbles are implicated in decompression sickness, we have been forced to abandon the concept that "bubbles = bends" and additionally, that quaint tautology, the "metastable state." With this in mind, research has been directed over the past few years into the patho-physiological consequences of a gas phase in the body as a whole. The working hypothesis is that decompression sickness, at the tissue level, is a composite of at least three factors. Figure 20 shows this as (1) the rate of gas uptake and elimination, (2) the tendency for cavitation to occur in a given micro-region, and (3) that the gas phase formation occurs in an as yet unidentified "critical tissue." It would be expected that for limb-bend decompression sickness, skin rash, and vertigo, the "critical tissue" would not change. The events in the other two circles, however, would be postulated to vary from day-to-day or possibly on an even shorter time scale.

As Figure 20 illustrates, gas uptake and elimination occurs in all tissues of the body as does the tendency towards gas phase formation. It is only when we experience an unfortunate conjunction of these three circles that we experience some degree of limb-bend decompression sickness. This most likely occurs for eighth nerve

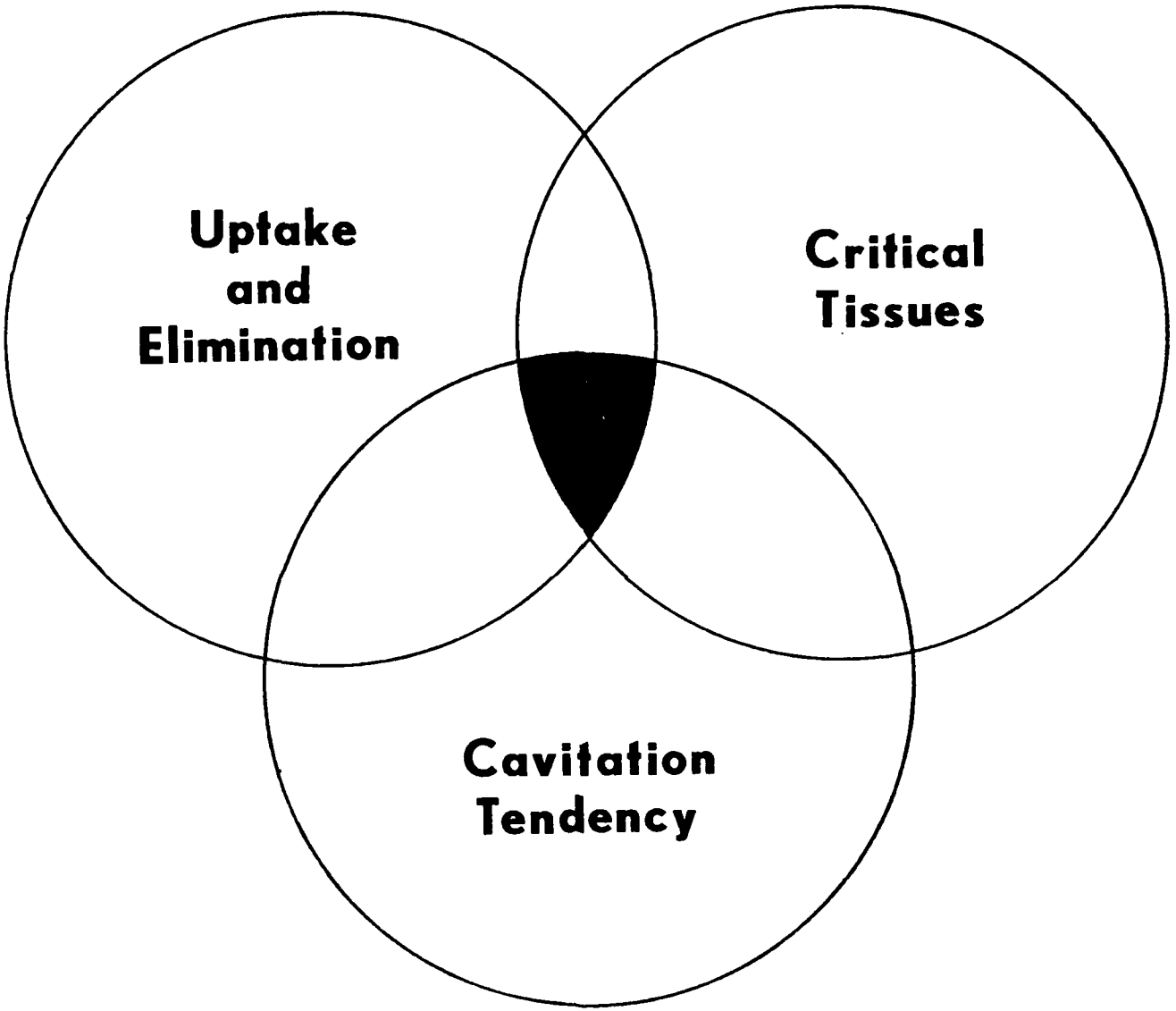

Figure 20. Graphical depiction of events leading to decompression sickness.

problems also. From a premonitory standpoint, at the present time, we appear to have the best handle on what we shall call the "cavitation tendency."

Following decompression, there exists the possibility of gas phase formation in many tissues of the body. The best method of gas phase detection in the body would most likely be a direct interrogation of the so-called "critical tissues" for example, with through-transmission ultrasound, mentioned earlier in this report. Exactly what tissues are involved is, at present, unknown. Through-transmission systems are interesting from a research point of view (Powell, 1971), however, in that beam attenuation can give an indication of the time course for the growth and decay of the tissue gas phase, in particular, the stationary phase. Similar information, with some anatomical detail, can come from echo systems (Mackay and Rubissow, 1971). This attenuation has been interpreted as growth, and later resolution, of a micro-vascular gas phase. This stationary microvascular phase persists longer that the moving "shower" of bubbles in the central venous system (Powell, 1972) and most likely represents the origin of these bubbles which can be released by expression of muscle. Whole mount histological specimens of rat and rabbit leg muscle tissue indicate that the predominant locus for gas phase growth is in the microvasculature (Powell and Weydig, 1974; Powell, 1975). While the initiating micro-gas nucleus may be extravascular, growth occurs in the vascular channels as can be seen in Figures 21 and 22 in muscle tissues, and even predominately intravascular in adipose tissue, Figure 23. As this microcirculatory gas phase grows, bubbles will eventually appear in veins draining that tissue.

From autopsies of large rats subjected to increasing time at pressure it has been noted that gas bubbles could be detected earliest in veins draining abdominal tissue (Powell, 1972). The femoral vein, for example, is a contributor of bubbles, but it is by no means the only or even a major source. Thus, for purposes of premonitory decompression sickness detection by the precordial Doppler detector, we must fully recognize that we are monitoring bubbles not only from "bends-producing tissue" but from many tissues of the body. Additionally, subjects possessing a significant proportion of adipose tissue will place a larger number of bubbles into the vena cava following decompression than non-obese ones. Similarly, a less fat soluable gas (such as helium or neon) will produce fewer caval bubbles than nitrogen. Figure 24 shows an overall hypothesis of pathophysiological consequences of a gas phase in the various portions of the body.

First presented in 1971 (Powell), this scheme has been further refined to its present form. Gas remaining in solution following decompression, no doubt, will not produce a damaging effect. A gas phase forms in the region of the micro-circulatory systems following a reduction in pressure as this is the region of highest gas tension and low hydrostatic pressure. this initial gas phase is "thrombic-like" (Class 1) and grows in place; at least in muscle tissue, the locus of this growth is intravascular (Figures 21 and 22). It is clear that the term "bubble with its geometrical connotations is

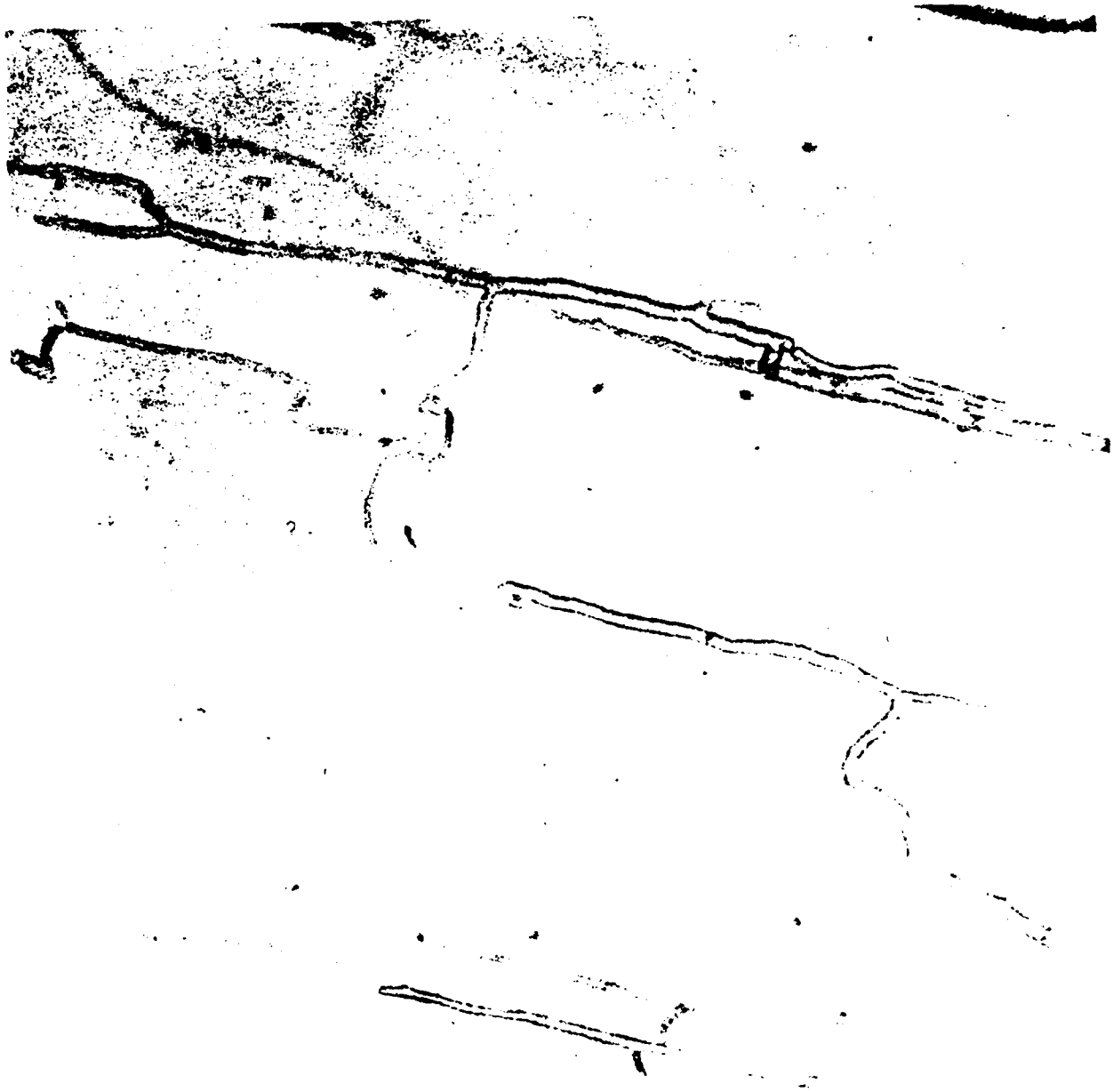

Figure 21. Gas phase in the capillaries of rat abdominal muscle. Note that the gas phase is cylindrical, not a round "bubble."

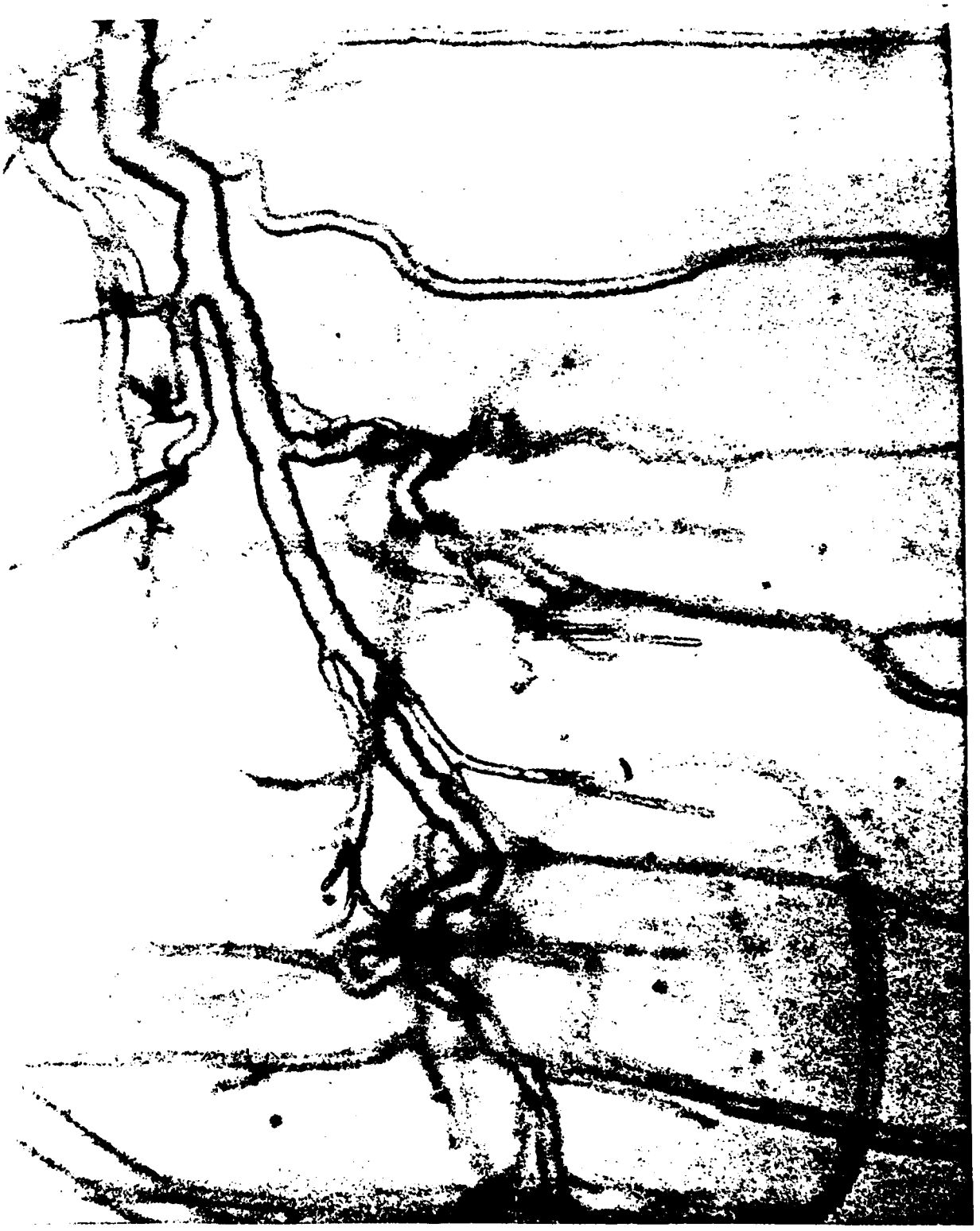

Figure 22. Gas phase in the capillaries and venule of rat abdominal muscle. Unprepared, whole tissue mount.

Figure 23. Gas phase in the microcirculatory system of rat abdominal adipose tissue. Note the absence of extravascular bubbles.

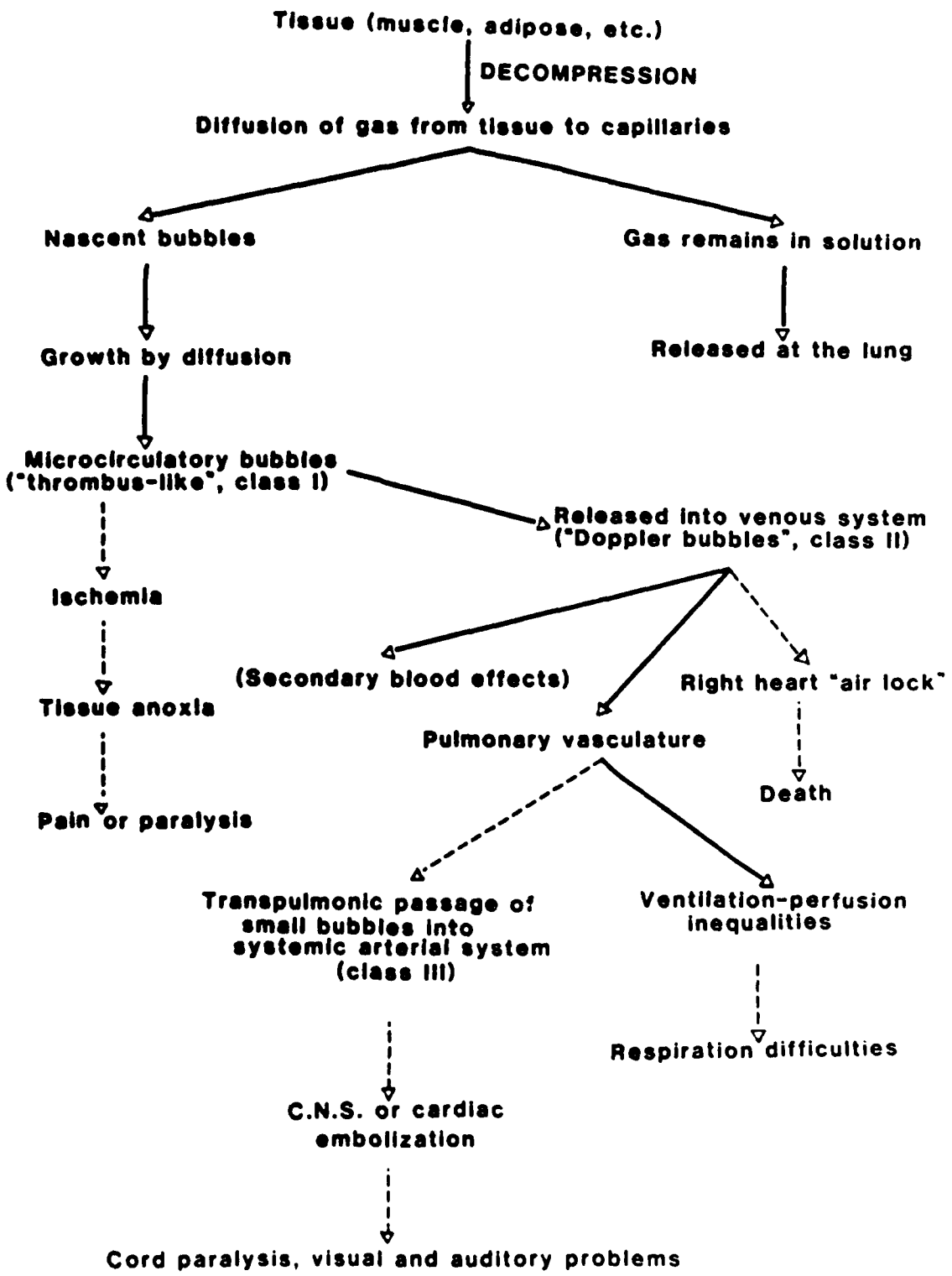

Figure 24. The various pathophysiological consequences of the presence of a gas phase in different anatomical locations of the body following decompression.

incorrect to describe the gas phase. We can also note that a cylindrical gas phase will change its length considerably with a pressure change, this is to be contrasted with the small diameter change of a sphere with pressure. If a cylindrical gas phase was to grow to the poit of a bifurcation of the arteriolar tree and block adjacent blood vessels, small pressure changes could cause it to retreat sufficiently to reopen the occluded channels thereby relieving anoxia.

Unquestionably, stagnation anoxia would result from the intravascular gas occlusion. Whether this would result in the pain as indicated in Figure 24 is, presently, only speculation.

As stated above, the preponderance of the gas phase which forms is not in tissues associated with limb-bend decompression sickness (adipose, for example). When these are released into the central venous system, they account for the majority of gas bubbles (this time, round) which are detected by Doppler precordial detectors (Class II). When in limited quantity, they appear to produce negligible pathological consequences, although they are no doubt, associated with some of the reported blood-bubble interactions.

Large quantities of gas will result in an air lock in the right heart with death following. This "decompression death" is the principal effect noted following decompression in small rodents, and its association with "limb-bend" decompression sickness in these subjects must be treated with great reservation.

In lesser quantities, ventilation-perfusion inequalities result in dyspnea is observed. The quantitative effect of the shunting on inert gas elimination is at present not known.

We have detected passage of inert gas bubbles into the systemic arterial circulation in both sheep and rats following deep hyperbaric exposure (160 fsw) followed by decompression in which the stops have been eliminated. (This is to be contrasted with rapid decompression where "burst lung" can occur.) Right ventricular systolic pressures were not necessarily found to be elevated more than 30% above the pre-dive value before the systemic bubbles were found in sheep in these inadequate decompressions. The transpulmonary passage of gas bubbles appears to be associated with both bubble size and pulmonary artery pressure. In that these arterial bubbles could be associated with visual and other central nervous system problems, the mechanism of trans-pulmonic passage needs further research.

2. Precordial Monitoring and Decompression Sickness

An easy method of treating precordial data appears to be by the scheme of a "grading system". The more subtle this scheme, the greater predictive value appears to be. One which has been developed over the past several years at the Institute of Applied Physiology and Medicine is a refinement of the earlier system of Spencer and Johanson (1974). This represents a fairly workable system, we believe, for both human and animal diving subjects. It is similar at

the O-IV grades to allow conversion of data from earlier work.

PRECORDIAL GRADING SCHEME (Powell and Smith)

GRADE	CHARACTERISTICS
0	No bubbles can be detected
I	Bubbles/cardiac cycle less than 1
II	Bubbles/cardiac cycle = 1
III	Bubbles/cardiac cycle much greater than 1
IVa	Bubbles heard throughout cycle, and -- numerous but discrete, or
IVb	-- numerous but not discrete
V	Individual bubbles not discernable, flow sound louder than cardiac motion sounds

Granting that we are in reality detecting gas bubbles from a large number of tissues of the body, it is proposed that what we are in fact physiologically measuring in bubble detection is the "whole body cavitation tendency" at approximately the time of listening, (that is, they must be both formed and released). This "cavitation tendency" in conjunction with tissue gas uptake and elimination rate will determine gas phase formation in any given region. It is by no means certain that this so-called "whole body cavitation tendency" will necessarily reflect the cavitation tendency in any given micro-region. Indeed, the fact that we can only get a probability of "bends outcome" as a function of bubble grade would seem to argue that this is not always the case.

We can view the process of Doppler bubble detection by considering two possible extremes; these are illustrated in Figure 25. Here we see that at one extreme local problems could be the result of all of the gas phase which is formed remaining in the micro-vasculature and no bubbles would be detected in the venous drainage. The other extreme would be that the formed gas phase is totally released with no local problems resulting; in this case many Doppler-detectable bubbles would be observed when there were no "bends". As is generally the case, the real world lies between the two extremes.

In many cases a prediction of dive outcome is possible because a percentage of the locally formed bubbles are released, and it appears that we can get a "downstream" view of what is occuring "upstream". "Upstream" we can expect bubble formation in "critical tissues" and reduced inert gas elimination (Powell, 1973). (We should realize that in detecting bubbles in the pulmonary artery, the final venous confluence, we are much like the drunk searching for a dime under a street lamp. While he has lost the coin in the alley, he is out on the street "because the light is much better there".)

Some experience gathered by various groups over the years and analyzed by Dave Johanson (Powell & Johanson, 1978), has indicated that predictive use can often be made of precordially detected bubbles. The "dive outcome vs. grade" is given in the next several tables. These are composites of both old and recently collected

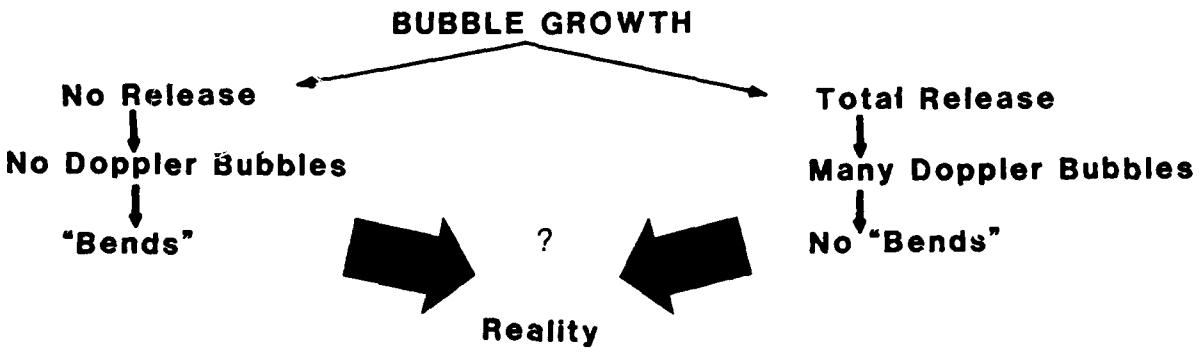

Figure 25. Depiction of two extremes in Doppler bubble detection. The left-hand side shows that the worst case would be a complete accretion of all autochthonous bubbles. The result would be "bends" without Doppler bubbles. The right-hand side depicts a total release of the tissue gas phase such that many Doppler bubbles could be detected and "bends" would not occur. Reality appears to fall in middle ground. While much of the gas phase remains in tissue to probe symptoms of limb-bend decompression sickness, enough bubbles are released to give evidence of its presence. The success of the Doppler monitoring technique depends upon the absence of a strange prevalence for either side.

data and have been amalgamated into the newer grading system. What is emphasized here is that to compile the data in these tables, the "dive outcome" has not been altered by treatment of the subjects or by changes in the decompression schedule. With animal subjects, this is, of course, fairly easily accomplished, while with human subjects it requires monitoring of subjects without a change in the decompression protocol. This is easily done, for example, during decompression table development. These findings are then retrospective. Air dives with pigs and sheep are given in Table II. The symptoms, or dive outcome, are given only as "none" or "mild" as a composite study in animals has not yet yielded better refinement. A similar probability table for helium or neon with pigs is given in Table III. For human divers, a compilation of data for air (from: Spencer and Johanson, 1974; Neuman, et al., 1976) is shown in Table II, and for helium or neon (Powell and Johanson, 1978), is given in Table III. It is obvious from these tabulations that a prognostication of dive outcome cannot be made on the basis of simply "listening for some bubbles."

Whatever use can be made of doppler ultrasonic bubble detectors will come from combined experience in diver monitoring with retrospective observation of the dive outcome until better probability tables can be made. It can be observed that, on the basis of the tables, the value of "N" was seldom greater than 15, and this situation needs to be improved.

For purposes of prediction, in sheep at least, it does not appear that monitoring of certain veins, for example the right and left femoral, provides any better results than the easier precordial monitoring. There is a close parallel between bubble grade in an individual vein and the pulmonary artery, the confluence of all of the veins.

An example of monitoring several long deep dives with human subjects is shown in Figures 26 and 27. These are the "Access" series (Hamilton, et al., 1974) performed at the Union Carbide Laboratories in Tarrytown. The solid circles indicate the times of monitoring when zero to grade II bubbles were detected. The open circles indicate monitoring sessions in which Grade III and IV bubbles were found. Arrows indicate the points at which decompression sickness occurred. We note again, that problems occurred on Grade IV.

(M.R. Powell)

TABLE II

AIR DIVES (HUMAN)

LIMB BENDS / BUBBLE GRADE	NONE	MILD	MODERATE
0	100% (n = 85)		
I-II	88% (n = 30)	12% (n = 4)	
III	60% (n = 9)	33% (n = 5)	7% (n = 1)
IV	67% (n = 14)	14% (n = 3)	19% (n = 4)

AIR DIVES (Pig and Sheep)

BENDS OUTCOME / BUBBLE GRADE	NONE	MILD
0-II	100% (n = 5)	
III	100% (n = 5)	
IVa	90% (n = 9)	10% (n = 1)
IVb-V	38% (n = 12)	62% (n = 20)

TABLE III

HELIUM OR NEON DIVES (Human)

LIMB BENDS / BUBBLE GRADE	NONE	MILD	MODERATE
0	100% (n=1)		
II-I	93% (n=13)		7% (n=1)
III	73% (n=8)	9% (n=1)	18% (n=2)
	39% (n=9)	13% (n=3)	48% (n=11)

HELIUM OR NEON DIVES (Pig)

BENDS OUTCOME / BUBBLE GRADE	NONE	MILD
0-II	100% (n=1)	
III	100% (n=9)	
IVa	89% (n=8)	11% (n=1)
IVb-V	25% (n=3)	75% (n=9)

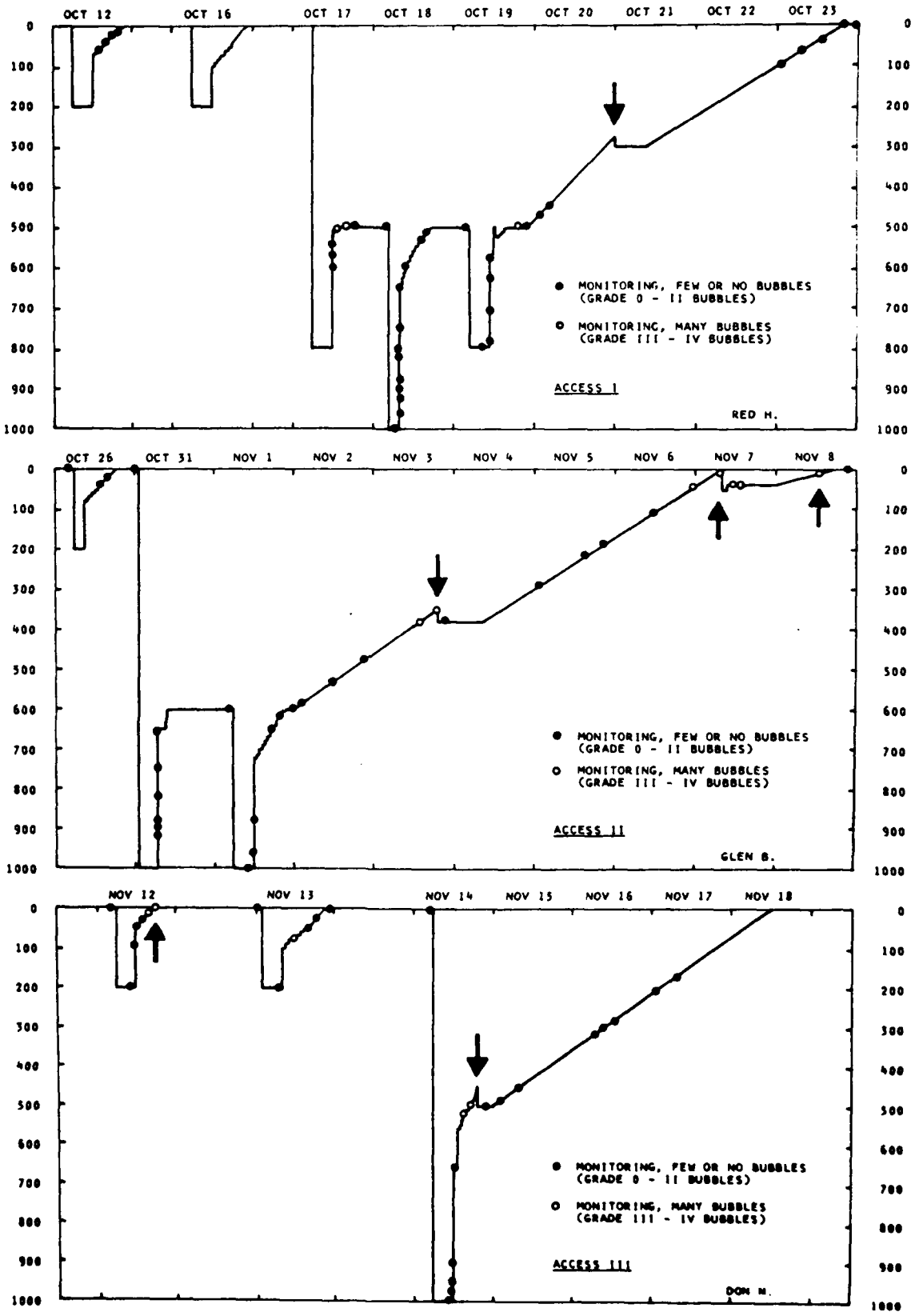

Figure 26. Doppler monitoring during the "Access" series. Circles indicate times of monitoring; arrows indicate points of decompression sickness.

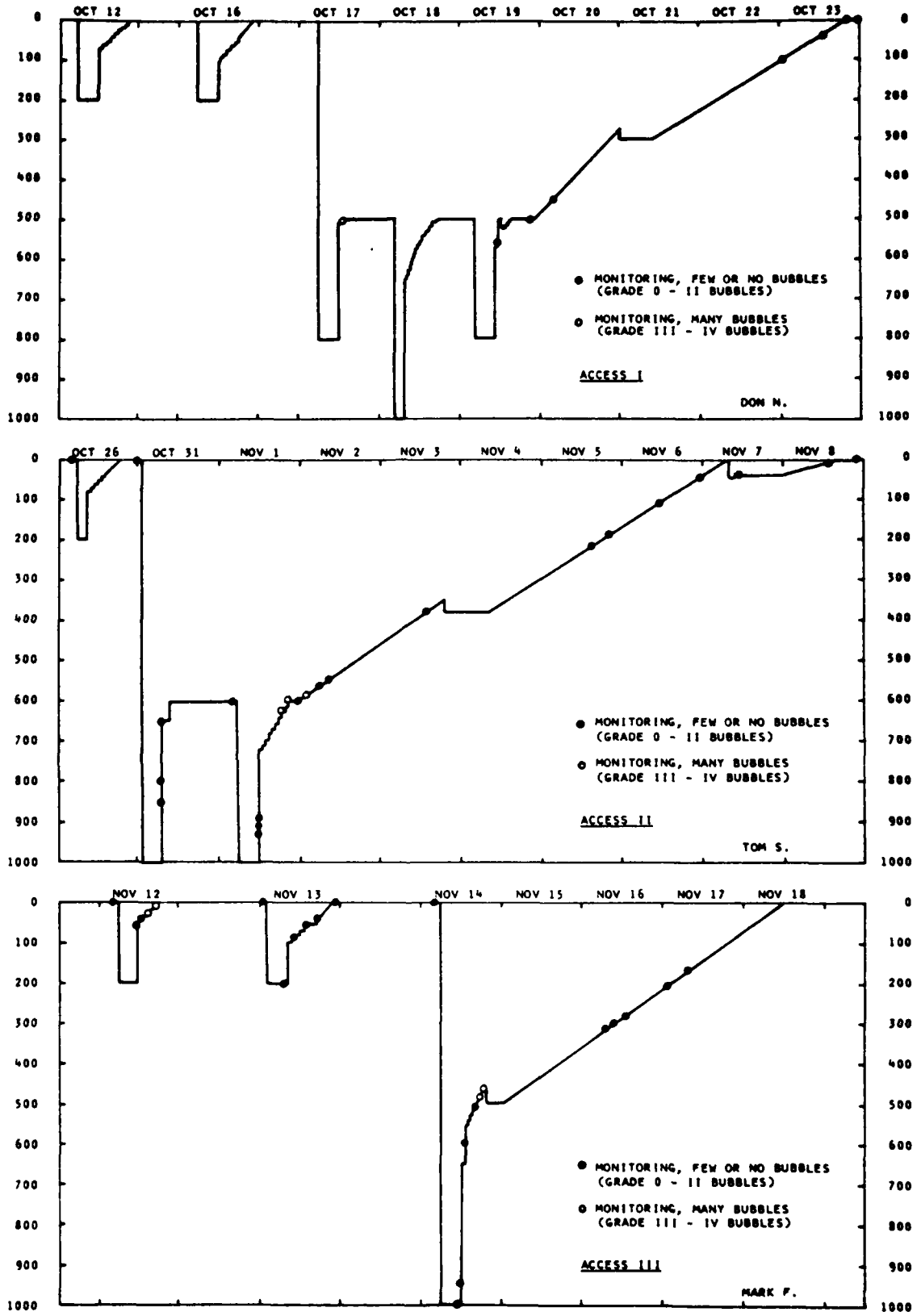

Figure 27. Same as previous figure.

B. DETERMINATION OF OPTIMUM SATURATION DECOMPRESSION SCHEDULES USING DOPPLER ULTRASOUND AND A CALIBRATED VENOUS GAS EMBOLI SCALE

1. Introduction

Our preliminary experiments have demonstrated the practical use of Doppler-detected blood bubbles as an index of proper decompression from saturation and the determination of whole-body tissue outgas half-times in sheep. Our purpose has been to show the effective use of Doppler ultrasound in detecting saturation decompression venous gas emboli and its practical application for investigating controlling tissue half-times in human saturation decompression.

Controlling tissue outgas half-times were investigated in sheep for 100 fsw saturation exposures. By monitoring Doppler-detected bubbles in the pulmonary artery, the longest controlling tissue half-time for sheep (36.3 & 37.6 kg) was determined to be 120 minutes. This half-time value is a result of controlling the decompression schedules to give no greater than a grade II bubble rate throughout the decompression.

An electronic bubble counting technique (discussed in the next section) was designed and used to quantitate large numbers of pulmonary arterial bubbles and to define, in terms of those numbers, traditional clinical bubble grading.

2. Methods

Two sheep were used for the 5 experiments represented in this section each having had ultrasonic transducers of the Spencer hemicup design surgically implanted on the pulmonary artery proximal to the bifurcation. Blood flow velocity and audio flow signals from the Doppler were recorded by an Offner 8 channel strip chart recorder and a TEAC 4 channel reel-to-reel tape deck.

Bubbles detected by the Doppler electronics elicited an increase in audio signal amplitude accompanied by a noticeable strip chart pen deflection above the flow recording. This allowed for easy counting of bubbles if they occurred at less than 5 bubbles per second. If the bubble rate was higher than 5 per second another electronic method, based on zero crossing measurements, was employed.

Saturation of the animal commenced during the evening, and decompression was initiated at 8 a.m. the following morning. During the exposures the chamber was vented for approximately 60 seconds every 10 minutes.

The first exposure was made at 100 feet for 12 hours. The saturation profile used for all other exposures is shown in Figure 28, and will give 98% saturation to a 252 minute half-time tissue. (although the 120 minute tissue is slightly supersaturated at the end of the 16 hour exposure (0.13 fsw) we feel that this supersaturation is negligible.) The rational behind this profile change was to make certain that all bubble contributing tissues with relatively longer half-times (120 to 240 minutes) would be 98% saturated. We

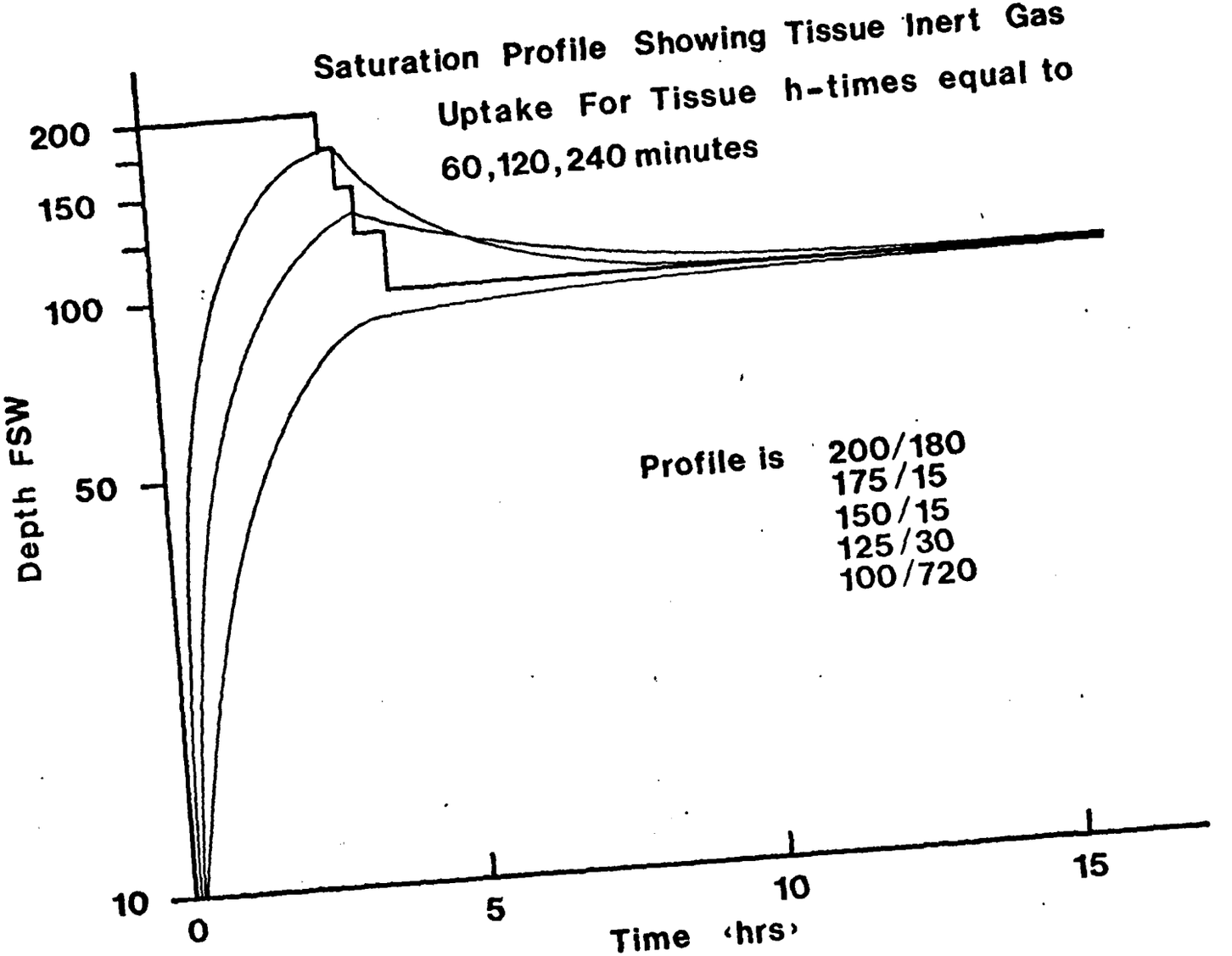

Figure 28. Accelerated saturation schedule used during the sheep saturation studies.

arbitrarily assumed that no contributing tissue half-time would be longer than 240 minutes.

In planning the compression profile, we have assumed that the uptake of inert gas by the tissue follows:

$$Y = D_c (1 - e^{-kt})$$

where k is equal to the tissue half-time constant, t is post compression time, and Dc is equal to the depth to which the body compressed. Tissue depth (Y) can be calculated at any time during the compression phase of the saturation exposure using this formula.

The elimination of tissue inert gas follows:

$$Y = D_{dec} (e^{-kt})$$

where all variables retain their previous meanings with the exception that D dec is the depth from which the body is decompressed and t is post decompression time. This equation is used to plot tissue depth for a given decompression schedule and again can be used to calculate tissue depth at any time during decompression.

Five separate exposures were made with 2 decompressions according to controlling tissue half-times equal to 60 minutes; two decompressions according to half-times equal to 80 minutes; and a single decompression according to a half-time equal to 120 minutes. As can be seen in Figures 29 through 31, decompression always started with an initial 50 foot depth change with successive stops of no greater than 10 foot changes and always 5 foot changes after the 25 foot stop. The stops were drawn in a fashion so that the half-time sloop line bisected (or nearly so) each decompression stop. Enough stops were made to bring the tissue depth below the calculated surfacing pressure (Spencer, 1976) with the exception of the last exposure.

3. Results

The criteria used to determine the controlling tissue half-time was a bubble rate equal to grade II. Referring to Table IV, Jeannette developed a no greater than grade I bubble rate when decompressed according to a procedure designed around a 60 minute half-time. During the third dive both animals were exposed at the same time and decompressed according to a procedure designed around a tissue half-time equal to 80 minutes. Jeannette bubbled less than previously and Kathy had severe bubbling (Grade III) which required treatedment on oxygen (30 feet for 30 minutes). Kathy was re-exposed two days later and decompressed according to a half-time equal to 120 minutes. Throughout the decompression procedure, her bubble rate was less than grade II, comprised mainly of grade I showers and occasional periods of grade 0. She was decompressed to the surface before reaching her calculated

surfacing pressure at which time her bubble rate increased to grade III. It was then necessary to treat her on oxygen at 30 feet for 30 minutes. In both instances, treatment on oxygen alleviated the higher bubble grade leaving a bubble grade of I.

The tabulated data below concisely shows these experimental results. Jeannette shows a marked reduction in bubble grade between the 60 and 80 minute half-time profiles. Kathy exhibited this same reduction from grade IV to grade II between her 80 minute and 120 minute half-time profiles.

Table IV

sheep weight (kg.) \ half-time (min)	60	60	80	120
Jeannette (9-27) 37.6 kg	I	I	I	
Kathy (9-28) 36.3 kg			IV	II

4. Discussion

Decompressions from 100 foot saturation exposures on air can be safely and efficiently done with an initial 50 foot reduction in pressure followed by the exponential decompression. The decompression stops less than 10 feet are necessary to prevent dangerous gas phase separation defined such that the decompression schedule allows the pulmonary bubble grade to become greater than grade II. At least in the case of sheep, we have found that the grade II is an optimum bubble grade with regard to safe and quick decompression. Stops below 10 feet allow a continuous pull on the tissue which brings the tissue depth below the surfacing pressure much quicker without the sudden release of a large volume of a gas phase.

When comparing bubble rate vs. decompression profile (Figures 29-31), the venous gas emboli rate becomes constant when the excess pressure gradient becomes constant for the limiting tissue. In the five studies performed, it was determined that a tissue half-time equal to or less than 120 minutes will satisfy safe and efficient decompression for sheep in the 40 kg range.

5. Conclusions

We feel that a viable and practical means of determining optimum

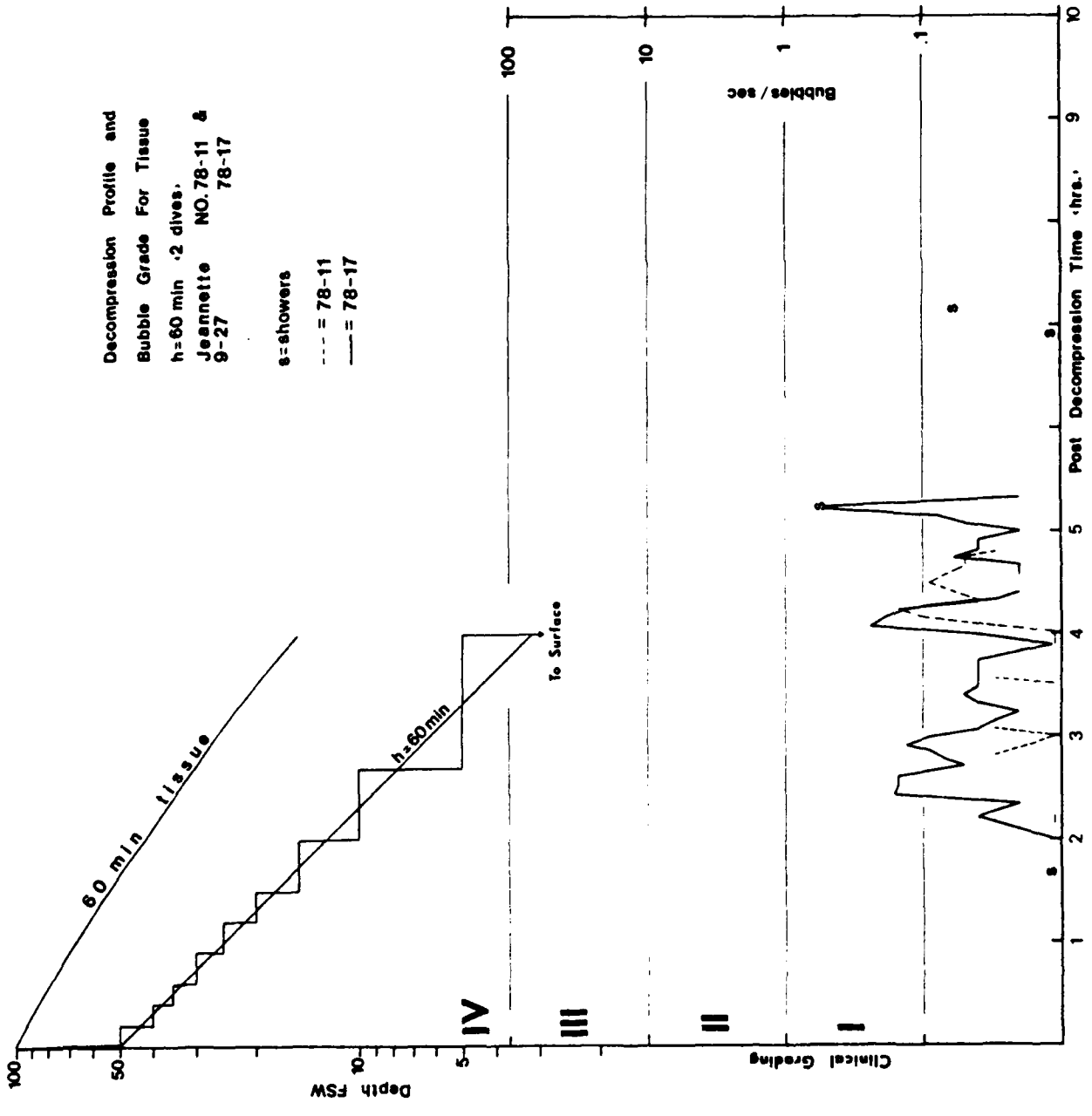

Figure 29. Saturation decompression schedule calculated gas tension (in FSW) in the 60 minute tissue and number of gas bubble detected in the pulmonary artery of sheep.

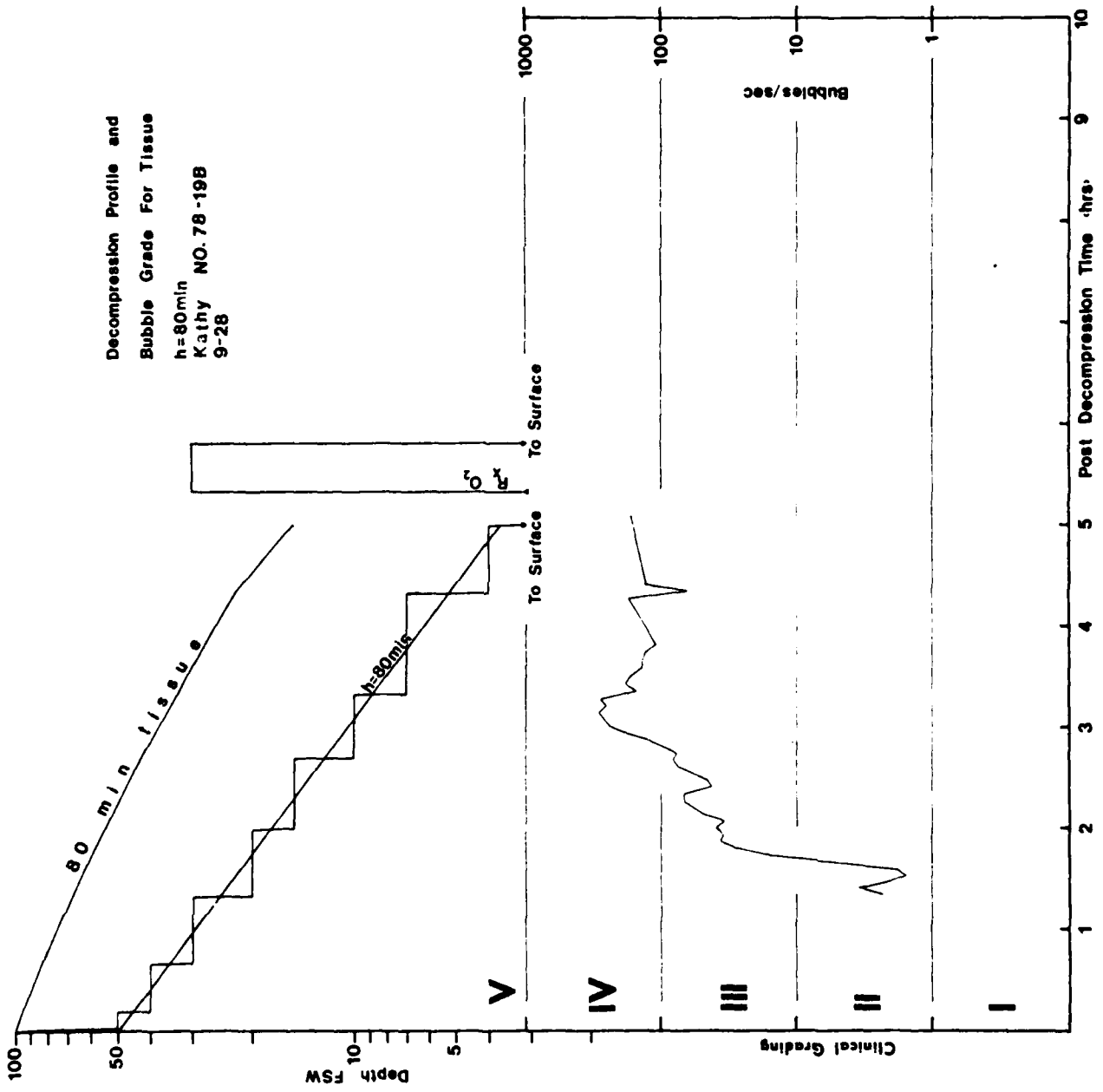

Figure 30. Saturation decompression schedule, calculated gas tension (in FSW) in the 80-minute tissue and number of gas bubbles detected in the pulmonary artery of a sheep.

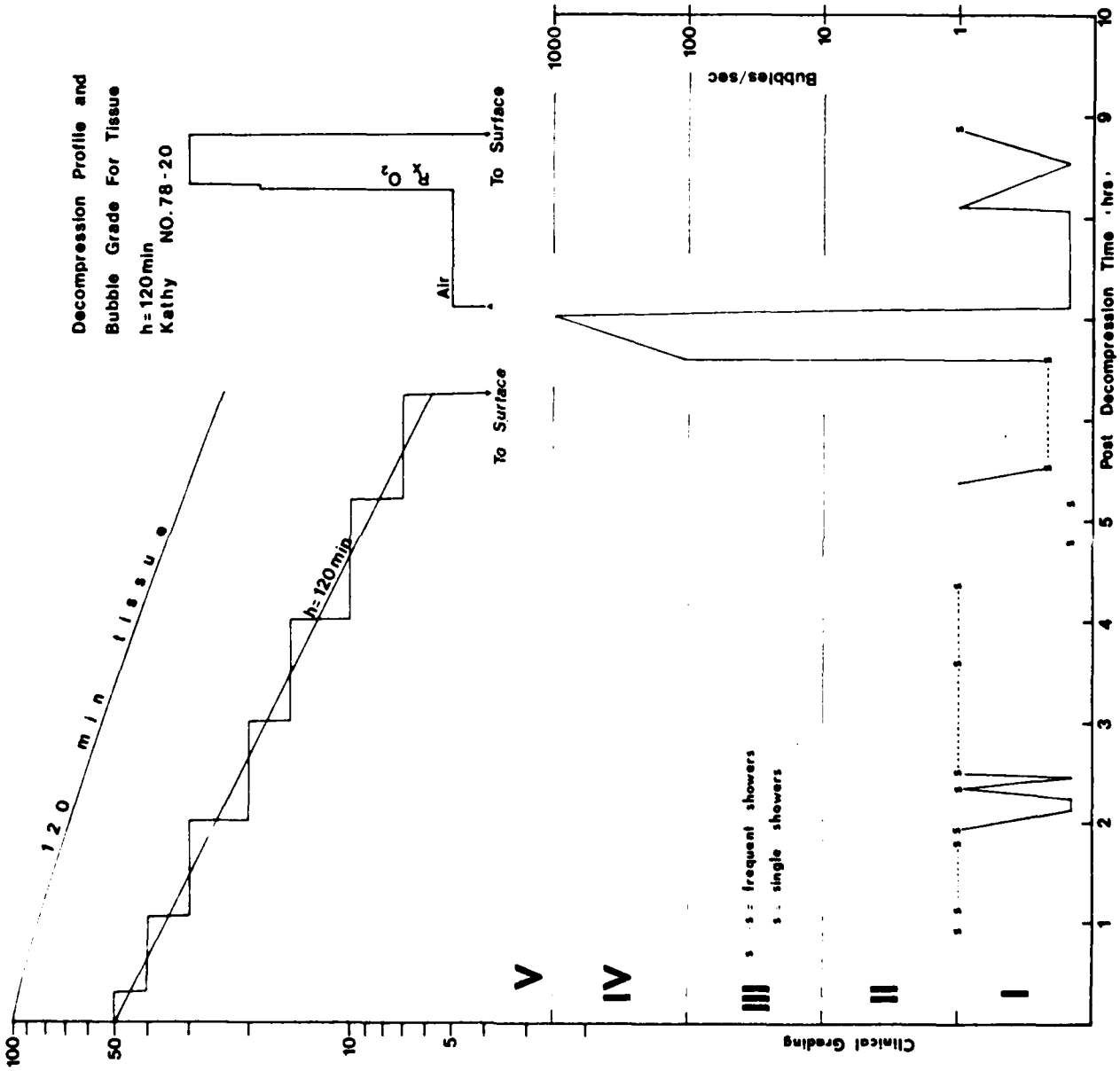

Figure 31. Saturation decompression schedule, calculated gas tension (in FSW) in the 120 minute tissue and number of gas bubbles detected in the pulmonary artery of sheep.

decompression schedules from saturation decompression conditions has been developed. The major advantages of this type of a decompression system as opposed to strict adherance to tables are:

(1) The ability to "tune" a decompression schedule to an individual eliminates ambiguities inherent in "standard" decompression tables. Removal of these ambiguities reduces the occurance of dangerous gas phase separation or decompressions that are too long.

(2) Having an online system to monitor bubbles in the blood during decompression allows a real-time update of whole-body tissue outgas status.

(3) A model based on biological feedback instead of mathematics has been used to design safe decompression procedure.

(M.T. Smith)

C. ELECTRONIC COUNTING OF DOPPLER BUBBLE SIGNALS

1. Introduction

In conjunction with our saturation studies, we have developed an electronic bubble counting system in order to alleviate the long data reduction time involved with each experiment. The system measures the audio output of the Doppler signal for zero crossings above a variable threshold.

2. Methods

The threshold is adjusted above the cardiac signal. This "above threshold" signal is inputted to a multi-channel strip chart recorder, can be used on-line (real time), or can analyze audio recordings made on magnetic tape. Pen deflection above the base line occurs when audio bubble artifacts drive the Doppler signal amplitude above the threshold. The height of the pen deflection is relative to the number of zero crossings measured and therefore related to the number of bubbles passing within the Doppler transducer beam. The number of zero crossings occuring above the threshold is dependant upon the audio gain of the input signal. Therefore, it is critical to maintain the same audio gain between recordings. In the case that this audio gain is changed, it is necessary to recalibrate the system. Zero crossings are measured and displayed on a digital meter.

3. Calibration

A section of tape containing cardiac and bubble sounds is replayed, where the number of bubbles per cardiac cycle (found to be between 0 and 7 bubbles per cardiac cycle) can be manually counted by listening to the audio recording. The number of bubbles per cardiac cycle is recorded with the concomitant hertz measurement displayed by the digital meter. A plot of hertz (ordinate) vs. number of bubbles (abcissa) is made, and a least squares fit program* is run to determine the slope of the line intersecting these points. The slope of the line is then taken to be the number of cycles per bubble. It is then possible to replay the audio recording through the frequency measuring system and dividing the digital display value per cardiac cycle by the number of hertz per bubble to obtain bubbles per cardiac cycle. Figure 32 illustrates the system.

4. Discussion

With only a moderate amount of experience (1/2 - 1 hr.), an operator can become confortable enough with the counting technique to analyze audio signals containing bubbles. There are, at present, some unresolved difficulties.

* Hewlett Packard HP-65 Program #STAT 1-22A

Block Diagram of Bubble Counter

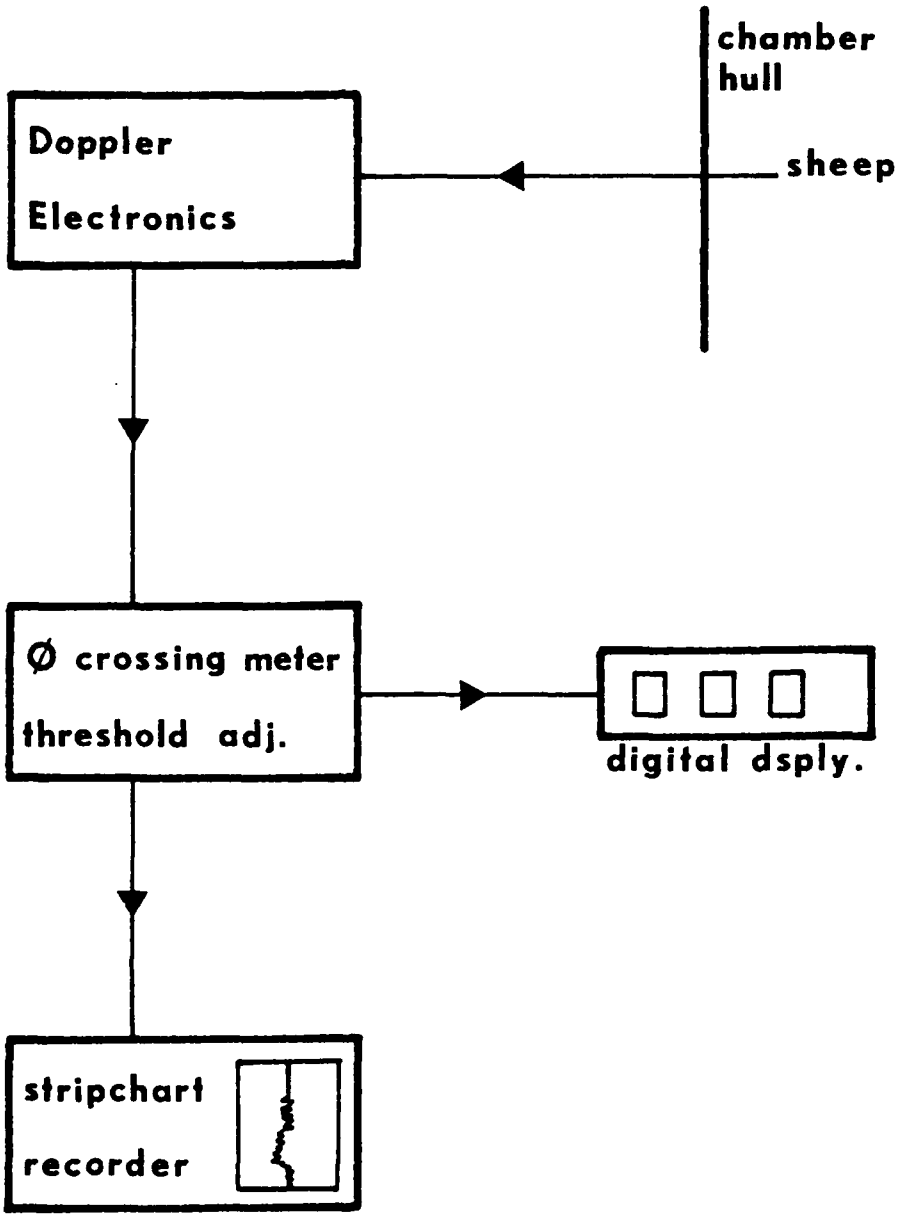

Figure 32

The counter is not designed to selectively count bubbles but rather all zero crossings above the threshold including electronic noise. The operator must use his discretion as to which measurements may have electronic noise artifacts. In addition, because the counter has no automated output of hertz measurements, it is necessary for the operator to manually annotate these measurements. This makes it practically impossible to maintain real-time analysis except for individual calculations at a sampling rate greater than 1/minute. Future systems will be automated and able to eliminate noise artifacts.

A revised form of our clinical bubble grading scheme in terms of bubbles counted by our system appears below.

Clinical Grade	Definition	Bubbles/Second
0	no bubble artifacts	0
I	1 VGE/heart cycle	1
II	1 VGE/heart cycle	1-10
III	1 VGE/heart cycle	10-100
IV	numerous but discrete	100-1,000
V	masks heart sounds	>1,000

The calculated numerical bubble rate models a logrithmic progression rather well. Grades 0 to IV each represent an absolute bubble number one decade higher than the next.

Grade V (1,000 bubble/second) has not been adequately measured, and it may be that Grade V shares the upper end of the Grade IV decade.

(M.T. Smith)

III. PULMONARY EMBOLISM STUDIES

A. BACKGROUND

The gross manifestations of pulmonary gas embolism are rarely seen in diving medicine. Cases usually only follow emergency situations in which a major violation of proper decompression practice has occurred. However, since the advent of Doppler bubble detection devices (Spencer and Campbell, 1968; Gillis, et al., 1968), it is evident the gas bubbles occur in many decompression situations not resulting in decompression sickness. What effects this pulmonary air embolization, long and short term, could have on a diver is unclear.

Much of the background for gas embolization in the pulmonary vasculature following diving comes from earlier research done in which air was introduced into the circulatory system at one atmosphere.

It is well known that there is an important relationship between the rate of injection of air and the time necessary to produce death when air is administered intravenously. Harkins and Harmon (1934) determined that the minimum lethal dose of intravenous air in the anethetized dog was approximately 8 cc/kilogram of body weight when injected within 20-30 seconds. Extrapolating to an adult, that would be about one-half liter of air in the 20-30 second period. In that injection of such a large volume in such a short period of time is difficult to imagine, the consequence of smaller amounts over a longer period of time was examined by Richardson, Coles and Hall (1937). They fould there existed a definite relationship between the rate of injection and the time necessary to cause death, noting that very large volumes of air could be injected if done at very slow rates. One dog, injected at the rate of 0.12 cc/kilogram/minute and weighing 23 kilograms, received 1,377 cc of air before death 460 minutes (7.8 hours) later. Thus, in the dog, air injected at a rate of less than 1 cc/kilogram/minute can be tolerated. Rates greater than 1 cc/kilogram/minute produce a marked decrease in tolerance to the gas load.

In other experiments in which a bolus of gas was injected, (Richardson, Coles and Hall, 1937), pulmonary blood pressure increased from 7.4 to 37 mmHg before death occurred. The right ventricle was greatly dilated and the left ventricle was contracted in systole. Experiments were also performed in which air was injected into unanesthetized free-standing dogs, one receiving 3,910 cc of air with a constant injection rate of 0.033 cc/kilogram/minute over a period of 87 hours before death ensued. When sudden sub-lethal injections of air were made into unanesthetized animals, they noted a pronounced bradycardia, cardic irregularity and water-wheel murmurs. This would occur for several minutes after which the animals would recover. At autopsy, they found air extensively distributed in the vena cava, vessels of the right heart and pulmonary arteries; however, air was never demonstrated in the left heart or systemic arteries. They also noted that the air in the right heart was in a churned-up, frothy state. Lungs were noted to be heavy and edematous with the bronchiols and bronchi containing

considerable quantities of clear, frothy fluid. Lung tissue was found to be markedly edematous with the capillaries being congested. Edema was not noted, however, in dogs which died suddenly. They concluded that small amounts of injected air produced no signs of respiratory or cardiac distress. Large volumes produced evidence of cardiac distress and respiratory embarrassment, but the animal could survive. Larger amounts of gas produced acute cardiac dilation and death, or if the animal did not expire immediately, it would progress to acute pulmonary edema and die or develop bronchial pneumonia and die from otherwise non-fatal pulmonary edema. Furthermore, animals which hyperventilated well could tolerated larger volumes of gas than those whose respirations were much less markedly affected. Noted also was the fact that much less air was fatal to an animal with low systemic blood pressure than one which was normotensive.

Durant, Long and Oppenheimer (1947) made a study of pulmonary venous air embolism with the prime interest of their study being the mechanism of death in air embolism and what life saving measures could be instituted. They noted that an injection of 25 to 150 cc of air into the femoral vein of a dog produced a gallop rhythm and a loud water-wheel murmur, audible even without a stethoscope over the precordium. Tachycardia, tachypnea, cyanosis, and the elevation of the venous pressure followed.

Four factors involved in fatality in experimental pulmonary air embolism were first described by Durant et al. (1947).

(1) The total amount of air injected.

(2) The injection rate.

(3) The position of the animal. (They were the first to note that the dog could tolerate more air when lying on the left side than in any other position. Even animals which demonstrated marked right ventricular failure while lying on their back would frequently recover if turned on their left side. The right lateral position was found to be the worst, and they reasoned that when the outflow track was the most superior portion of the right heart, an air lock developed. This did not follow when the animal was on his left side. It was observed that if an air lock did not form, the air was mixed with the blood forming a froth which was then transported to the lungs where the gas was expelled.)

(4) Animals which developed tachypnea could tolerate larger amounts of gas than those with an unchanged respiration rate.

In open chest experiments, it could be seen that large volumes of gas produced myocardial ischemia, and they hypothesized that the presence of air caused a large increase in right ventricular pressure. In conjunction with this was a reduction in systemic arterial blood pressure. These two factors combine to reduce the aortic-right ventricular pressure gradient thus reducing blood flow in the myocardial muscle with resulting ischemia.

In a parallel study of arterial air embolism, Durant, Oppenheimer, Webster and Long (1949) found that a considerably reduced gas volume was needed to produce effects when in the systemic arteries as compared to the venous system. Air reaching the terminal arterial branches of an organ produced not only mechanical obstruction but also vasoconstriction in that air emboli are strong vascular irritants (Chase, 1934). Thus, ischemic effects are greater than would be expected on the basis of the size of the air embolus alone. Death from arterial air embolism usually resulted from coronary and cerebrovascular involvement.

Niden and Aviado (1956) studied arterial venous shunts which developed following pulmonary embolization. Pulmonary embolization in dogs was produced by glass beads of various known diameters. Immediately following injection of 5 to 8 grams of glass beads, they noted apnea, bradycardia, and hypotension. The terminal signs of this fatal dose of glass beads was a failure of respiration and fall of carotid blood pressure, signs of a massive obstruction of the pulmonary circulation. Early signs of embolization were abolished following vagotomy, but the later gradual and persistent fall in carotid blood pressure occurred despite vagotomy. Blood gas studies in 12 dogs showed a simultaneous fall in arterial carbon dioxide and oxygen tension after embolization. The anoxemia could be prevented by administration of 100% oxygen. This provided a reversal for not more than 30 minutes after which anoxemia occurred again and the animals died in spite of the oxygen administration. This experiment suggested changes in the alveolar capillary circulation, and they investigated the possibility of arterial-venous passages in the lungs which could cause the anoxemia. Glass beads from 60 to 420 micra were injected into the pulmonary arteries, and the beads were recovered from the venous blood leaving the injected lobe by means of a sieve. They noted that:

(1) Pulmonary A-V shunts of at least 420 micra in diameter must exist.

(2) The number of beads passing through the pulmonary circulation was a function of pulmonary artery pressure.

(3) The ventilation of the lungs with 100% oxygen decreased the number of beads recovered while a 10% oxygen mix increased the number of beads recovered.

It was concluded that shunts open either when pulmonary pressure was increased or alveolar oxygen tension decreased.

Their experiments revealed at least three components to pulmonary embolization:

(1) a primary mechanical obstruction to the vessels;

(2) a secondary vasoconstriction which is at first local;

(3) a vasoconstriction which extends to the other lobes.

Stimulation of respiratory depth immediately following embolization was the result of both anoxemia and intrathoracic sympathetic receptors. Thus plumonary shunts appear to reduce the rise in pulmonary artery pressure at the expense of a concommitant anoxemia.

It has been questioned that blockage of the outflow track by gas bubbles is the principal cause for reduced pulmonary blood flow. Vasoconstrictive substances such as seratonin have been implicated (Mustard, et al., 1969; Dolen, et al., 1967). Hartveit, et al. (1968) confirmed that air bubbles were arrested in the terminal branches of the pulmonary artery, but their work with heparinized subjects has cast doubt on the conclusion that the air bubbles per se arrest the flow of blood in the pulmonary circulation. Blood in the right ventricle and the major branches of the pulmonary artery was found to be abnormal in appearance, and they noted that, in the terminal arteriols, bubbles were less frequently found and the smallest vessels contained mainly fibrin. Larger pulmonary arteries contained a network of fibrin and air bubbles while, in the major pulmonary vessels, the red cells were stuck together with strands of fibrin and separated by gobules of fat. They postulated that the air in blood is whipped together in the heart causing the production of fibrin as a result of platelet damage. Their conclusion that death is the result of fibrin present in the pulmonary artery is supported by their finding that prior heparinisation will protect mice from death due to air embolism if the dosage of air is low. This finding may explain the purported effect of heparin on decompression sickness in rodents where death is taken as the end point (i.e., pulmonary embolism). Heparin is ineffective in higher air dosages. Their experiments suggested that the pathophysiology of venous air embolism is similar to that of pulmonary embolism produced by blood clots and that heparin therapy may be indicated in both cases.

Measurements have been made of pulmonary artery pressure, pulmonary arterial wedge pressure, left atrial pressure, cardiac output, systemic pressure in the aorta, pulmonary vascular resistance, and systemic vascular resistance (Berglund and Josephson, 1970) following repeated embolization with air in the dog. Their experiments were performed on anesthetized dogs using an injection of 1 ml/kilogram of body weight with a bolus injection. It was found that within 20 seconds after injection, pulmonary artery pressure rose 140% above control while wedge and left atrial pressure were almost unchanged. There was a 28% decrease in cardiac output and a decrease of 12% in systemic blood pressure. Vascular resistance increased in both pulmonary and systemic systems, 248% in the former and 30% in the latter. All of the changes were temporary and values returned to control levels within 13 minutes. Inter-experimental basal levels were not influenced despite multiple repetitions of embolization. Repeated embolizations yielded results with similar numerical values. Similar effects were noted with plastic bead injections, but the changes were longer lasting, as might be expected, in that dissipation of the embolizing material was not possible.

Embolization studies (Deal, Fieldon and Monk, 1971) on sheep have yielded information on righ ventricular pressures, cardiac output and arterial PO_2 following the rapid injection of a large bolus of

air. Shortly following the injection, right ventricular pressure was found to rise with a concomitant fall in cardiac output. Within less than 10 minutes, cardiac output was quickly regained and right ventricular pressure rose and then returned to its pre-injection level. Arterial PO_2, however, fell precipitously and only slowly started to rise over the period of study. By the use of bubble traps in the aorta, trans-pulmonary passage of large volumes of gas bubbles could be monitored. None were found except in the case of one sheep with a patent foramen ovale.

Spencer and Oyama (1971), using sheep, made a quantitative study of the capacity of the pulmonary system to absorb and eliminate intravenous bubbles of various gases and the maximum tolerable gas dosages which occur before the passage of gas was made into the systemic circulation. Their study was made using three injection rates and three gases: carbon dioxide, nitrogen and oxygen. Maximum increases of right ventricular systolic pressure were seen with nitrogen; oxygen produced smaller increases and carbon dioxide, even at high injection levels, produced but a small increase. Arterial oxygen tensions were decreased most by nitrogen, less by oxygen, and least of all by carbon dioxide injections. With the highest gas injection rates, 0.15 cc/kilogram/minute, a pronounced tachycardia was seen in the nitrogen injection experiments, reaching 42% above control at the end of the injection period, 19% increase with oxygen and 4% increase for carbon dioxide. Arterial oxygen tension decrease through the entire 30 minute injection and began to return to normal at the conclusion of the gas injections. A continuous fall of PO_2 in the systemic circulation was not found. Only at the highest injection rate were systemic arterial bubbles detected by the Doppler ultrasound flowmeter placed on the brachiocephalic artery. This occurred in one of five oxygen experiments and three of five nitrogen experiments. Right ventricular pressure at the time of appearance of arterial bubbles in the oxygen injection experiment was 155% of initial (34.4 mmHg) and in the three nitrogen experiments it was 180-200% of initial (39 , 42 and 45 mmHg). At each of the injection rates, the animals did not exhibit any signs of decompression sickness problems but remained calm throughout the study. In later terminal experiments, however, when large quantities of air were injected, the detection of arterial bubble showers with Doppler flowmeters was quickly followed by paralysis, unconsciousness and death.

In that bubbles are not normally found in the systemic arterial circulation following decompression (Spencer and Oyama, 1971; Emerson et al., 1967; Powell, 1972), it was concluded that the gas was dissipated by solution into the blood or direct passage through the alvealor membrane and into expired area. Nitrogen with its lower solubility is dissipated more slowly than oxygen and carbon dioxide. The rapid recovery to control values of both right ventricular systolic pressure and arterial PO_2 indicate the dissipation of the gas is rapid and continuous, apparently reaching a plateau in the cardio-pulmonary responses where the dissipation rate is matched by the dosage rate although true plateau levels were not reached in their experiments (30 minute injection periods). Spencer and Oyama calculated that a 5% right to left shunt existed following nitrogen

embolization at the 0.15cc/kilogram/minute rate. This they concluded was the most important factor for arterial anoxemia following pulmonary gas embolism. In addition to effecting a reduction in arterial PO_2, these shunts could also provide the passageway for bubbles to enter the systemic arterial circulation. From these experiments, they concluded that death from pulmonary air embolism did not result solely from circulatory obstruction or right heart failure. Nitrogen or oxygen injection levels required to produce vascular overload and passage of gas into the systemic circulation were less than those needed for right heart failure, and death or morbidity from cerebral or myocardial ischemia had to be considered.

(M.R. Powell)

B. RIGHT VENTRICULAR SYSTOLIC PRESSURE FOLLOWING GAS EMBOLIZATION AND VENOUS GAS PHASE CONTENT

1. Introduction

Doppler-shift bubble detectors demonstrate the fact that gas phase formation is a common occurrence in decompressions. The pathological significance of small gas emboli passing to the lungs and, in particular, their part in the arterial embolization often seen following inadequate decompression are important to the etiology of the various forms in which decompression sickness is encountered. This holds true both for human divers and for small experimental animals; this latter group is often subjected to great dysbaric stress which provokes more than the limb-bend decompression sickness for which they are the supposed models.

A quantitative determination of gas phase volume reaching the pulmonary vasculature with ultrasonic bubble sizing has not yet been possible. However, when listening to the large number of audible "bubble events" detectable in the pulmonary artery, either with implanted or transcutaneous Doppler bubble detectors, one distinctly receives the impression that they are listening to a fairly large volume flow of gas. It is sometimes even noted that a "roaring" sound can be heard with Doppler bubble detectors throughout the cardiac cycle following decompression with the animal displaying but minor signs of distress (usually only dyspnea). However, the gross manifestations of pulmonary gas embolism are rarely seen in diving medicine; cases usually follow situations in which a major violation of proper decompression practice has occurred. Gas phase formation occurs in many portions of the body following hyperbaric decompression and generally involves the growth of "bubbles" in the microvasculature which later "bud off" and enter the venous drainage channels; it is the volume of this gas phase in the central venous system which we seek.

2. Experimental Measurements of RVSP Increase with Gas Quantity

This semi-quantitative method to determine the volume of the inert gas (in the gaseous phase) reaching the pulmonary vasculature, is by measurement of the increase in right ventricular systolic pressure (RVSP). The increases in RVSP following hyperbaric decompression were then compared to similar increases following air injection into the venous circulation at various rates performed while the subject was at the surface. The increases in RVSP were the result of a blockage of portions of the pulmonary vasculature by the inert gas emboli. It is assumed that the processes, and thus, the RVSP increases, would be similar whether the gas emboli reaching the pulmonary circulation were either internally (from decompressed tissue) or externally (from a catheter) generated. We are also interested in the relationship between RVSP and the presence of gas bubbles in the systemic arterial circulation.

Subjects used in this study were adult sheep (weight range 55 to 58 Kg). All sheep were unanesthetized and free-standing during the surface air injections. Right heart catheterization was performed by

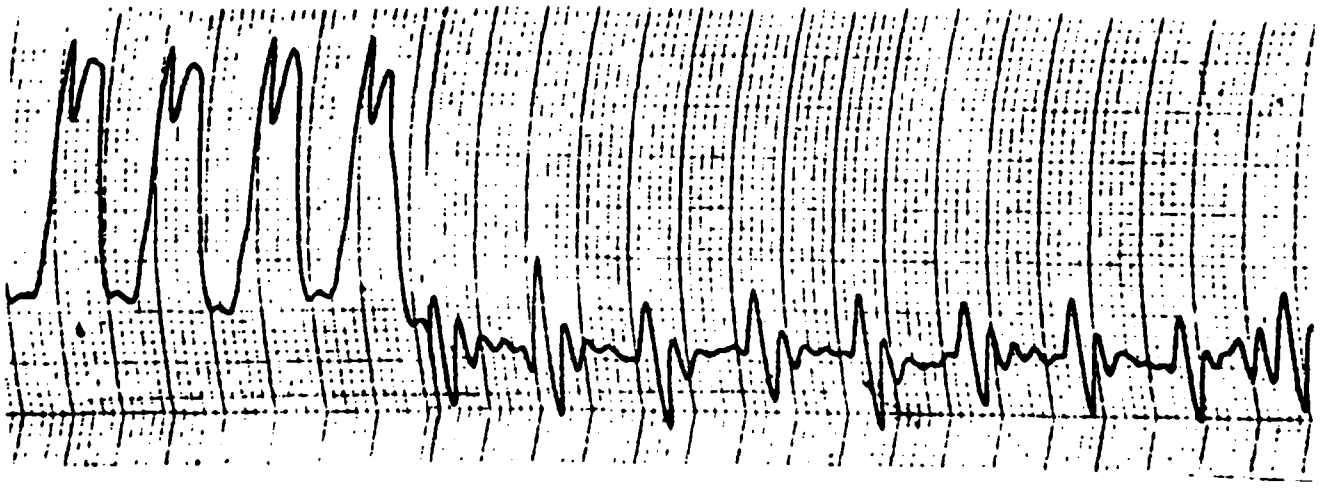

Figure 33. Right ventricular and right atrial pressure waveforms.

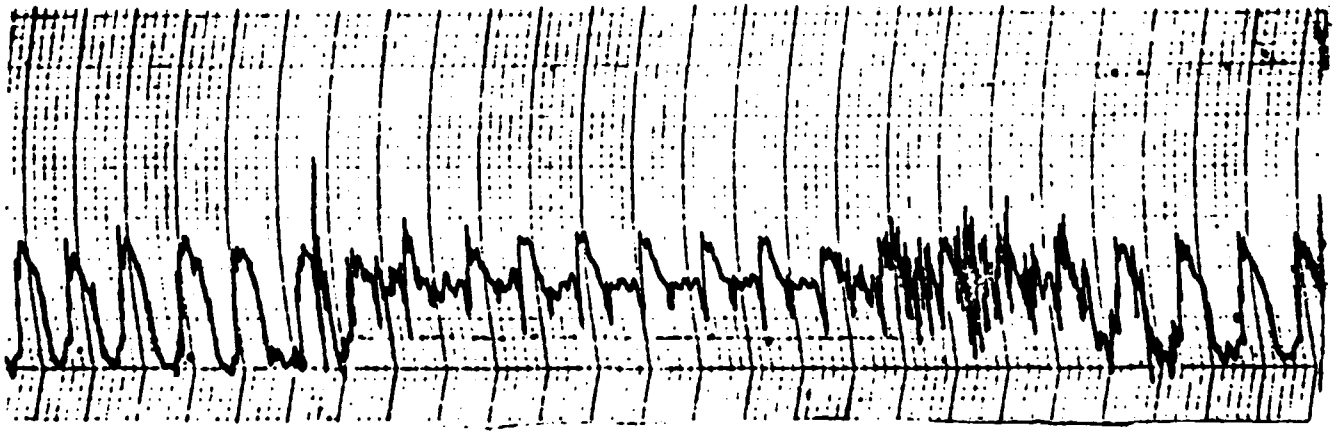

Figure 34. Right ventricular and pulmonary artery pressure waveforms.

passing a #7 Cordis pressure measuring heart catheter down the right jugular vein. We identified the position of the catheter tip by the wave form and the magnitude of the pressure pulses (Figures 33, 34). RVSP in one sheep was also studied by means of a Millar Mikro-Tip Pressure Transducer; measured values were similar to those made with the fluid-filled catheters. "Control" (pre-dive) right ventricular systolic pressures were in the range of 22 to 27 torr. RVSP was recorded on a strip chart, and measurements were taken from initial end-diastolic pressure to the shoulder of the systolic pressure.

The increase in RVSP with gas load was calibrated by injecting air at various rates into five sheep by means of a syringe pump, through a 0.58 mm I.D. catheter inserted into the jugular vein. (Bubbles produced into flowing water by this method were measured by the rate-of-rise method to have radii of 100 to 300 m.) The results of the calibration measurements for sheep are shown in Figure 35 where the maximum increase of right ventricular systolic pressure (percent of control) is plotted against the gas load in units of cc/kg/min.

Calibration data points for our sheep experiments were collected from five different subjects and are indicated by the squares and circles. Data points from an earlier study by Spencer and Oyama (1971) are indicated by the triangles. These triangles are the average of three sheep for each of the three points.

The results of our study on rats are likewise plotted for comparison. In this case, the rats were anesthetized. While qualitatively similar, it shows quantitative differences. We noted that rats often died shortly after the RVSP reached an approximate value of 170% - 180% of control after a proportionately smaller volume of gas as compared to sheep. This may give a clue as to the high percentages of death in rodents following decompression. During none of the surface air injections on either sheep (5 subjects) or rats (10 subjects) were systemic arterial bubbles detected; carotid artery Doppler probes were utilitzed for bubble detection in sheep and visual inspection of mesenteric arteries in the case of rats.

With air injection we found that right ventricular systolic pressures rose following a brief lag and reached a steady-state maximum after 15 to 35 minutes in sheep, and with a shorter time in rats. These steady-state maximum values are the RVSP increases which are plotted in Figure 35. The RVSP returned to the pre-injection pressures with approximately the same time course as the rise to maximum in both species. From this effect we can conclude that the pressure increases are most likely the result of (1) embolic blockage of the pulmonary vasculature by gas emboli and/or (2) reflex vasospasm of the vasculature resulting from irritation. This is contrasted with blockage of the vasculature by fibrin clots generated by the mixing of blood and air in the right heart. The "decrease curve", were this "solid embolis" theory correct, would be expected to be considerably longer than the initial "increase curve". In none of our air injection experiments was this found to be true. Long term injection, however, may result in fibrin clot formation; we have not tested this as yet.

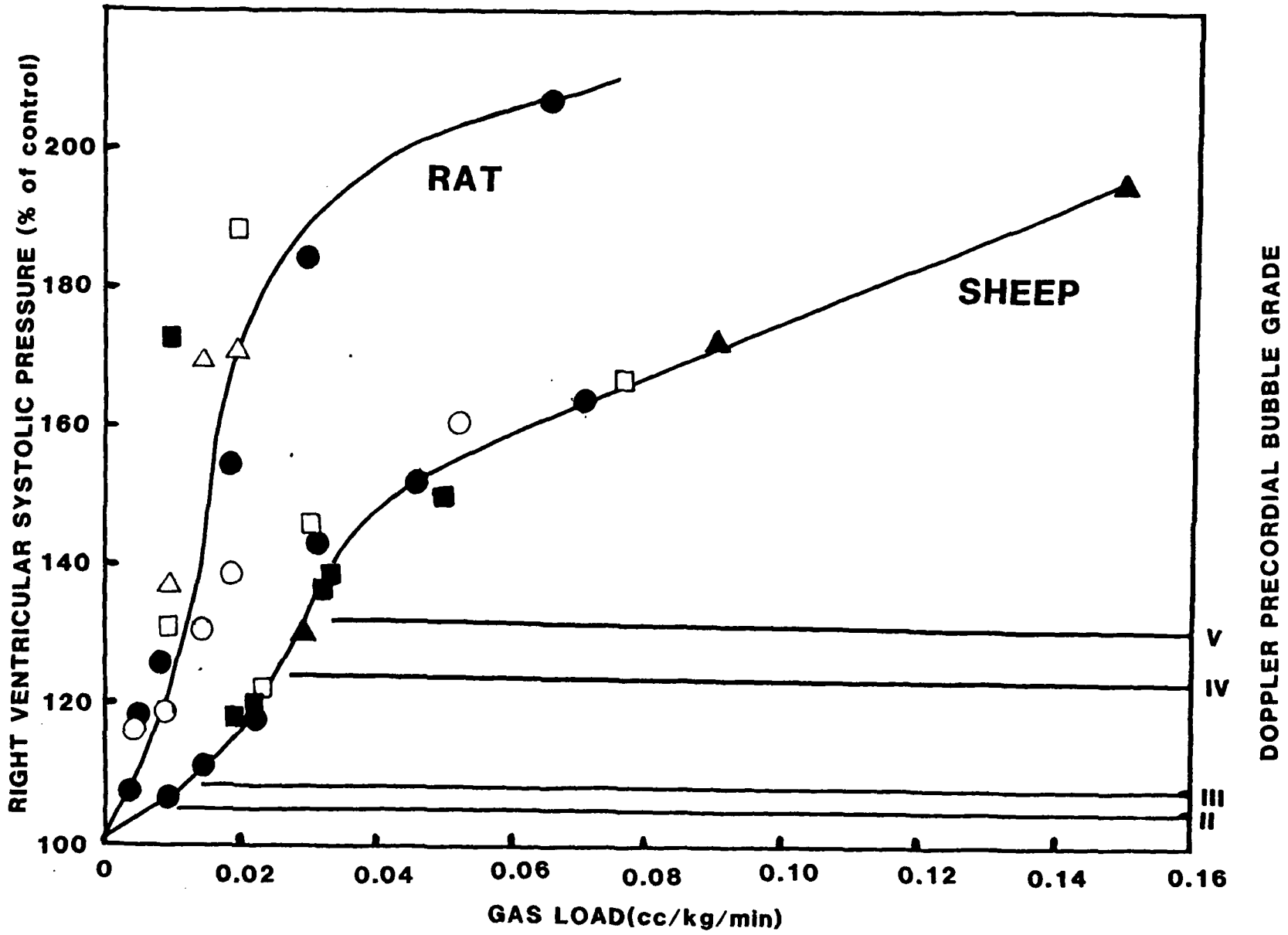

Figure 35. Maximum steady-state increase of right ventricular systolic pressure as a function of gas load. Subjects were sheep and rats. Triangles on the "sheep curve" are from Spencer and Oyama (1971). Average RVSP following hyperbaric exposures is indicated on the right with its conjugate precordial Doppler grade.

3. RVSP Increase Following Decompression

Measurements of the increase in right ventricular systolic pressure following decompression were performed in a manner similar to the air-injection experiments. All dives were made with compressed air and decompressions were made directly to the surface without stops at a rate of 60 fsw/min. Thus, all measurements of the post-decompression RVSP were made at 1 ATA as were the calibration measurements. Averages of post-decompression RVSP measurements are shown in Figure 36.

This increase in RVSP following decompression was also measured in conjunction with the precordial bubble grade. We were thus able to relate the volume of gas embolizing the pulmonary vasculature (in terms of steady-state volumes) with the precordial grade. The results of 22 post-decompression measurements on 7 sheep are given in Table V. We can see the RVSP increases are small even up to Grade IV (124%). These points are also indicated on the curve in Figure 35.

Our sheep generally did not display signs of decompression sickness on air when exhibiting a Grade IV bubble signal; on Grade V the incidence is approximately 80 percent. We can note from air injection and RVSP that "Grade V" is not the maximum amount of venous gas phase which sheep can sustain and live; surface injected sheep display only signs of dyspnea, at least for injection periods of less than one hour.

There is a range for grade V as the precordial Doppler is operating in a "saturated" capacity and simple aural discrimination of "high" and "low" Grade V is not possible in this range. For a very large venous gas bubble load, RVSP measurements whould provide more information than Doppler monitoring.

4. Estimations of Venous Gas Load: A Semi-quantitative Method

Decompressions which do not result in limb-bend decompression sickness produce increases of RVSP on the average of not more than 120 percent, that is, Grade IV and less. From the calibration measurements (Figure 35) this maximum represents a gas load of 0.02 cc/kg/min in our sheep.

On an air dive of 160 FSW for 20 minutes the sheep in this series typically displayed an elevation of RVSP of about 120% of control for about 60 minutes. Insofar as subjects display Grade IV bubbles precordially, a grade generally encountered in cases of limb-bend decompression sickness in both human and animal subjects, it would be of interest to determine the total gas bubble load to the lungs. This, of course, would represent inert gas absorbed during the dive and now released in gas phase from the tissue micro-circulatory system into the major venous channels. For a short dive of this type, we assume that most of the gas is taken up by fast aqueous tissues. Taking the value for the solubility of nitrogen in man as 18 cc/kg./atm, for a 48 kg sheep, the whole body gas uptake would be at least 864 ml/atm at saturation. Empirical measurements of Behnke and Willmon (1941) indicate that approximately 30% of the saturation

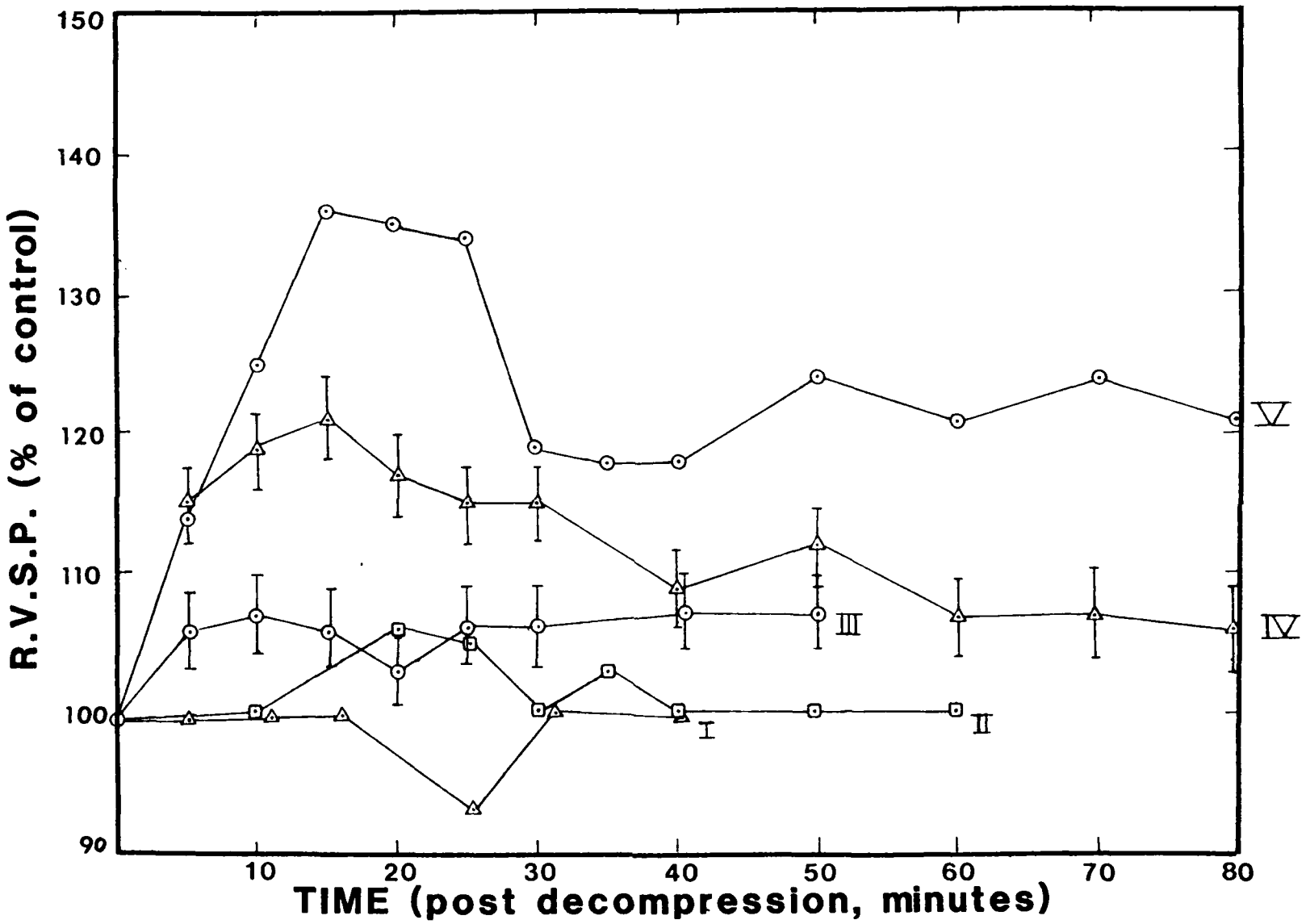

Figure 36. Change in right ventricular systolic pressure with time following decompression. Roman numerals at the right indicate the precordial bubble grade.

TABLE V

RIGHT VENTRICULAR SYSTOLIC PRESSURE

VS.

PRECORDIAL BUBBLE GRADE

Precordial Bubble Grade	Maximal (20-25 minutes) R.V.S.P. (% of control)	S.E.M.	$X10^2$ Gas Load (cc/kg/min.)
II-III	105	2.5	1.0
IV	124	5.0	2.5
V	137		3.5

TABLE VI

PRECORDIAL GRADING SCHEME (Powell and Smith)

GRADE	CHARACTERISTICS
0	No bubbles can be detected
I	Bubbles/cardiac cycle < 1
II	Bubbles/cardiac cycle ≈ 1
III	Bubbles/cardiac cycle $\gg 1$
	Bubbles heard throughout cycle, and
IVa.	- numerous but discrete, or
IVb.	- numerous but not discrete
V	Individual bubbles not discernable; flow sound louder than cardiac motion sounds

gas volume is taken up in 20 minutes. Thus, we can estimate that the typical inert gas load in the body at the start of decompression for this type of dive (160/20) is 1260 ml. with air as the compression gas.

From the calibration curve (Figure 35), a rise in RVSP of 120% of control would be produced by a gas load to the right heart of approximately 0.03 ml/kg/min. The RVSP is elevated typically for approximately 60 minutes. For our 48 kg sheep, this yields a value of 86.4 cc. of gas. Comparing this to the estimated gas uptake load gives 7% of the decompression-released inert gas appearing in the vena cava in the gaseous state.

In that these are moderately severe dives, we could extrapolate this finding and state that gas phase separation, in the body as a whole, is small (5-10%) in "clean" to "limb-bends-only" producing dives. These measurements of the gas phase in the central venous system do not, of course, indicate the degree of gas phase separation in any given organ which, locally at least, may be large. The temporal relation between the formation of the gas phase in the tissue and appearance in the vena cava is presently not known.

Dives which result in evidence of spinal cord involvement may be associated with larger pulmonary gas loads as we have found that bilateral weakness of hind limbs often occurs in our unanesthetized sheep when RVSP increases of 150% are noted. (This was also found by Bove, Hallenbeck and Elliot (1974) on anesthetized dogs.) In typical cases, an elevation of RVSP to 150% is noted up to the point at which sheep are unable to sustain weight on their hind limbs; this is equivalent to a gas injection range of 0.04 to 0.06 cc/kg/min. However, it is a rate which the sheep are easily able to tolerate if the gas is injected, that is, from an external source. When the body tissues themselves are the source of gas bubbles rather than an outside (catheter) source, we note that the effects of a venous gas phase are different with limb-bends resulting. This is most likely the result of the fact that (1) only a portion of the total tissue-gas phase is released into the venous system (a large portion may remain at the local tissue level), (2) there is a reduced regional gas elimination resulting from an increase in arterial inert gas tension from ventilation-perfusion inequalities (also with concomitant arterial anoxemia), and (3) in some cases, there are also arterialized gas bubbles which will embolize various tissues. We wish to point out that hind-limb weakness has also occurred in sheep in cases of RVSP elevations of no greater than 120%.

During none of the surface gas injections were bubbles detected in the systemic arterial circulation in either sheep (5 subjects) or rats (10 subjects). This, however, was not found to obtain following hyperbaric decompression. Carotid arterial bubbles could be found following severe decompression in sheep even at a point when the RVSP was elevated to only 120% of the pre-dive value. Bubbles could also be detected ultrasonically at the arch of the aorta in rats following hyperbaric decompression. They did not necessarily parallel RVSP (See Section IV). It appears that passage of a gas phase through the pulmonary vasculature following decompression is more complex than a

simple increase of pulmonary artery pressure forcing bubbles through either pulmonary capillaries or shunts. We suspect that small size dysbarogenic bubbles (generated most often in the time shortly following initial decompression) and elevated RVSP are functioning in concert (See also Section V).

(M.R. Powell)
(M.P. Spencer)

AD-A093 485 INSTITUTE OF ENVIRONMENTAL MEDICINE AND PHYSIOLOGY S--ETC F/G 6/19
THE PATHOPHYSIOLOGY OF DECOMPRESSION SICKNESS AND THE EFFECTS O--ETC(U)
DEC 80 M R POWELL, M P SPENCER N00014-73-C-0094

UNCLASSIFIED NL

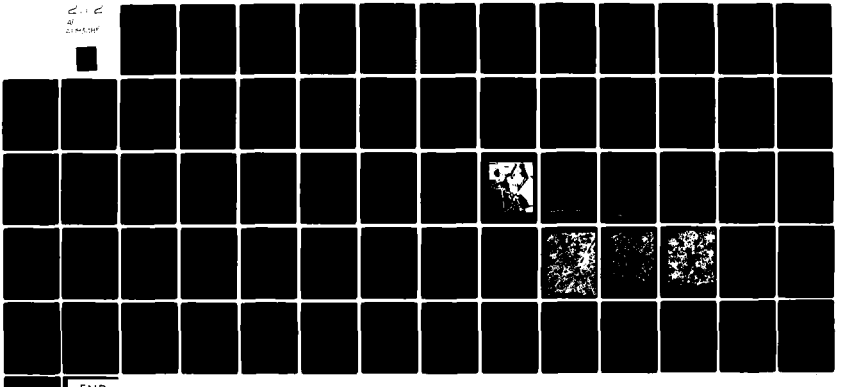

END
DATE FILMED
2-81
DTIC

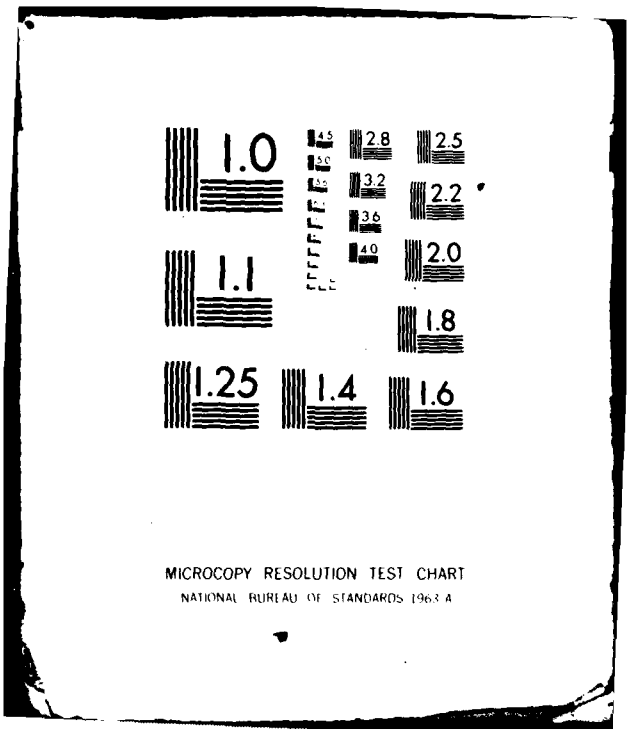
1.0
1.1
1.25
1.4
1.6
1.8
2.0
2.2
2.5
2.8
3.2
3.6
4.0
4.5
5.0
MICROCOPY RESOLUTION TEST CHART
NATIONAL BUREAU OF STANDARDS 1963 A

C. EFFECTS OF PULMONARY GAS EMBOLISM ON THE DEVELOPMENT OF LIMB-BEND DECOMPRESSION SICKNESS

1. Introduction

As was reported in Section II. A. of this report, there is a correlation between precordial bubble grade and the probability that the dive outcome will result in limb-bend problems. There exist several explanations for this effect. There is the possibility that:

(a) the large venous gas phase indicates a high tendency for the body as a whole to cavitate and produce stationary tissue bubbles at that particular time (this "cavitation tendency" is considered in Section II A.), or

(b) the large venous gas phase *per se* is influencing gas phase formation in the tissues, possibly by reducing inert gas elimination at the lungs, or

(c) by opening pulmonary A-V shunts, venous bubbles can produce arterial anoxemia, or

(d) promote systemic embolization by the arterialization of venous system bubbles through increases in RVSP.

2. Methods

To determine if it is possible to initiate, or to exacerbate limb-bend decompression sickness by an increase in the bubble load to the pulmonary vasculature, three sheep (47, 48, and 76 kg.) were first injected with a gas load of 0.03 cc/kg/min through a fine catheter in the jugular vein. Bubbles produced in flowing water by this catheter were measured by the rate-of-rise technique and found to have radii of 100 to 300 μm. With the volumes administered here, this is equivalent to approximately 10^5 bubbles/min. ($r \approx 150$ μm).

These control experiments indicated that these subjects could tolerate this total pulmonary gas volume of 90 (2 sheep) or 137 (1 sheep) cc. for 60 minutes with no untoward effects. The load was chosen as it represents an amount greater than that found in asymptomatic to marginal (that is, Grade IV) decompressions, and yet substantial enough to be just less than the amount found in cases of limb-bends in sheep (i.e., Grade V). The gas load values were determined from previous experiments described in detail in the preceding section.

A "titration" method was chosen for the decompression stress for these experiments. Here, the bottom time is increased and the resulting decompression stress and precordial grade are both noted. We get a spectrum of responses as the tissue gas loads are increased; a suitable end-point can be chosen dependent upon the response required (i.e., minor limb-bend problems, severe limb-bend problems, paralysis, or death). In our series of experiments, we worked in the range of asymptomatic to moderate limb-bend problems.

All dives were made on air to a pressure of 5.85 ATA (160 fsw); decompressions were made directly to the surface at a rate of 18.3 m./min. (60 ft/min). Subjects were observed, at surface, for signs of decompression sickness. Precordial bubble grades were also monitored at approximately 10 minute intervals.

The signs of decompression sickness were as follows:

0 = no observable problems
\+ = uneasy on legs
++ = reluctant to stand on hind legs and lies down
+++ = down for extended period, paralysis on following day.

They were discreet, objective, and easily recognizable signs to allow a clear comparison between the "air injected" and the "non-injected" series. Because a wide range of exposures was employed, it was not necessary to monitor for subtle signs of problems; subtle signs are, of course, often a matter of the observer's opinion. It is necessary, however, to not provoke 3 + signs until the end of the series as these subjects must be eliminated from further trials.

Gas injections were commenced approximately 8 to 15 minutes following the start of decompression; this represents the time needed to bring the animal to surface and to attach the tubing and syringe pump. The time to develop a maximum bubble grade was also approximately 10 to 15 minutes following the initiation of decompression. This is illustrated in Figure 37 and reflects the RVSP curves shown in Section III. B. The air injection period totaled 60 minutes.

In addition to grading the bubbles in the pulmonary artery (by precordial detectors), the relative number of bubbles in the right and left femoral veins were also monitored. An example of this is given in Figure 38 showing the progressive growth and decay of the number of femoral bubbles. The grading system for the superficial veins is as follows:

0 = none detected
1 = infrequent
2 = approximately 1/sec
3 = approximately 5/sec
4 = greater than 5/sec to continuous "whizzing" sound

At the present time, it does not appear that a more effective premonitory method can be devised by utilizing the superficial veins of the legs than by using precordial monitoring. It was, however, noted that numerous gas bubbles could be detected in the femoral veins even when no bubbles were detectable with precordial monitoring. This represents the difference in limits of detectability because of the difference of signal-to-noise ratio between the femoral vein and pulmonary artery.

3. Results

The results of the dives, with and without injected gas, are shown in Tables VII to IX. Within the scope of these gas injection loads, one can conlude that a high gas volume load per se to the pulmonary vasculature does not exacerbate limb-bend decompression sickness.

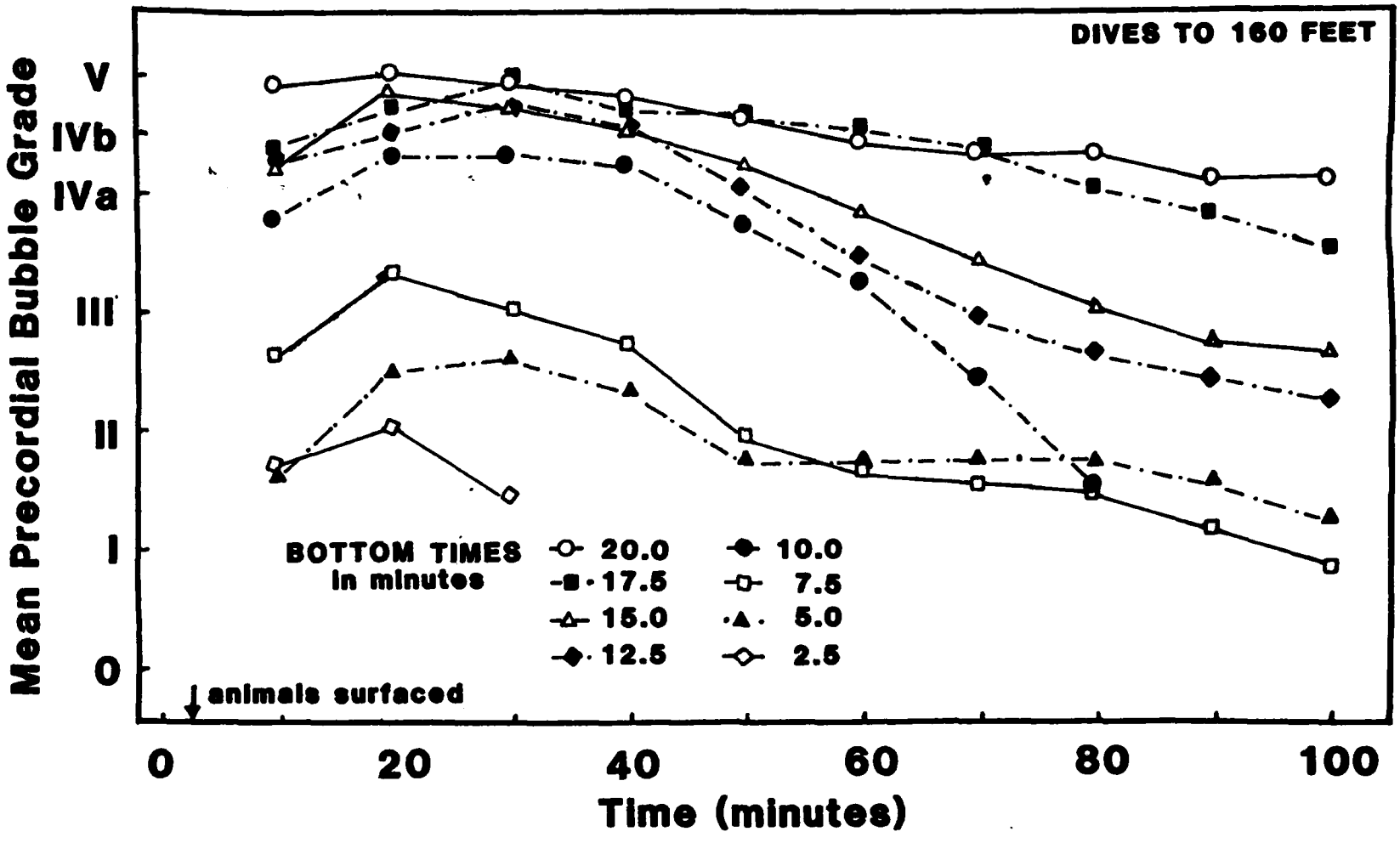

Figure 37. Average growth and decay of precordially monitored bubble grade.

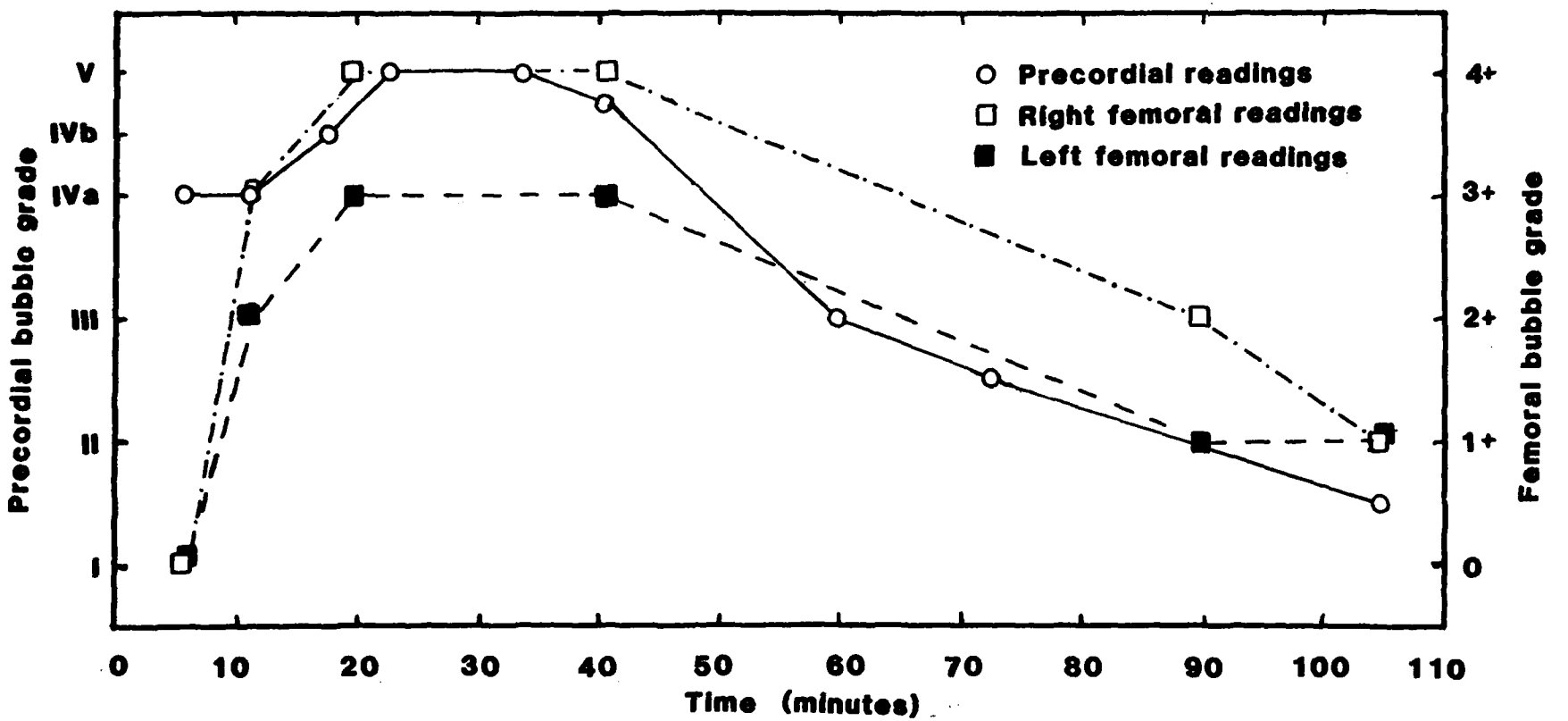

Figure 38. "Femoral Grade," on right, is as follows: 0 = clear, 1 = infrequent, 2 = about 1/sec., 3 >1/sec., 4 >5/sec. to a continuous "roar" in the vein.

TABLE VII

SUBJECT: "MARQUETTE" (#9-18)

DIVE OUTCOME FOLLOWING VARIOUS BOTTOM TIMES, ALL 160 fsw

Bottom Time (minutes)	2.5	5.0	7.5	10.0	12.5	15.0	17.5	20.0
Maximum Bubble Grade	II	II /III*	IVa	IVb/IVa	IVb/V	IVb/IVa	V	V/V/ V
Decompression Sickness	0	0/0	0	+ +/0	0/++	+/++/0	++	+/+/++
Maximum Femoral V. Grade	-	0/3	-	-/-	-/4	-/4/4	4	4/4/4

WITH AIR INJECTION (0.03cc/kg/min)

Bottom Time (minutes)	2.5	5.0	7.5	10.0	12.5	15.0	17.5	20.0
Initial Bubble Grade	I	III	IVa	III	IVa	IVa	V	IVb/IVb
Grade with Injection	IVa	IVb	IVa	IVa	V	V	V	V/V
Decompression Sickness	0	0	0	0	0	0	+	++/0
Maximum Femoral V. Grade	0	0	3	1	0	0	4	4/4

*Multiple dives at a given bottom time are indicated by a slash(/).

TABLE VIII

SUBJECT: MEGALON (#9-21)

DIVE OUTCOME FOLLOWING VARIOUS BOTTOM TIMES, ALL 160/fsw

Bottom Time	2.5	5.0	7.5	10.0	12.5	15.0	17.5	20.0
Max. Bubble Grade	II/I*	III/III	IVa/IVa	IVa /V	IVb/IVb /V	V/V	IVb/V	V
Decompression Sickness	0/0	0/0	0/0	0/0	+/0/++	+/++	0/++	++
Max. Femoral Grade	-/-	-/2	3/-	-/4	4/-/4	4/4	4/4	4

Bottom Time	2.5	5.0	7.5	10.0	12.5	15.0	17.5	20.0
Initial Bubble Grade	0	III	IVa	IVa	IVb	V	IVb	IVb
Max. Grade with Injection	IVa	IVb	V	V	V	V	V	V
Decompression Sickness	0	0	0	0	0	+	+	+
Max. Femoral Grade	0	1	3	2	3	4	4	4

* Multiple dives at a given bottom time are indicated by a slash (/).

TABLE IX

SUBJECT: CODA (#9-23)

DIVE OUTCOME FOLLOWING VARIOUS BOTTOM TIMES, ALL 160/fsw

Bottom Time	7.5	10.0	12.5	15.0	17.5	20.0	22.5	25.0
Max. Bubble Grade	-	-	IV	IV	IVb	IVb /IVb	V	V
Decompression Sickness			0	+	+	+/+	++	++

Bottom Time	7.5	10.0	12.5	15.0	17.5	20.0	22.5	25.0
Max. Grade with Injection	-	-	-	-	IVb	IVb	IVb	IVb
Decompression Sickness	-	-	-	-	0	+	0	+

The signs employed were rather clear-cut and any difference between the two types of titrations (gas injection and noinjection) could be clearly recognizable.

4. Discussion

We can conclude from these gas injection experiments that a high gas bubble load per se to the pulmonary vasculature does not exacerbate limb-bend decompression sickness. The signs employed were rather distinctive and any difference between outcomes of the two types of titrations (gas injection and no injection) could be clearly recognized.

We even note that there was an apparent reduction of severity in the signs of decompression sickness problems in all three subjects of the air-injected series (Figure 39) and a slight reduction in the number of femoral bubbles.

Studies into the question of decompression sickness amelioration by external gas injection are presently under investigation.

It therefore seems necessary to reject the hypothesis that short-term, large central venous gas loads per se can detrimentally influence the outcome of decompression. It further appears that blood-bubble interactions initiated at the level of the central venous return were not playing a deleterious role insofar as limb-bend decompression sickness is concerned. The blood-bubble effects of a gas phase in capillaries can, of course, not be determined from these experiments. We restate that we have added a considerable amount of gas, bringing the central venous gas content to more than twice what would be encountered in severe decompressions, without the observation of any additional untoward signs. Thus, vis-à-vis Koch's postulate of the "infecting organism" being present in the body and causing the disease, it would appear that the gas bubbles in the central venous system are benign within the one-hour periods here tested.

In view of the apparent reduction in severity at signs of decompression sickness, the thought is provoked that certain unspecified bubble-blood interface interactions are effected which may be beneficial (if not initiated at the microcirculatory level).

Experiments have not yet been performed to determine if the hematological changes observed following hyperbaric decompression can also be observed following external air injection. Our experiments would indicate that even if changes are noted, they should not be large enough to be of physiological consequence with respect to limb-bend problems. Furthermore, correlations of blood viscosity and hematocrit with precordial bubble scores in human divers following decompression were not significant [Neuman, Harris, and Linaweaver, Jr., Aviat. Space Environ. Med., 47, 803, (1976)].

(M.R. Powell)

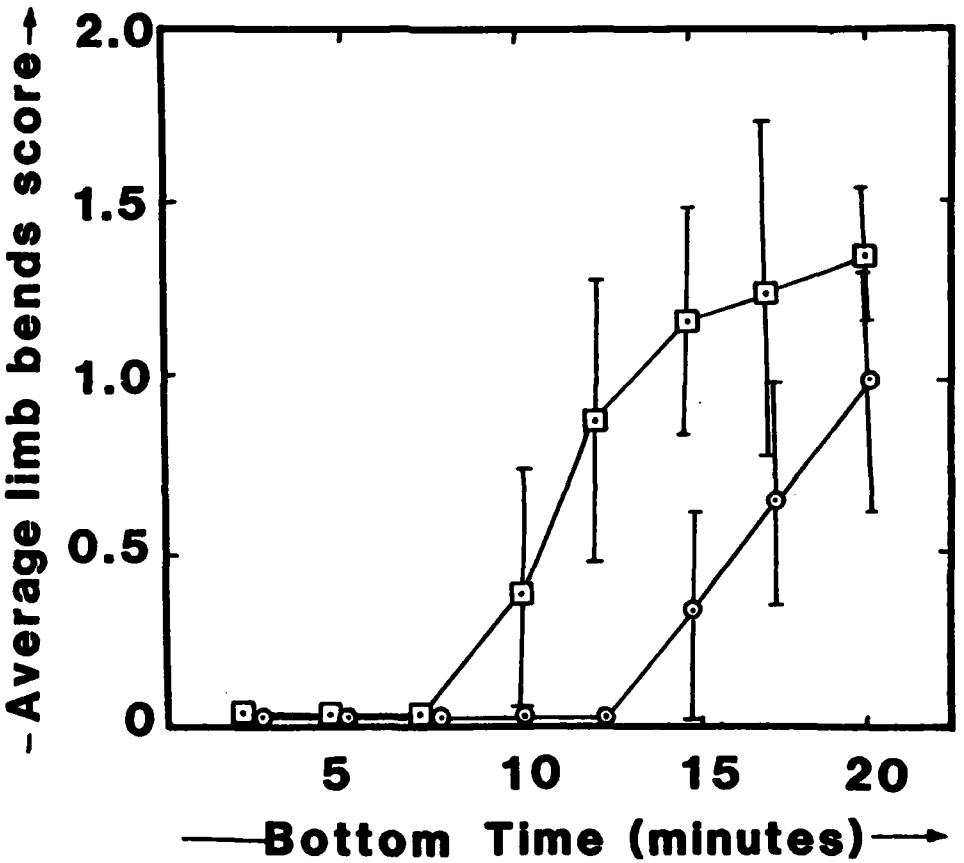

Figure 39. Average decompression stress as a function of bottom time for three sheep. Upper curve represents normal response to decompression, while lower curve is the response with augmented air injection (0.03 cc/kg/min).

IV. GAS PHASE FORMATION FOLLOWING DECOMPRESSION IN HIGHLY PERFUSED TISSUE

Doppler bubble detectors have demonstrated that large numbers of gas bubbles are found in veins which drain muscle tissue. So-called "skin bends" notwithstanding, a gas phase in dermal or muscle tissue appears to be benign. A gas phase forming in other organs which are also highly perfused, such as the brain or kidneys, could be more injurious. A study was thus initiated using Doppler flowmeters to determine if a gas phase could form in these two tissue types.

A. RENAL

1. Methods

To determine if highly perfused non-muscular tissue, such as kidney, forms a gas phase following decompression, Doppler perivascular cuff probes were surgically placed on the renal vein. Four subjects (domestic sheep) were employed, and various efforts were made to isolate blood drainage solely from renal tissue. (In addition to renal tissue flow, the renal vein also carries blood from the capsule, perirenal adipose tissue, and the drainage of the utero-ovarian vein.) Elimination of these gas phase sources, as was done most completely in the subject "Ruffian," resulted in few Doppler detectable bubbles. Bottom depths were generally at least 48.5 m. (160 fsw) (Table X), and bottom times were 10 to 20 minutes.

2. Results and Conclusions

From perfusion considerations only, the kidney half-time is on the order of 10 seconds. Thus we might not expect that so "fast" a tissue would exhibit gas phase separation and this appears to be true in the case of subjects (e.g., "Ruffian") treated to sample only renal tissue. In three of four times where renal bubbles were detected on "Ruffian," the presence of systemic arterial bubbles was also confirmed (by a probe on the carotid artery).

We could conclude that the few renal bubbles detected were simply gas bubbles which had passed from the renal artery through to the renal vein. The one exception to this hypothesis is dive #76-56 where a large number of renal vein bubbles (on the order of 500/min) were heard from 14 to 26 minutes; doubtlessly this could not have been purely of embolic origin, although systemic arterial bubbles were detected before the appearance of the renal vein bubbles.

B. CEREBRAL

1. Probe Design

Gas phase formation in cerebral tissue was investigated by a Doppler flow transducer implanted over the sagittal sinus. Considerable difficulty was initially experienced in getting adequate Doppler signals from the sagittal sinus using our single crystal probe

TABLE X

RENAL VEIN DOPPLER STUDIES

Experiment Number	Days Post Operative	Exposures FSW/Bottom Time	Stops FSW/ Minutes	Bubbles In Renal Vein*	Decompres. Sickness	Pre-Cordial Bubble Grade	Remarks
			"Polyester"				
75-32	3	160/20	D-D	80/ (50)	0	IV	
75-33	4	160/20	D-D	7/ (10)	0	IV	
75-34	7	160/20	20/3, -	38/ (36)	0	III	
75-35	8	160/20	20/3,10/5	4/ (80)	0	II	
75-36	9	160/20	20/3,10/11	22/ (45)	0	III	
75-37	10	160/20	20/3,10/5	67/ (25)	0	II	
75-38	11	160/20	20/3, -	73/ (20)	0	IV	
75-39	15	160/20	D-D	0	0	IV	
75-40	16	160/20	D-D	0	0	IV	
75-42	18	160/20	D-D	7/ (20)	0	IV	
75-44	46	240/10	D-D	0	0	IV	
			"Dry-Clean-Only"				
75-41	2	160/20	D-D	0	0	I	
75-43	6	160/20	D-D	2/ (20)	+	IV	
			"Innominate"				
76-27	3	160/20	D-D	7/ (21)	+	IV	
76-28	4	70/70	D-D	0	0	IV	
76-29	7	160/20	D-D	74/ (15)	0	IV	
76-31	11	160/20	D-D	50/ (7)	0	IV	

*(maximum no. bubbles/min. @ time of maximum)

(continued)

Experiment Number	Days Post Operative	Exposures FSW/Bottom Time	Stops FSW/Minutes	Bubbles In Renal Vein*	Decompres. Sickness	Pre-Cordial Bubble Grade	Remarks
76-33	15	160/20	3/20,11/10	0	0	IV	
76-34	16	160/20	D-D	10/(6)	0	IV	
76-35	18	350/10	D-D	79/(15)	+	V	Recompressed at 15 min.
76-37	23	60/100	D-D	0	0	IV	
76-38	35	160/20	D-D	0	0	IV	High velocity flow
76-39	37	160/20	D-D	0	0	-	
			"Ruffian"				
76-50	6	160/20	D-D	10/(5)	0	II	
76-51	7	160/20	D-D	0	0	II-III	
76-52	8	70/90	D-D	0	0	0	
76-53	9	210/15	D-D	0	0	V	
76-54	12	220/20	20/10	0	0	IV	
76-55	15	180/20	D-D	4/(12)	0	V	carotid bubbles
76-56	16	180/20	D-D	500/(14-26)	+	IV	carotid bubbles
76-57	19	180/20	D-D	0	+	IV	carotid bubbles
76-58	20	180/20	D-D	0	0	IV	carotid bubbles
76-59	27	180/20	D-D	0	0	III-IV	
76-60	28	180/20	D-D	0	0	IV	
76-61	33	180/20	D-D	0	0	IV	
76-62	34	230/15	D-D	0	0	IV	
76-63	47	180/25	D-D	0	0	V	
76-64	48	180/30	D-D	0	+	V	carotid bubbles
76-65	60	180/30	D-D	68/(17)	+	V	carotid bubbles

implanted in sheep. We improved the probe performance by (1) using double crystals on the probe, with the crystals slightly tilted to provide overlapping ultrasound fields of transmission and receiving, (2) using a special backing material, (3) improvement of the electrical connectors and cabling, and (4) improving the surgical technique for trephination and implantation of the probe. The combination of these improvements, working with generally improved Doppler ultrasonic electronics, has resulted in excellent signal-to-noise ratio.

The overall geometry of the sagittal sinus probe is 1/4 inch in length with the cabling emerging at right angles to the end of the probe opposite the crystals. 10 MHz crystals, rather than 5 MHz, are used for both the transmitting and receiving in order to elevate the audio-frequencies of the low venous blood velocity in the sagittal sinus. Each crystal is mounted with the facing crystal on the ground side of the circuit and the opposite side at the high RF voltage level. By tilting the crystals to an approximate 10 degree angle between the faces, a sufficiently broad area of overlapping transmitting and receiving beams has been achieved so as to flood the sagittal sinus with ultrasound.

The backing material developed consists of a mixture of microscopic glass beads and epoxy cast into 1/4-inch diameter rods and sectioned into 1/2-inch lengths. These pieces provide a sturdy base for the crystals as well as an acoustical mismatch when cemented in place allowing efficient radiation of the ultrasound. This material is superior to air backing because it provides structural security and will not allow a space to be filled with body fluids or to be subject to fracture by hyperbaric exposures. The probe bodies are drilled for passage of the shielded electrical wiring of the crystals and stress relieved with a plastic tubing covering.

The cabling is of low microphonic quality and is connected to specially designed pull-away connectors, each pair being secured with heat shrink tubing. The length of the cable is about 4 inches and is mated to an extension cable at the time of its use in the experiments. The cable extending to the Doppler ultrasonic control boxes at the time of the experiments also had improved connectors and cabling considerably reducing the artifacts caused by microphonics of the previous alligator clips.

Doppler ultrasonics have been improved by the use of low noise integrated circuits which have become available. Improvements in the signal-to-noise aspects of the circuitry have been incorporated into the two Doppler Model 1027 boxes (manufactured by the Sound Products Division, Institute of Applied Physiology and Medicine) previously built for this contract and allow the simultaneous monitoring of two Doppler instruments of different ultrasonic carrier frequencies. The flexible feature of this Institute's Doppler electronics is the utilization of interchangeable frequency control crystals in the Doppler Model 1027 boxes. This considerably increased the yield of the probes because it allows for variation in the probe resonant frequency.

2. Surgical Technique

A major improvement in the surgical implantation technique has been the ability to trephine the skull of standing unanesthetized sheep using tranquilizers and local anesthetic. This capability provides a quicker recovery for the animals so that they may be utilized on the same day of the experiment as a result of their better general condition. The debilitating effect of a general anesthetic and long surgical procedure necessary in the past is avoided. The past requirements for several days of recovery compounded the probe electrical leakage problem which is present in all implanted electrical transducers. With more immediate availability of the animals, a higher success ratio of the implanted probes is achieved and, in addition, if a nonfunctioning probe is encountered on a given day, the part can be easily removed through the existing incision and can be repaired or replaced with a new sagittal sinus flow probe. Of additional value has been the employment of a special adjustable "stop" for the trephine drill to prevent penetration of the brain at the moment of passage through the skull. No significant brain damage has been encountered since the development of this adjustable stop.

3. Hyperbaric Exposures

The design of the experiment has been to implant carotid artery Doppler cuff-type detectors routinely on our experimental sheep for use in all experiments. The sagittal sinus probe is placed at a later time after the animals have been utilized for other procedures. Because of the severe nature of the gas loadings and subsequent decompressions, sagittal sinus experiments are essentially terminal experiments. The hyperbaric exposures varied from 48.5 m. for 20 minutes to 63.6 m. for 40 minutes. In most instances, a decompression rate of 60 feet per minute has been utilized; however, in the most recent experiments we have increased the surfacing rate to 120 feet per minute in order to further challenge the highly perfused brain tissue. Good sounds of blood flow were heard in all cases here reported.

4. Results and Conclusions

The results of the experiments and our attempts to produce a sagittal sinus gas phase in sheep has been consistent in all of the animals and are tabulated in Table XI and Figures 40 and 41. They demonstrate that even in severe decompression procedures, where maximum grade precordial bubbles are routinely detected, venous gas bubbles are detected from the brain only after arterial gas embolization occurs. Sagittal sinus bubbles are detected approximately 30 to 60 seconds following the first arterial gas emboli (detected with the carotid probe).

These experiments accord with the original hypothesis that gas phase separation does not occur in the highly perfused brain tissue following otherwise acceptable decompression tables and, in fact, the brain does not produce detectable gas bubbles without prior arterial embolization in the most severe exposures we have performed, namely, 60.6 m. (200 feet) for 30 minutes followed by decompression at the

TABLE XI

SAGITTAL SINUS BUBBLES FOLLOWING DECOMPRESSION

Dive Number	Subject	Dive Profile	Precordial Grade Bubbles	Carotid Artery and Sagittal S. Bubbles	Remarks
76-5	9-10 "Blue Streak"	160/20 10 fsw stop removed	IV	no bubbles	
76-6	9-10	160/20 10 fsw stop removed	III-IV	no bubbles	
76-7	9-9 "First Stop"	160/20 10 fsw stop removed	IV	no bubbles	Signs of mild decompression sickness noted, subject recompressed for treatment.
76-8	9-10	160/25 direct decom-pression	IV	no bubbles	
76-9a	9-9	160/40 direct decompression	V	Sagittal sinus: possible 4 bubbles detected.	
76-9b	9-9	160/30 direct decompression	--	no bubbles detected.	30 minutes surface interval.
76-9c	9-9	180/20 direct decompression	--	no bubbles detected.	18 minutes surface interval.
76-9d	9-9	185/20 direct decompression	--	no bubbles detected.	11 minutes surface interval.
76-9e	9-9	210/40 direct decompression	V	Sagittal Sinus and Carotid artery: bubbles detected in artery followed by sinus, subject convulsed and expired.	17 minutes surface interval.

Dive Number	Subject	Dive Profile	Precordial Grade Bubbles	Carotid Artery and Sagittal S. Bubbles	Remarks
76-12	9-10	160/20 direct decompression	IV	no bubbles detected.	
76-13	9-10	270/10 direct decompression	IV	no bubbles detected.	
76-15	9-10	250/10 direct decompression	IV	no bubbles detected.	Mild decompression sickness.
76-16	9-10	240/15 direct decompres.	V	no bubbles detected.	
76-19	9-10	190/20 direct decompres.	IV	no bubbles detected.	
77-83	9-18 "Marquette"	160/15 direct decompres.	IV	no bubbles detected.	
77-84a	9-18	160/20 direct decompres.	IV	no bubbles detected.	No decompression sickness (or mild).
77-84b	9-18	160/40 (75 min. interval from 77-84a)	V	Numerous sagittal sinus bubbles following carotid artery bubbles.	No obvious effect on sheep.
77-85	9-18	200/30 (ascent: 120' per minute)	V	Numerous sagittal sinus bubbles following carotid artery bubbles.	Bubbles gone on recompression, terminal experiment.
77-87a	9-22 "Kojak"	200/30 (ascent: 120' per minute)	V	no bubbles detected.	
77-87b	9-22	200/30 (ascent: 120' per minute)	V	Numerous sagittal sinus bubbles after carotid artery bubbles.	

rate of 120 feet per minute. Previous calculations from perfusion rates of 0.21 ml per minute per ml of tissue, representing a half-time of 143 seconds, indicate the white matter should sustain a surfacing pressure of 130 feet.

An additional result of the data appear to be that the brain and cord can often tolerate many arterial gas emboli without convulsions or collapse. The appearance of sagittal sinus bubbles shortly after their detection in the carotid artery would further indicate that the rete mirabile does not restrict gas bubbles in the sheep.

5. Discussion

One would not suspect that spinal cord tissue could produce a gas phase sufficient to cause paralysis if the brain itself cannot, as shown in these experiments. Thus, with regard to brain and spinal cord decompression sickness, two hypotheses are suggested: (1) that all neurologic symptoms resultant from decompression exposures in hyperbaric atmospheres are the consequence of arterial gas embolism, rather than in situ formation of gas bubbles in local tissue, or (2) that because the cord is situated within articulated joints, mechanical stress may generate micro gas nuclei. Thus, local gas phase transformation may occur in blood vessels feeding cord nerve tissue.

Neurologic decompression sickness as manifested in the brain would then be the result of arterial gas embolization to non-silent areas (visual, vestibular, etc.) and areas with terminal arteries. Vein stasis (a result of accumulation of venous gas emboli in the lumbar veins) may be a contributing etiologic factor in lower extremity paralysis as suggested by Bove et al (1974). In some dives which yielded spinal cord problems in our sheep, right ventricular systolic pressures were not elevated above 20% of pre-dive control. Neurologic lesions of the cord in dogs were found by Bove, et al, when RVSP rose to 150% of control; the required elevations may be smaller than this.

(M.P. Spencer)
(M.R. Powell)

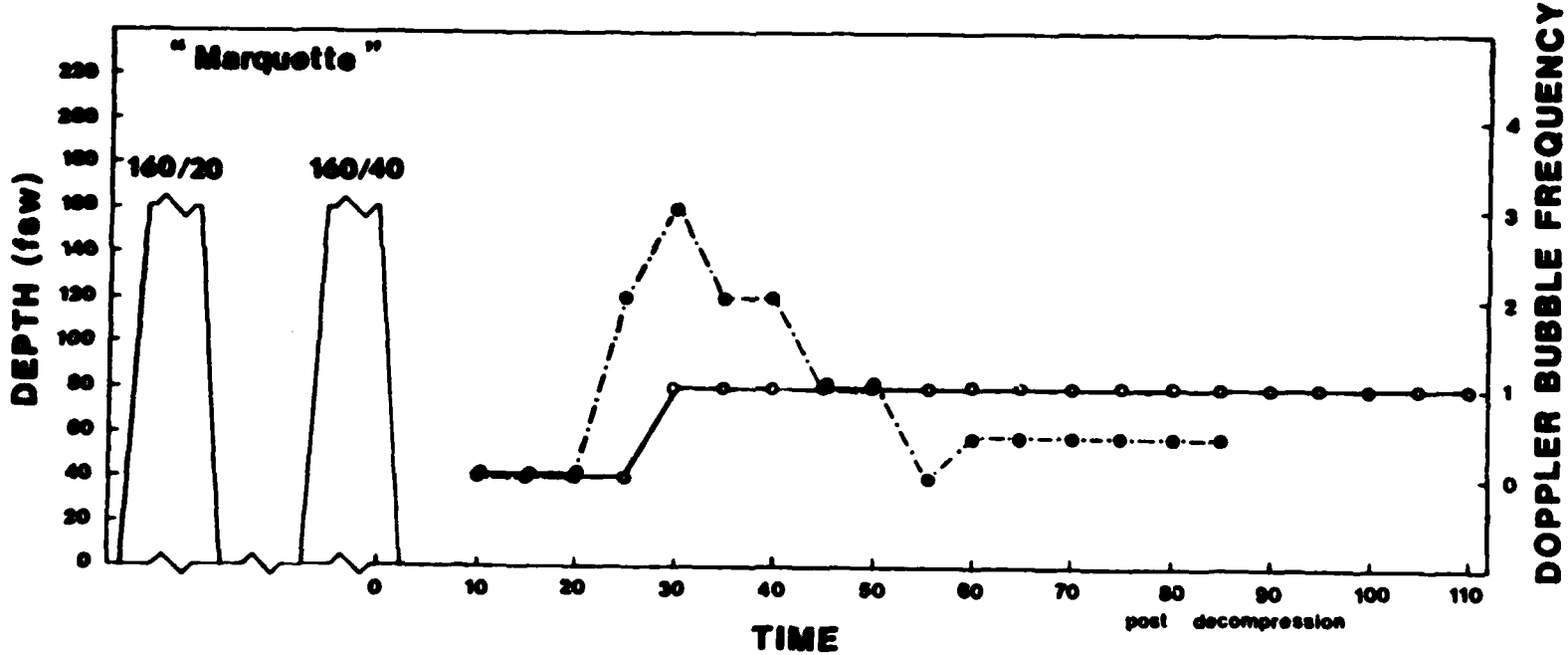

Figure 40. Multiple dives to provoke Doppler-detectable bubbles in the sagittal sinus. It can be seen that none were detected despite rather severe gas loadings. Following the final dive (240/40) carotid artery bubbles were detected and, shortly thereafter, bubbles in the sagittal sinus. Both were reduced by recompression. ("Doppler Bubble Frequency" is explained in Section D.)

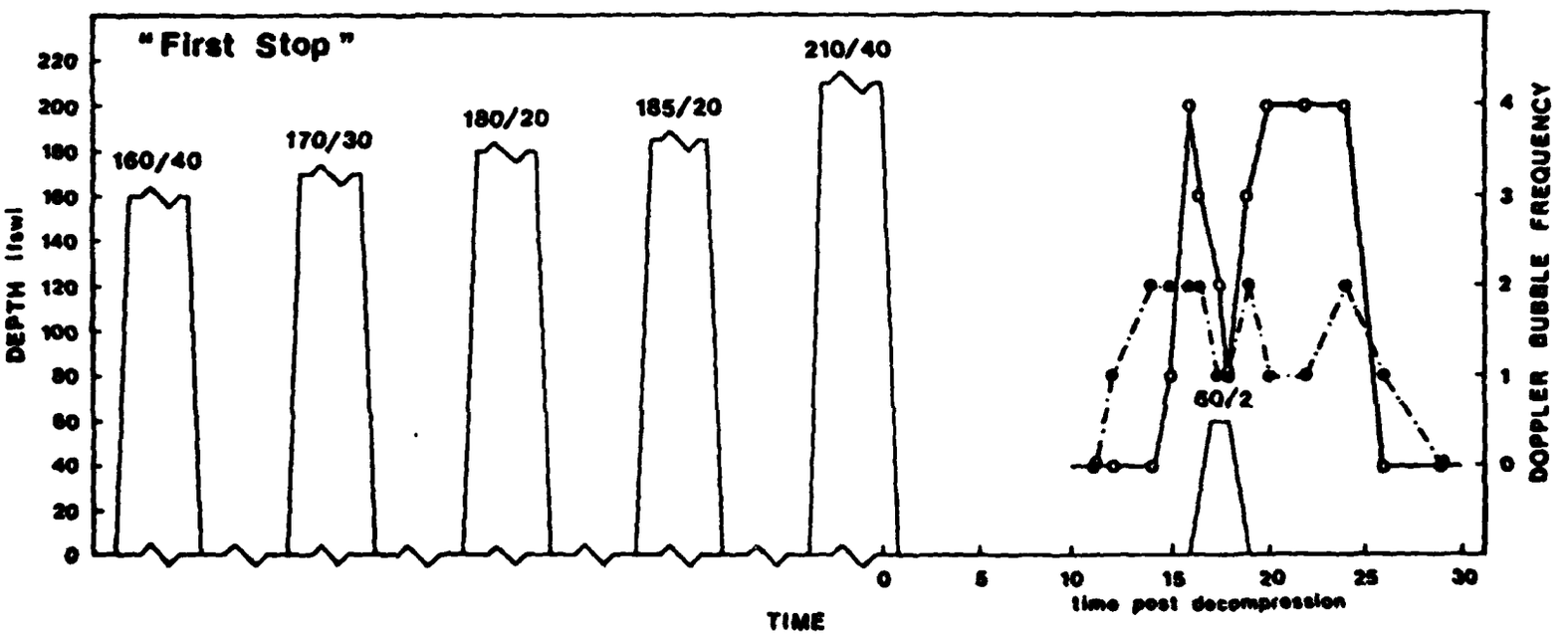

Figure 41. Multiple dives to provoke Doppler-detectable bubbles in the sagittal sinus. It can be seen that none were detected despite rather severe gas loadings. Following the final dive (240/40) carotid artery bubbles were detected and, shortly thereafter, bubbles in the sagittal sinus. Both were reduced by recompression. ("Doppler Bubble Frequency" is explained in Section D.)

—.●.— Carotid artery

—○— Sagittal sinus

V. SYSTEMIC ARTERIAL BUBBLES; SOURCE AND PATHOGENESIS

A. INTRODUCTION

One very important contribution of Doppler ultrasonic bubble detectors to hyperbaric physiology has been the demonstration that bubbles appear copiously in the central venous return, but only rarely in the arterial system. Our studies on gas separation in two highly perfused organs (kidney and brain) have indicated that these tissues do not readily produce a gas phase following decompression--even when rather heroic efforts are undertaken to induce one. Neurologic and sensory manifestations of decompression illness do exist, however. Among these are vertigo, visual disorders, nausea, paralysis and disorientation and loss of consciousness. While the etiology of neurologic forms associated with the cord appears to have a strong base in circulatory alterations, particularly venous vertebral plexus congestion (Bove, et al., 1974), arterial embolic events cannot be discounted.

The changes in right ventricular systolic pressure described in Section III. B. are below those given by Bove, et al. (1974) in their studies of cord lesions on dogs. One might conclude that while venous vertebral plexus congestion occurs and results in cord lesions when RVSP reaches 159% of predive control (in dogs), dives resulting in severe hind leg weakness and paralysis (in sheep) when the RVSP is elevated but to 130% are observed.

As seen in the preceding section, highly perfused tissues seen to be resistant to gas phase formation in all but the severest cases of decompression. Neurologic decompression sickness could have an origin in arterial gas embolism. The question of transpulmonic passage of the gas phase was investigated to determine if, indeed, such an event occurred. Work by Emerson, Hempleman and Lentle (1967) had earlier indicated that a gas phase could not pass the pulmonary barrier under normal physiological conditions. Earlier studies with rats (Powell, 1971) had indicated that arterial bubbles could be found in those subjects which expired, although not all rats with arterial bubbles would necessarily die. The majority of these animal subjects showed no evidence of systemic arterial bubbles following decompressions on profiles known to result only in limb-bend decompression sickness. There often appears in the literature (e.g., Buckles, 1968) references to the fact that arterial bubbles precede venous ones. Doppler techniques have shown this is actually the exception in intact animal subjects. In that certain decompression maladies are hypothesized to have their etiology in arterial gas embolization (C.N.S. "hits"), it is of interest to determine what conditions mitigate for arterialization of venous system bubbles. It is generally assumed that since venous bubbles appear first, the source of arterial bubbles is the lung. Arterial gas tensions are thought to closely follow inspired pressures and thus not be supersaturated; this has, however, not been rigorously tested for hyperbaric conditions and rapid pressure changes.

B. METHODS AND RESULTS

1. Rats

In seven anesthetized subjects (Wistar rats, retired breeders, male, 500 grams), pressure-measuring catheters were inserted through the jugular vein into the right ventricle. Placement was determined from pressure tracings and waveform. All values of the ventricle pressures are given as percent of control. To minimize the effect of resistance loss in the fluid-filled lines, all lines were kept to minimum lengths and flushed with saline containing 1 I.U. heparin/cc.

A Doppler filament-tip probe (designed and constructed at I.A.P.M.) was inserted to the arch of the aorta through the mesenteric artery. A probe-type Doppler transducer was also positioned over the vena cava to detect venous bubbles transmurally.

The rats were subjected to a dive on air of 44.2 to 54.4 meters for 35 minutes. Decompression was accomplished in 3 to 4 minutes by means of a slow bleed (to avoid "burst lung").

Following decompression, subjects were monitored for ECG, RVSP and vena cava and aorta gas bubbles (chart recording and aural monitoring). Air was injected for certain phases of the experiment, through a fine bore catheter inserted through the femoral vein. Flow rate was determined by a syringe pump.

Following surface air injection in 10 rats, no evidence of a systemic arterial gas phase could be found, either by Doppler filament-tip monitors in the aorta or by examination of mesenteric arteries. The subjects used in all 10 cases expired from cardio-respiratory collapse. RVSP was measured in 5 cases and often found to be elevated as much as 200% of control. This finding of the absence of arterial gas bubbles was likewise noted in sheep during the air injection measurements shown in Figure 35. The bubbles must be considered larger than those generated by decompression.

Results of decompression experiments are shown in Figures 42 to 45. We note that only in Figure 45 did the rise in number of aortic gas bubbles significantly precede the rise in RVSP; there were also few bubbles at the time of maximum RVSP. In Figure 43, the rise in number of aortic bubbles came only after a fall in RVSP when the subject was moribund (end of second dive). This could indicate the opening of pulmonary A-V shunts although an increase of blood flow as grossly measured by the Doppler flowmeter was not evident. In the majority of examples, numbers of aortic bubbles paralleled RVSP. Not all elevater right ventricular pressure incrreases affected the arterialization of venous bubbles; presumable size of bubbles is likewise a consideration.

It is of particular interest to note that the appearance of systemic arterial gas bubbles did not necessarily result in the death of tne animal shortly thereafter, e.g., Figure 45. We can surmise that

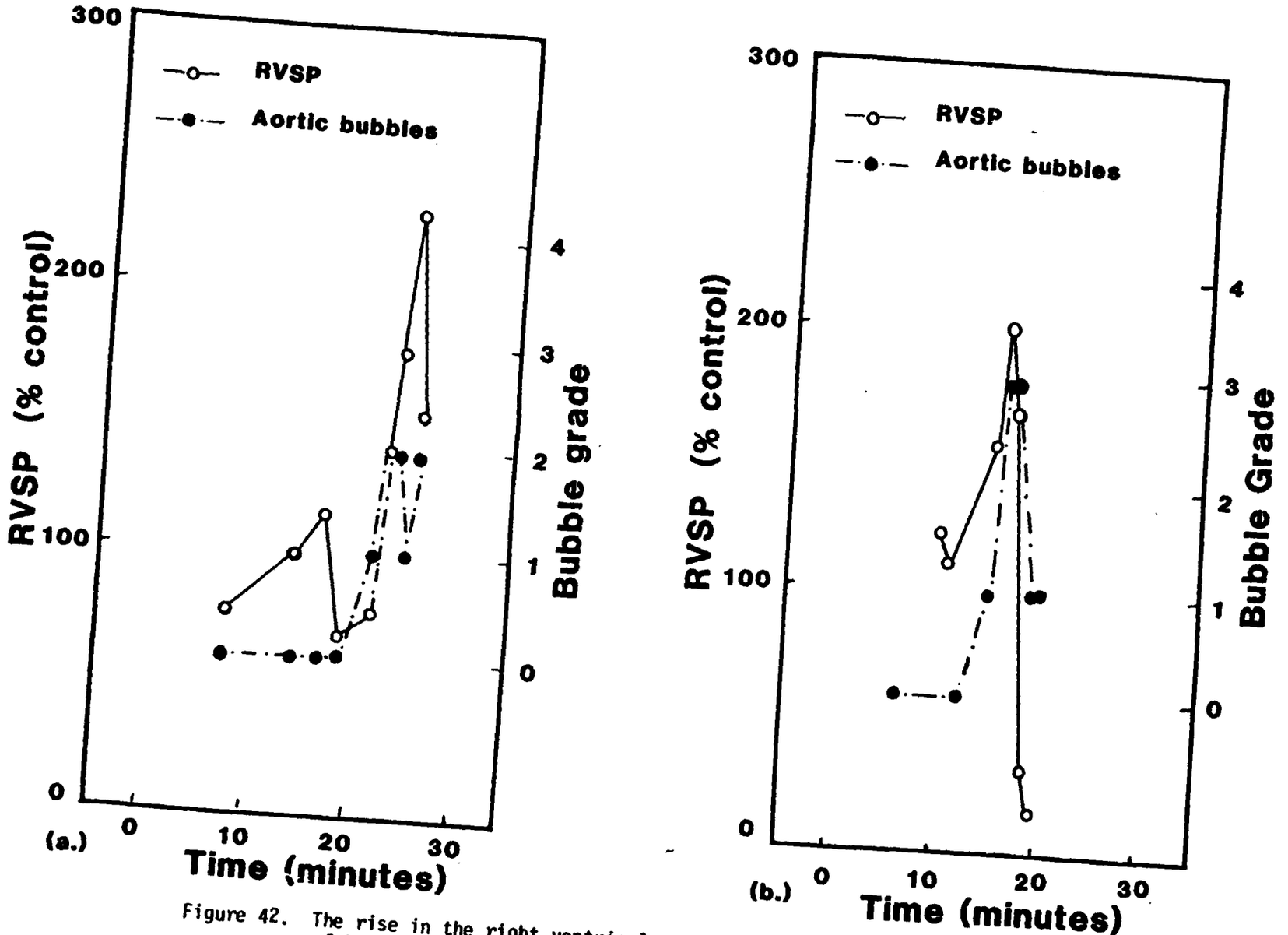

Figure 42. The rise in the right ventricular systolic pressure and the presence of Doppler-detectable gas bubbles in the aorta of rats following hyperbaric decompression (a.) 75 psi/35 min. (b.) 75 psi/30 min.

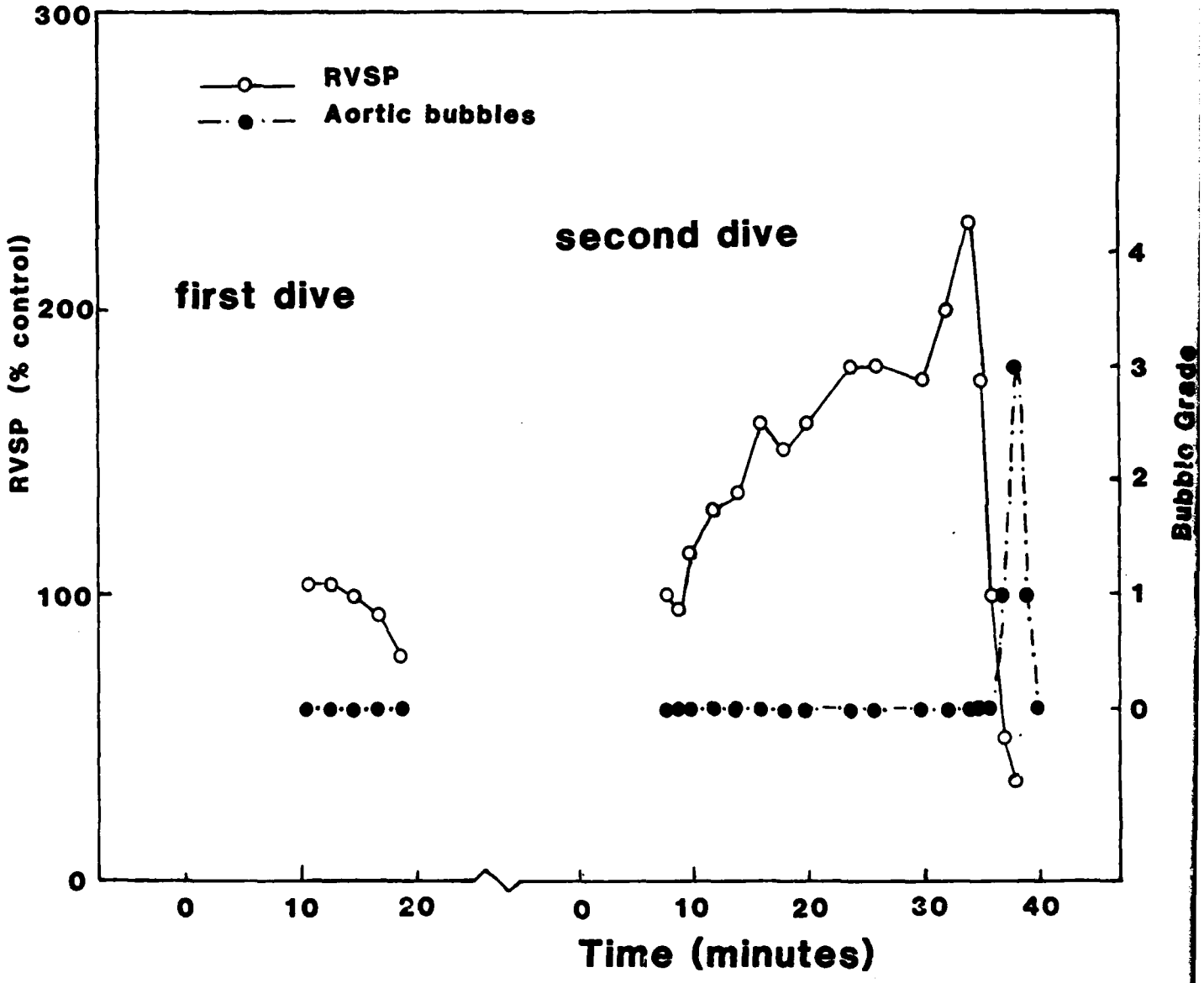

Figure 43. Examples of multiple dives to elicit aortic gas bubbles. Record made at 35 minutes for experiment in (a) is shown in Figure 47.
(a) 1st dive: 75 psi/25 min. 2nd dive: 80 psi/20 min.

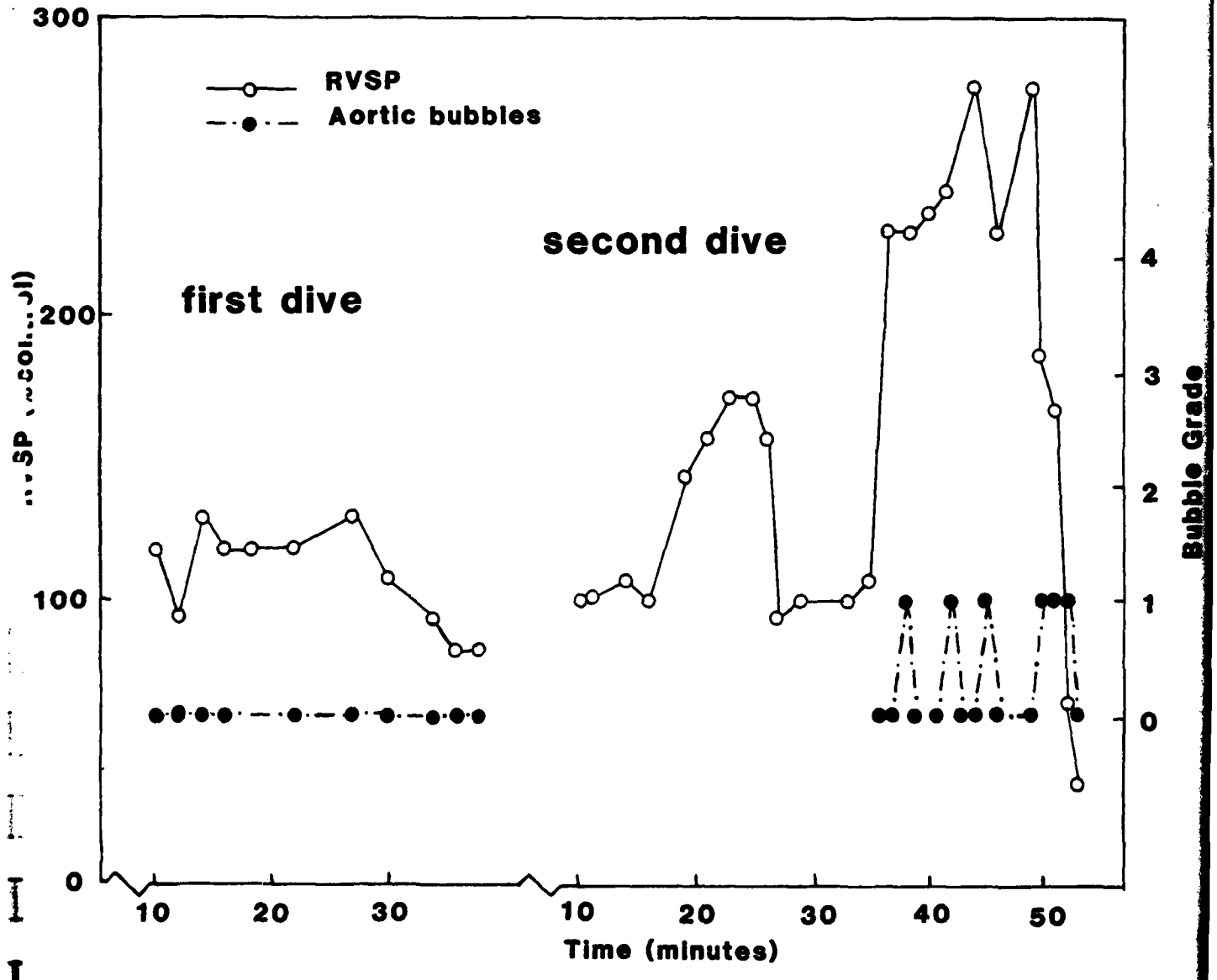

Figure 44. (b) 1st dive: 75 psi/30 min. 2nd dive: 75 psi/20 min.

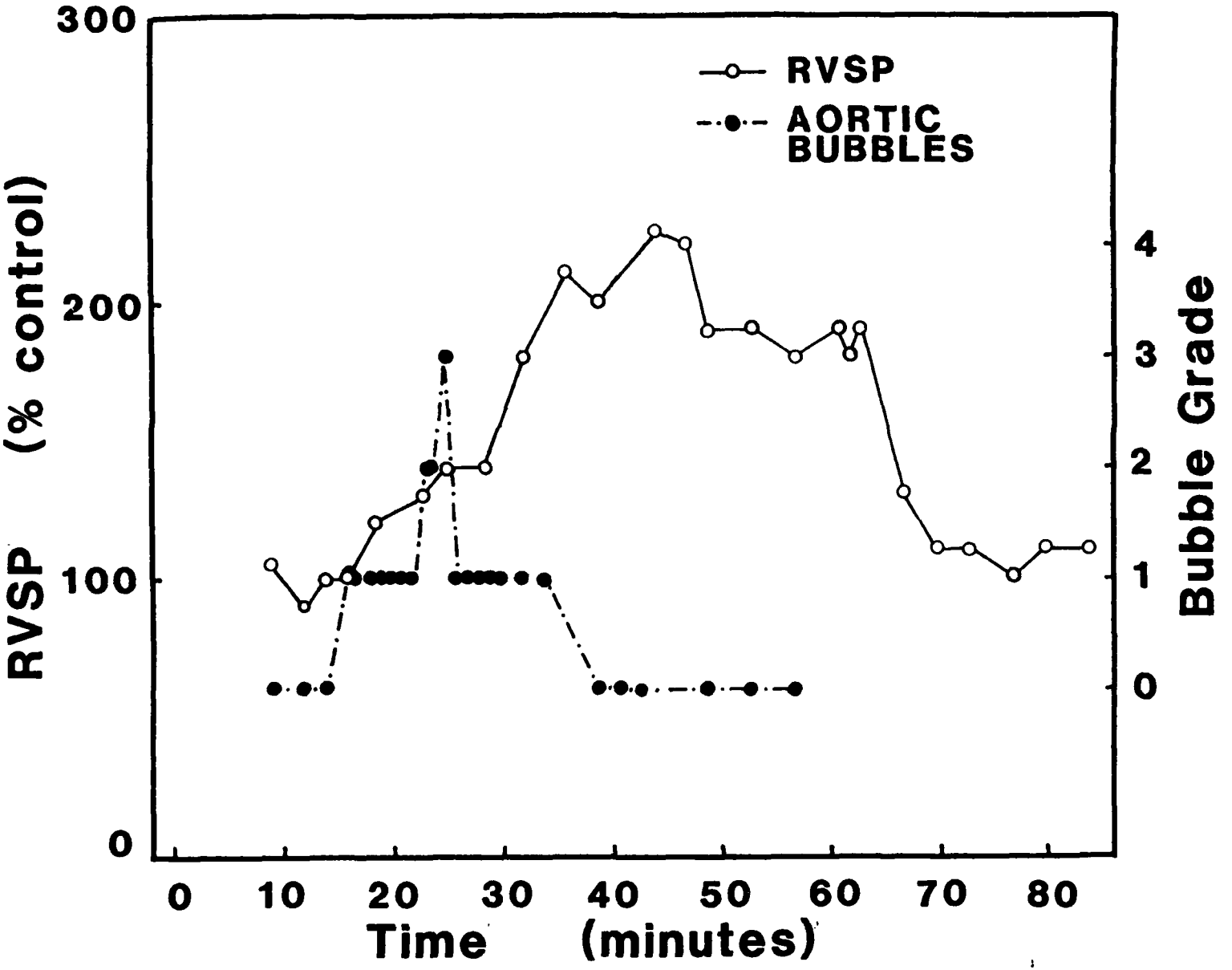

Figure 45. Doppler-detectable aortic bubbles and RVSP in a rat following hyperbaric decompression. Aortic bubbles on right hand scale.

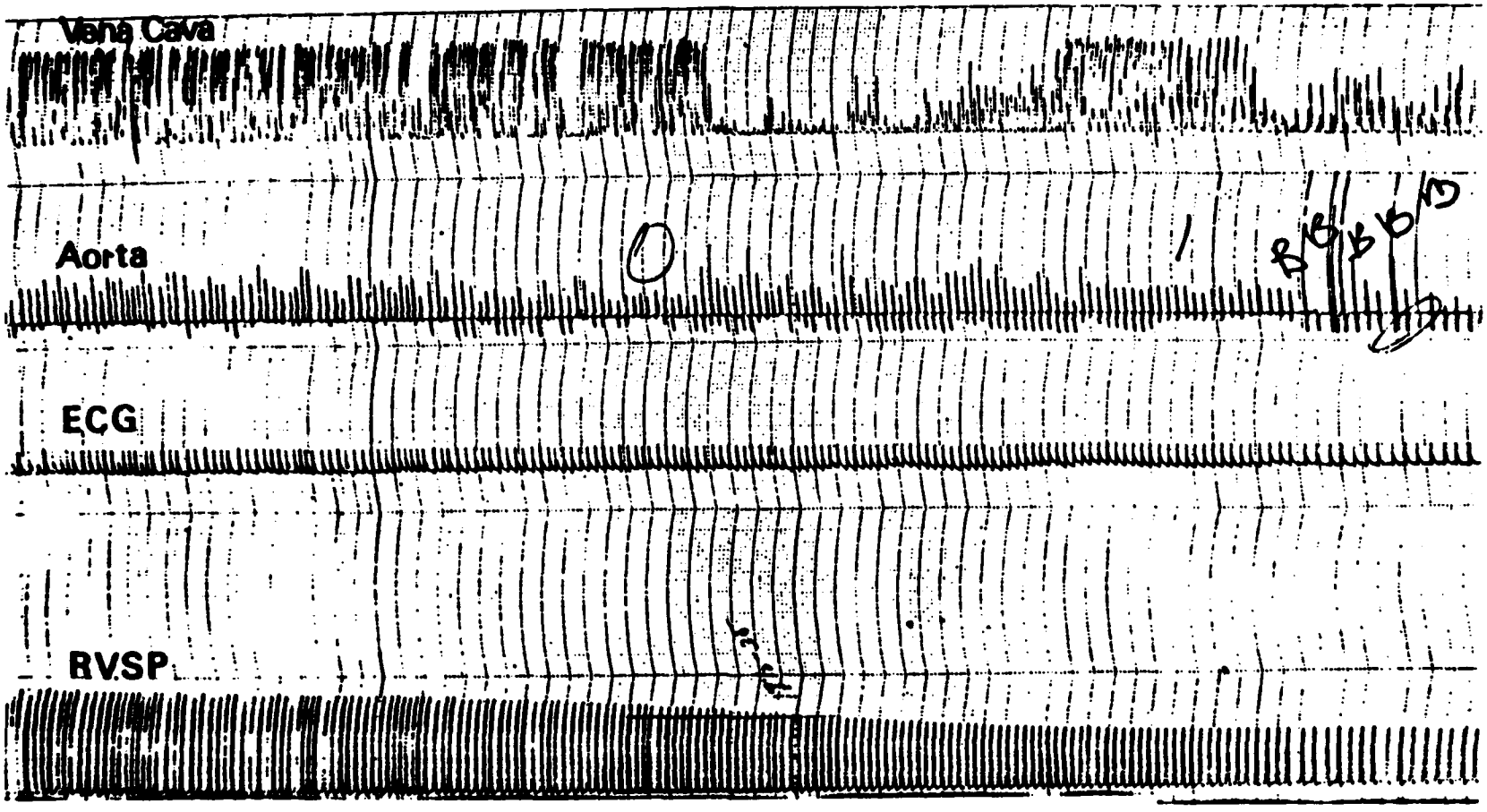

Figure 47. Chart recording of bubbles appearing in the aorta of a rat following the fall in RVSP. At this point, bradycardia is evident but no ECG abnormalities. Subject expired shortly after this recorded segment.

cardiac gas embolism and cardiac arrest are not the common aftermath of the presence of arterial bubbles.

2. Sheep

The results of a survey of 86 decompressions with sheep as subjects are given in Table XII. These dives were selected as all having at least Grade III precordial bubbles and using sheep with a Doppler probe implanted around the carotid artery. This is a useful implant position as it has ease of accessibility. Each carotid artery monitors approximately 5% of the cardiac output allowing one to estimate the number of systemic gas emboli. Furthermore, in the sheep the brain receives almost the entirety of its blood supply through both carotids (B. A. Baldwin and R. R. Bell, J. Anat., 97, 203-215, 1963); each vessel then gives a good indication of the degree of cerebral gas embolization.

All decompressions are based upon a truncation of approximately 10 to 30 minutes from U. S. Navy tables for any given depth and bottom time; most are direct decompressions. With Grade IV precordial bubbles, all would be considered marginal for sheep, and 12% provoked signs of decompression sickness. Grade V gave a decompression sickness incidence of 59%.

Bubbles were detected in the carotid artery in 7% of the subjects monitored displaying Grade IV precordial bubbles, and in 50% of those with Grade V (augmented gas loads not included here). As Grade V affects the greatest increase in RVSP, we suspected venous bubbles were arterialized by forced passage through A-V shunts (c.f. Niden and Ariado, 1965). Arterial anoxemia is, likewise, also strongly suspected to play an important role. As seen in Figure 46, carotid artery bubbles could be detected before a marked increase of RVSP.

D. DISCUSSION

While Grade V is not commonly encountered in human divers, it is not as rare event as one might imagine, especially where air is the compression gas (nitrogen is very fat soluble). In caisson workers, Grade V (or high Grade IV) could be a problem.

Emerson et al. (1967), earlier observed that gas bubbles could move antidromically in moribund subjects, and this led to the earlier conclusion that gas was not passing the pulmonary barrier. We now believe this conclusion to be in error, and bubbles can, indeed, be found to pass the pulmonary barrier following decompression.

It now appears that the appearance of gas bubbles in the systemic arterial circulation is a rare, but not totally improbable, event (even in cases where massive pulmonary vasculature overload is not occurring). Multiple small arterial gas bubbles could occur in some cases (the exact conditions are unclear) and some could be expected to embolize the central nervous system. Non-silent areas (vision, vestibular, auditory) could be expected to be the most sensitive. This applies to cases of tissue served by terminal arteries as has also been suggested by Guillerm et al. (1975).

TABLE XII. BUBBLES DETECTED IN CAROTID ARTERY

Dive Number	Subject	Profile	Precordial Grade	D.C.* Sickness	Bubbles Detected in Carotid Artery	Remarks
75-3	9-1	200/10	III	0	0	
75-4	9-1	200/15	V	+	0	
75-5	9-1	200/15	V	+	0	no c.a. bubbles upon recompression to 160
75-6	3-3	200/30	V	+	++	no c.a. bubbles upon recompression to 160 subject expired
75-12	9-3	100/40	IV	0	0	
75-16	9-4	60/100	III	0	0	
75-19	9-5	140/25	IV	+	0	no c.a. bubbles upon recompresstion to 160
75-20	9-5	140/20	IV	+	0	no c.a. bubbles upon recompression to 100
75-24	9-4	100/40	IV	0	0	
75-25	9-4	200/20	V	+	0	no c.a. upon recomp to 1
75-31	9-6	100/50	IV	0	0	
75-44a	9-7	240/10	IV	0	0	
75-44d	9-7	240/15	V	++	++	4th redive, convulsed and expired
76-5	9-10	160/20	IV	0	0	
76-6	9-10	160/20	IV	0	0	
76-7	9-9	160/20	IV	+	0	
76-8	9-10	160/25	IV	0	0	
76-9a	9-9	160/40	V	+	0	
76-9e	9-9	210/40	V	++	++	5th redive, convulsed and expired
76-12	9-10	160/20	IV	0	0	
76-13	9-10	240/10	IV	0	0	
76-15	9-10	250/10	IV	+	0	
76-16	9-10	240/15	V	0	0	
76-19	9-10	190/20	IV	0	0	
76-27	9-12	160/20	IV	+	0	
76-28	9-12	70/70	IV	0	0	
76-29	9-12	160/20	IV	0	0	
76-31	9-12	160/20	IV	0	0	
76-32	9-10	160/20	V	++	+	
76-33	9-12	160/20	IV	0	0	
76-34	9-12	160/20	IV	0	0	
76-35	9-12	250/10	V	++	0	2 c.a. on recompression to 60
76-40	9-13	210/10	IV	0	0	
76-46	9-13	260/10	IV	0	0	
76-47	9-13	250/10	III	0	0	
76-53	9-14	210/15	V	0	0	
76-54	9-14	220/20	IV	0	0	
76-55	9-14	180/20	V	0	+	
76-56	9-14	180/20	IV	+	+	no c.a. upon recomp.
76-57	9-14	180/20	IV	+	+	
76-58	9-14	180/20	IV	0	+	
76-59	9-14	180/20	IV	0	0	

*Decompression Sickness

Dive Number	Subject	Profile	Precordial Grade	D.C.* Sickness	Bubbles Detected in Carotid Artery	Remarks
76-60	9-14	180/20	IV	0	0	
76-61	9-14	180/20	IV	0	0	
76-62	9-14	230/15	IV	0	0	
76-63	9-14	180/25	V	0	0	
76-64	9-14	180/30	V	+	+	
76-65	9-14	180/30	V	++	+	
76-71	9-16	160/20	V	+	+	
76-72	9-16	160/20	III	0	0	
77-1	9-16	160/35	V	++	++	expired
77-59	9-18	160/5	III	0	0	
77-60	9-21	160/5	III	0	0	
77-61	9-18	160/7.5	IV	0	0	
77-62	9-21	160/7.5	IV	0	0	
77-63	9-21	160/10	IV	0	0	
77-64	9-18	160/10	III	0	0	
77-65	9-18	160/2.5	IV	0	0	
77-66	9-21	160/12.5	IV	0	0	
77-67	9-18	160/15	IV	0	0	
77-68	9-21	160/12.5	IV	0	0	
77-69	9-18	160/17.5	IV	+	0	
77-70	9-18	160/15	V	+	0	
77-71	9-18	160/20	V	+	+	augmented bubble load, gas injected
77-72	9-21	160/17.5	IV	+	+	augmented bubble load, gas injected
77-73	9-18	160/20	IV	0	+	augmented bubble load, gas injected
77-74	9-21	160/20	IV	+	+	augmented bubble load, gas injected
77-75	9-18	160/20	V	0	+	
77-76	9-21	160/20	V	+	0	
77-77	9-18	160/20	V	+	+	
77-79	9-18	160/17.5	IV	0	0	augmented gas load
77-80	9-22	160/10	III	0	0	
77-81a	9-22	160/12.5	IV	+	0	
77-81b	9-22	160/12.5	V	+	0	
77-83	9-18	160/15	IV	0	0	
77-84a	9-18	160/20	IV	0	0	
77-84b	9-18	160/40	V	0	+	redive, no deleterious effect
77-85	9-18	200/30	V	++	++	expired
77-86	9-22	160/15	V	+	0	
77-87a	9-22	200/30	V	0	0	ascent 120'/sec.
77-87b	9-22	200/30	V	+	++	re-dive, expired
77-97	9-23	160/25	V	++	0	
77-98	9-23	160/12.5	IV	0	0	
77-99	9-23	160/20	IV	+	0	
77-100	9-23	160/22.5	IV	0	0	
77-101	9-23	160/25	V	+	0	

*Decompression Sickness

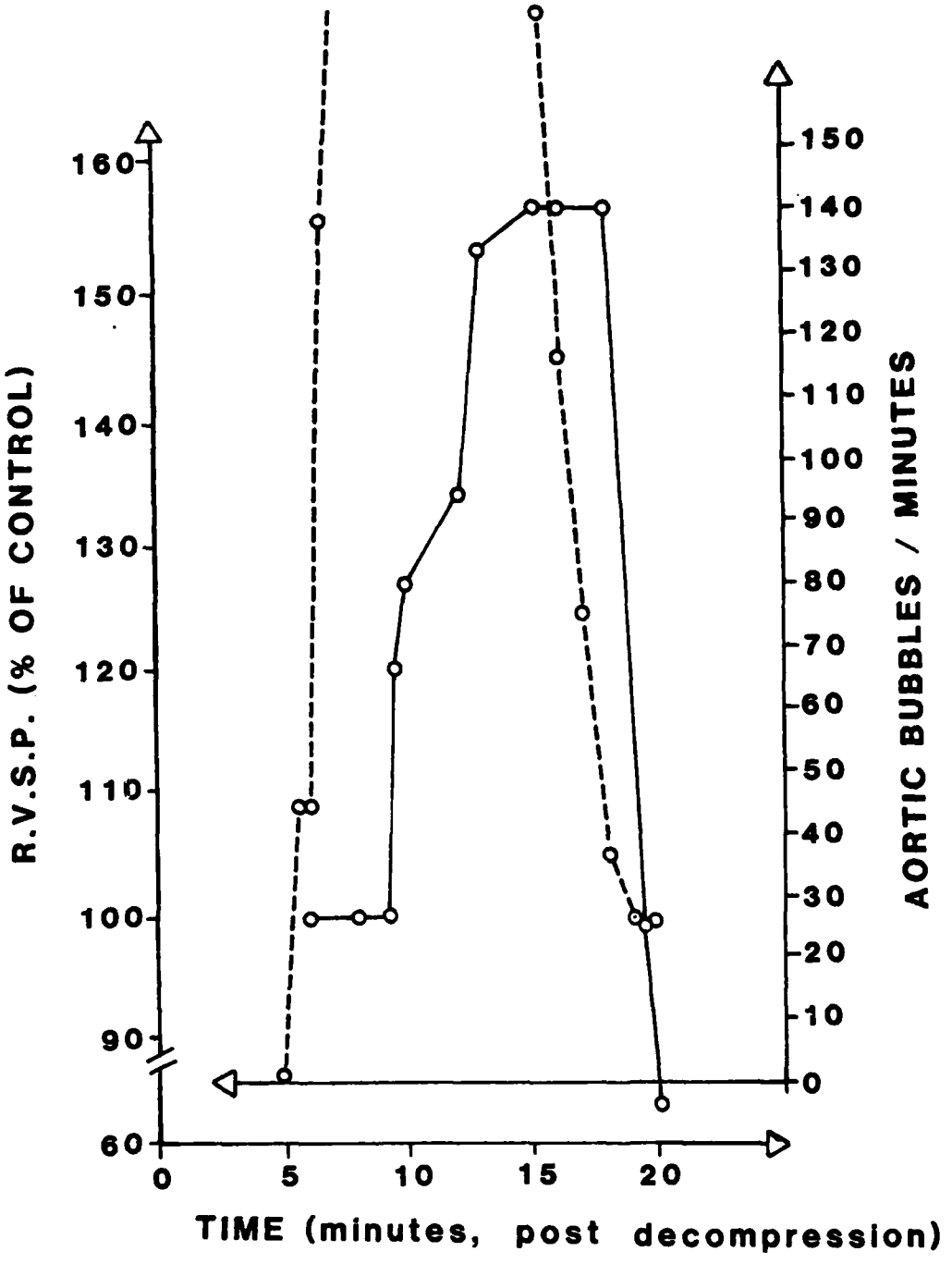

Figure 46. Number of aortic bubbles (dashed line) and right ventricular systolic pressure (solid line). Dive 160 fsw for 35 minutes with a sheep as the subject.

We may also postulate that spinal cord problems are associated with in situ gas phase growth, that is, not embolic. The problems associated with the cord are less random than cerebral problems, and appear to be more "regular" such as is seen in joint pain. It is possible that if a gas phase grows on micro-nuclei generated by tribonucleation, then anatomical areas most affected would be those in articular joints (cord and extremities) and muscle. We have noted a distinct lack of detectable venous bubbles from tissues not exposed to mechanical stress (cerebral and renal in the cases we have monitored; see Section IV).

We would recommend from the studies here conducted that, when Grade IV or V precordial bubbles are encountered in human divers, Doppler monitoring of the carotid arteries be carried out. Upon the appearance of systemic arterial gas phase, appropriate measures should be taken (halt, recompress). Increased oxygen ("breathing cocktails") may not be beneficial as the inert fraction is still high in the venous system, and this inert fraction stabilizes the gas bubbles (that is, there will be no "washout" of bubbles). Recompression, also, did not promote arterialization of venous bubbles as can be seen from the right hand column of Table XII.

(M.R. Powell)

VI. INERT GAS DYNAMICS IN TISSUES AND GELS

A. INTRODUCTION

Experiments have been conducted in the field of gas uptake and elimination in two areas; (1) *in vitro* in gels and (2) *in vivo* in rats at 1 ATA. The purpose of these experiments has been to investigate (a) the reproducibility of the data, and (b) to determine if the mass spectrometric devices can provide useful data of relevance to diving physiology (e.g., inert gas tensions in tissues).

Increased interest in mass spectrometry in hyperbaric environments has risen since the initial papers by Ackles *et al.* (1972) and Powell (1973) on tissue gas tensions as evidenced by the workshop held on the topic of mass spectrometry and hyperbaric environments at the Defense and Civil Institute for Environmental Medicine at Toronto in September, 1975. However, while extensive use is being made of mass spectrometers for respiratory work in hyperbaric environments, little use is being made of tissue gas analysis; this is, no doubt, the result of technical difficulties coupled with an uncertainty of what is actually being measured by these instruments.

Insofar as local tensions have not been measured for inert gases, it is difficult to evaluate the mass spectrometer against other, more classical, techniques. It is for this reason that we may expect some period of time before general understanding of the usefulness of this method results. This will be true only if the method, indeed, does measure a critical variable. In association with this is the fact that a so-called "critical tissue" has not been defined anatomically for problems associated with limb-bend decompression sickness. Moreover, we further recognize that, at the present time, only the gross features of gas transport in hyperbaric environments can be studied as the tissue gas probes realistically are not small with respect to cellular dimensions. We do believe, however, that the mass spectrographic method, using *in situ* probes, should be given a fair and unbiased evaluation without unrealistic claims being made either for or against it. Its employment to yield a definite numerical value for uptake and elimination constants in tissues may be less valuable than information gained regarding such things as the kinetics following gas switching or oxygen breathing. It would also be possible to study inert gas elimination in tissues with extensive gas phase formation present.

B. IN VIVO GAS TENSIONS, METHODS AND RESULTS

Gas loss through the probe will reduce the final measured tissue gas tension such that it is slightly less than that of the actual ambient gas tension, although it is proportional to the true value. For most of our measurements this factor is not important as we are primarily interested in kinetics. Here the experimentally measured tension is controlled by the diffusion of gas from the surrounding tissue to the surface of the probe through transudative fluid. If the probe is not disturbed during uptake and elimination measurements, diffusion distances will remain the same for both uptake and elimination and the replicatable steady-state point will be reached. The true value

of the tissue gas tension cannot be directly determined by any method which does not actually consume gas during the measurement process (as does mass spectrometry and in situ probes). However, it has been shown by Ackles, et al., (1972) that mass spectrometer measurements of tissue gas tensions of nitrogen, oxygen, and carbon dioxide do compare favorably with theoretical values determined by pulmonary physiology. Furthermore, estimates of true tensions are difficult only in the case of gases involved in metabolism. The tension of inert gases (of interest to hyperbaric physiology) tension can be measured if stable steady-state values are obtained after the subject has reached equilibrium. Thus, the in vivo tension of nitrogen is known from respiratory physiology, and the value measured by the mass spectrometer will be proportional, but reduced, because of gas uptake from non-moving transudative fluid. Non-moving fluids are known to give measured tensions less than the true values; they are, however, reproducible values (Nelson, et al., 1973).

We have made some measurements of pN_2 in rat muscle tissue with the equipment shown schematically in Figure 48. This consists of a rough pumping system (mechanical and diffusion pump) and the mass spectrometer analyser head (Figure 49). After pump-down, the analyser is sealed off from the rough pumping system, and a pressure of approximately 10^{-6} torr is maintained by a Vac-Ion pump.

Gas is admitted into the analyser head by means of a plastic-coated (Silastic or Teflon) stainless steel cannula. The mass range of the analyser can be controlled for both scan time and molecular species analysed. The output is recorded on paper for analysis (Figure 50).

These measured tissue tensions are not greatly different from the actual tensions estimated from respiratory physiology. Using our mass spectrometer, the measured pN_2 in thigh muscle at 1 ATA was 500 torr. This was determined from a two-point calibration of the probes in gas-equilibrated saline at 37 degrees C. This compares favorably with the expected value of 560 torr (from pulmonary physiology), and it also compares to the value of tissue pN_2 determined by Ackles, et al., (1972) with similar equipment. An example of measurement and calibration is given in Figure 51.

We are, therefore, confident that inert gas tensions as measured in vivo closely approximate the actual tissue gas tension. There is then an apparent anomaly between low gas tensions measured in fluids whose velocity has been reduced (c.f., Bondi, 1975) and the high (almost normal) gas tensions which we measure in a tissue, with supposedly non-moving transudative fluid. We advance the hypothesis that for in situ tissue gas probes, such as those we are using whose depletion is of the order of 10^{-9} cc. per second per torr, depletion is not more than 10%; the transudative fluid, therefore, acting as if it were a fairly well-stirred system.

C. IN VITRO GAS KINETIC MEASUREMENTS, METHODS AND RESULTS

To determine if a physical system with constant properties (such as thickness and viscosity) would give reproducible results, gels were prepared of either gelatin or agar. This arrangement is the same as

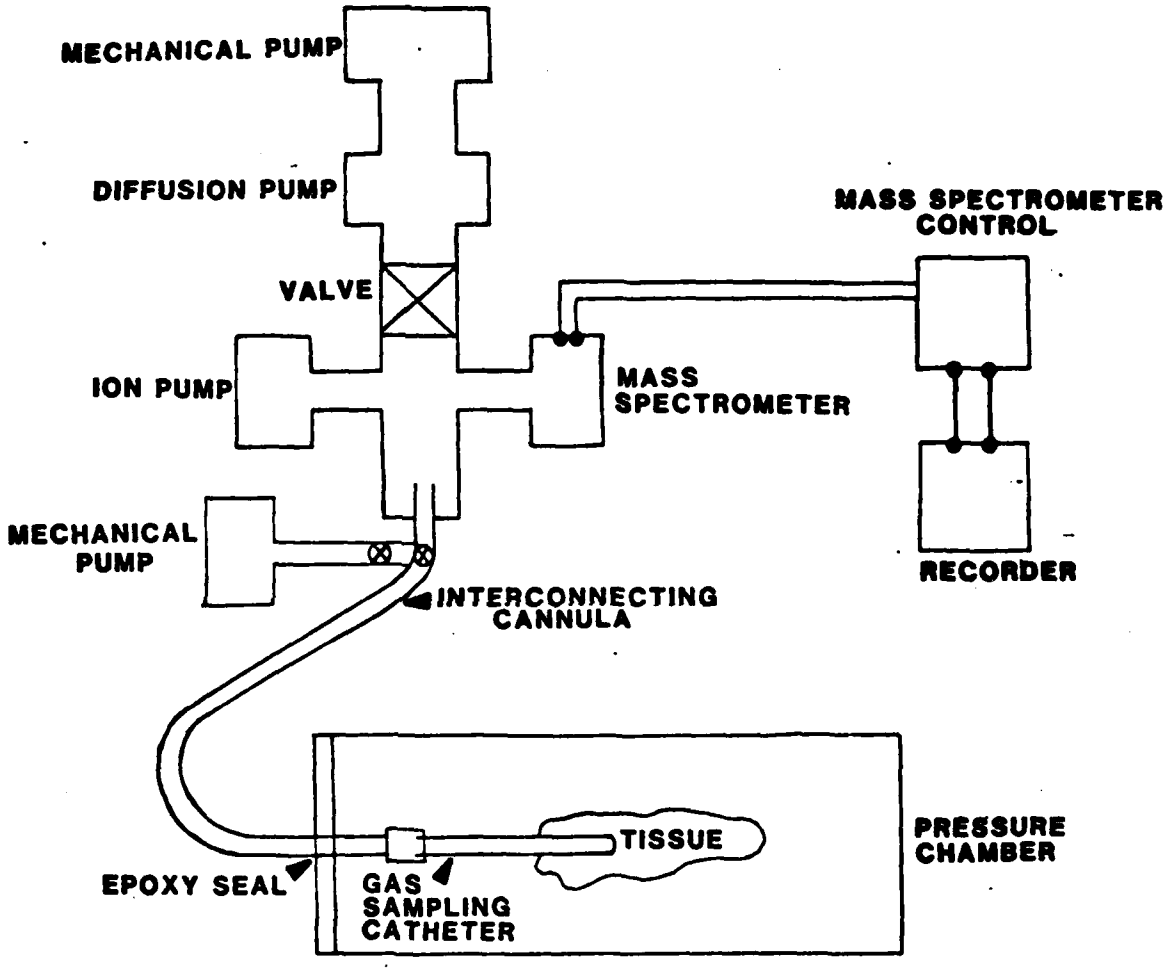

Figure 48. Schematic of mass spectrometer tissue gas analyser system.

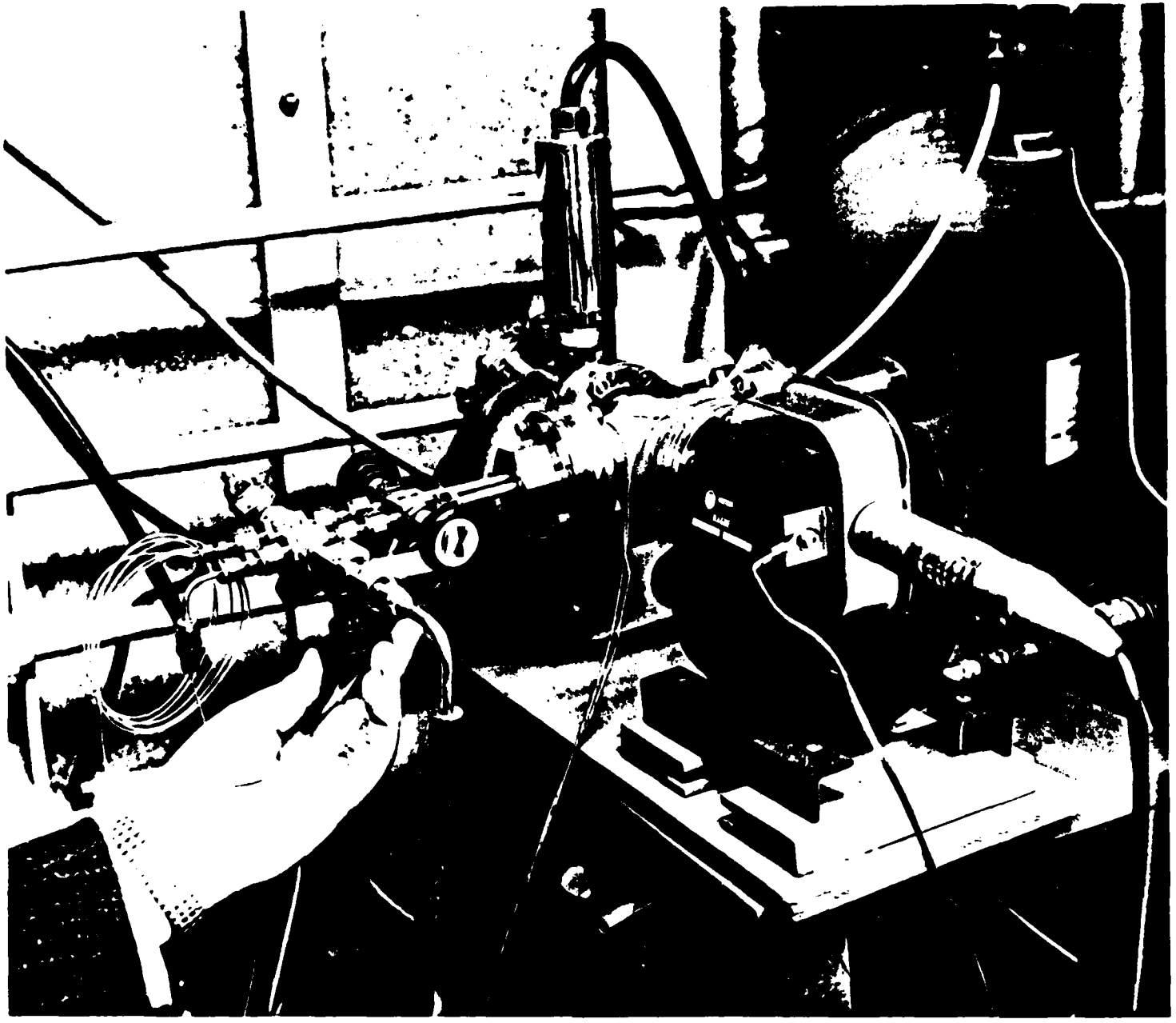

Figure 49. Detail of the pumping, inlet, and gas analysis system.

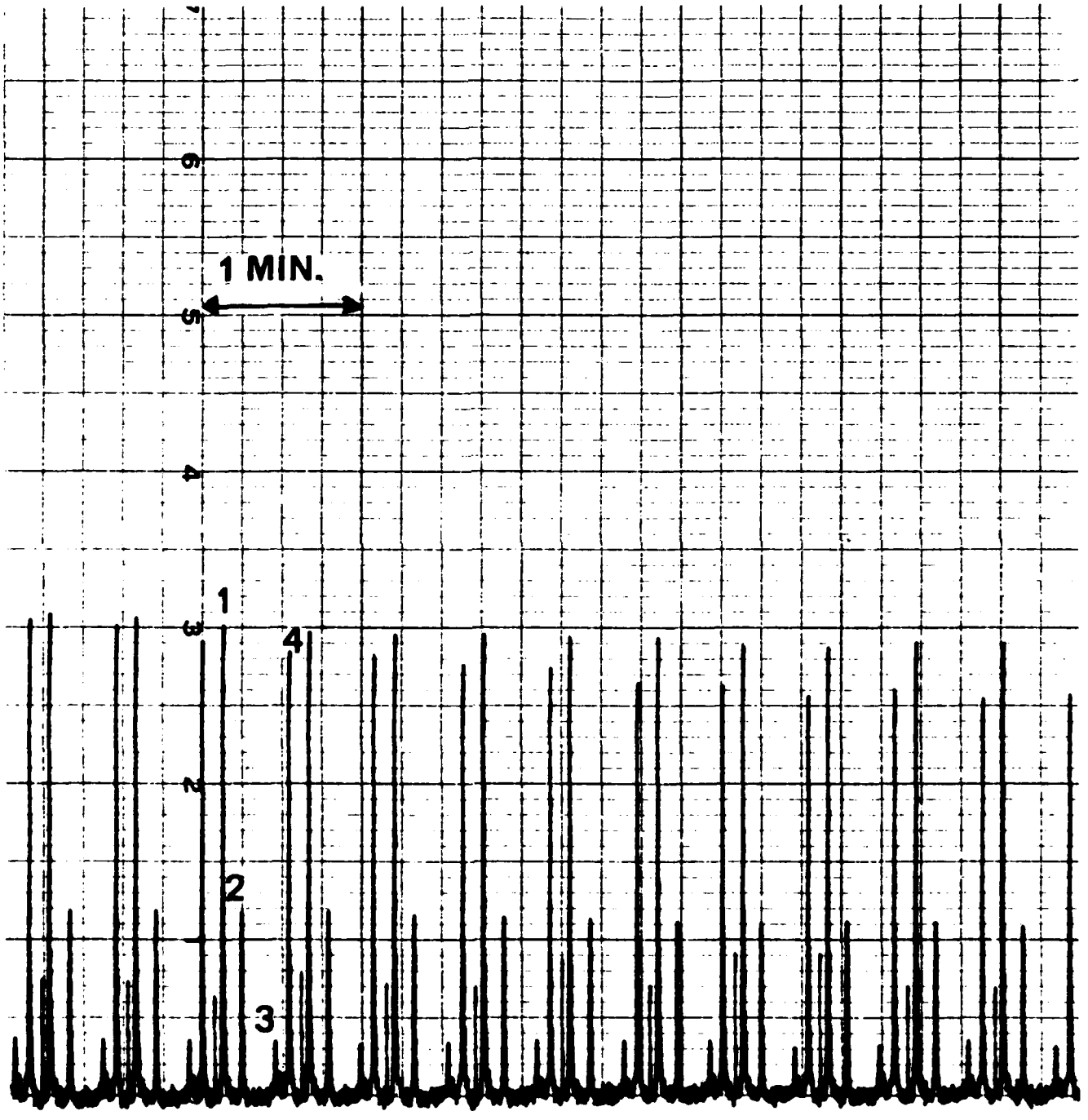

Figure 50. Chart recording of gas tension as a function of time. Peaks are: (1) nitrogen, (2) oxygen, (3) argon, and (4) carbon dioxide. Peak heights do not reflect relative tensions between different gases but rather a difference in instrument sensitivity for the species.

Figure 51. Comparison of nitrogen tension as given by gas-equilibrated saline at 37° C. and in situ mass spectrometer probe in the thigh muscle of rat. Two-point calibration yields a tissue nitrogen tension of 500 torr. Measured tensions are greater than would be expected from extrapolations of flowing solutions (cf. Nelson, et al., 1973).

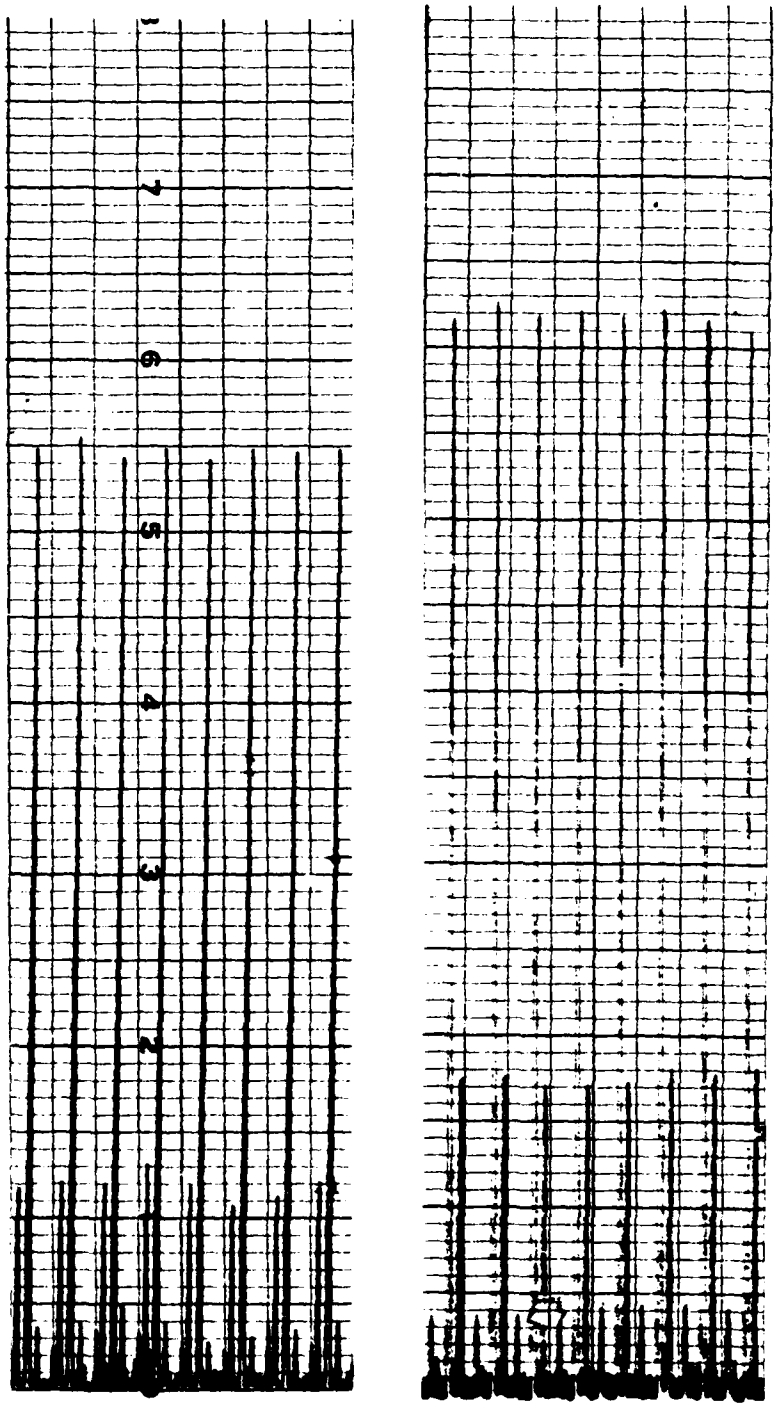

Rat thigh muscle (37° C.) Gas-equilibrated saline, 37° C.

that in Figure 48 with "gel" replacing "tissue". An in situ probe was inserted through a hole in the side of a petri dish and agar poured over and allowed to set to a depth of 3-5 mm. The gels were then either pressurized to 15 psi or placed in a bag and flushed with oxygen at 1 ATA.

The values for the uptake and elimination constants for nitrogen were found to be single valued in data corrected for the probe constant. The values are given in Tables XIIIa and b. As can be seen, within any one given day, the constants are approximately equal. (The major exception being the second run in B-2; the reason for this exception is not known. It is suspected that the optimum arrangement has not yet been found for an in vitro system to test the reproducibility of mass spectrometric measurements). On successive days, gel thickness decreased as a result of desication; half-times likewise decreased.

As can generally be suspected, more viscous gels should have longer uptake and elimination half-times and the same would be true of thicker gels. This was noted experimentally with in situ probes, the thinnest gels giving uptake and elimination half-times which were essentially identical to the probe constants.

D. IN VIVO GAS KINETIC MEASUREMENTS, METHODS AND RESULTS

To determine the degree of reproducibility of the measurements of uptake and elimination kinetics, repeated experiments were performed on the same subjects. Teflon probes (Scientific Research Instruments) were inserted into thigh muscles of lightly anesthetized rats and wash-in and wash-out measurements were made while the subject breathed alternately air or oxygen at 1 ATA. The results are given in Table XIII (the letter prefix designating a given day and the number suffix indicating the experiment on that day).

Day-to-day variation is no larger than the variations during any one day. The standard error of the mean for the uptake elimination half-times for the gels is in the same range as the S.E.M. for rats as seen in Tables XIIIa and b. The S.E.M. is 7.7% of the value for gels, 7.9% for rats, and 4.5% for probes in gas-equilibrated saline.

(M.R. Powell)

TABLE XIIIa

EXPERIMENTALLY MEASURE NITROGEN UPTAKE

AND

ELIMINATION HALF-TIMES IN AGAR GELS

Agar Preparation	Day Number	Uptake Half-Time (Min.)	Elimination Half-Time (Min.)	Average ± S.E.M.
A	1	26 26.5	26	$\overline{(26.2 \pm 0.17)}$
A	2	17.1 18.6	23.3	$\overline{(19.7 \pm 1.87)}$
A	3	14.7 18.7 17.9	22 18	$\overline{(18.3 \pm 1.16)}$
A	4	12.5 15	11	$\overline{(15.3 \pm 1.87)}$
B	1	27	22	
B	2	9	25 10	
C	1	21 29	28	$\overline{(26 \pm 2.52)}$
D	1	62	62	

TABLE XIIIb

UPTAKE AND ELIMINATION HALF-TIMES FOR RATS;

NITROGEN MEASURED BY IN SITU PROBES IN RAT THIGH MUSCLE AT 1 ATA.

Subject	Experiment Number	Uptake Half-Time (Min.)	Elimination Half-Time (Min.)	Average ± S.E.M.
# B-1	a-1	16	20	
	b-1	--	17	
	b-2	--	10	
	c-1	--	14.3	
				(15.5 ± 1.65)
# P-1	a-1	9	11	
	a-2	12.5	9	
	a-3	10	13	
	a-4	9.6	11.5	
				(10.7 ± 0.55)
# U-3	a-1	10.8	14.7	

VII. AMELIORATION OF CHRONIC PULMONARY OXYGEN TOXICITY BY INERT GAS DILUTION

A. INTRODUCTION

The observation that oxygen at higher than normal pressures has a deleterious effect upon lung tissue dates back to Lavoissier. Two effects are generally noted. The first, or acute oxygen toxicity, occurs when oxygen tension is increased to greater than three atmospheres. Here, a neurological component is prominent with convulsions occurring and death following. It was Paul Bert who, in 1878, first showed that the toxic substance responsible for this central nervous system effect was the oxygen in compressed air. The second effect, so-called chronic pulmonary oxygen toxicity, was first described by J. Lorraine-Smith in 1899 and is noted following a long exposure when the oxygen pressure is less than three atmospheres. It is primarily directed toward the pulmonary tissue with death the ultimate outcome.

The literature is replete with conflicting evidence concerning the effect of added amounts of inert gas on each of these two types of oxygen toxicity. Added amounts of inert gas appear to exert a potentiating influence on acute oxygen toxicity, which has a very rapid onset, although Burns (1972) did report increased latency to convulsions when helium was added to the oxygen as did Almquist et al. (1969) with oxygen-nitrogen mixtures.

There does exist some experimental evidence in the literature that increased amounts of inert gas will ameliorate the effects of chronic pulmonary oxygen toxicity. The early investigations of Penrod (1956) indicated that gross pulmonary damage in rats was reduced by the presence of inert gas. He postulatd that, to a great extent, the chronic toxic effects of oxygen were the result of a locally high oxygen tension in the lungs. Norman and co-workers (1951) found that pulmonary damage in rats and mice was reduced when breathing a given oxygen tension with added nitrogen. Protection was not found when systemic oxygen levels were reduced by the addition of carbon monoxide to the oxygen, although anemia and pulmonary denervation were found to be protective by Moss et al. (1976). The protective effect of nitrogen and oxygen was reported by Smith and co-workers in dogs (1971). No protection in mice with 13.5 atmospheres of added nitrogen was noted, as reported by Rokitka and Rahn (1977).

B. BLOOD GASES IN SHORT-EXPOSURE SUBJECTS, METHODS AND RESULTS

To investigate the effect of inert gas diluents on pulmonary dysfunction, arterial oxygen tensions in rats exposed to equal partial pressures of oxygen (but with differing pressures of inert gas) were studied. For these experiments, male Wistar rats of approximately 450 grams were used as the subjects. The rats were housed in pairs and given food and water ad libitum. Chamber gas composition was maintained by a gas controller which added either oxygen or inert gas as required against a constant chamber flush.

A total of 103 rats were used in this study. In the low-inert series, fifty-seven rats were divided into three groups of approximately 20 subjects each, and each group was exposed to 0.8 atmospheres of oxygen and 0.2 atmospheres of nitrogen, or 20% inert gas, in a hyperbaric chamber. In the high-inert series, 32 rats were divided into two groups, one group exposed to 0.8 atmospheres of oxygen with 4.2 atmospheres of helium added. Thus the rats in this series were exposed to 84% inert gas. The chamber temperature was maintained at 35 degrees C. for those subjects in helium and at room temperature, approximately 23 degrees C., while in the other gases. No significant difference in the parameters measured were seen between the nitrogen and helium diluents so they have been here grouped together. An additional 14 rats served as controls, remaining in the chamber for 52 hours with a slow air flush at one atmosphere.

Pre-exposure values for pH, arterial oxygen and carbon dioxide tension and hematocrit were made on blood removed from the caudal artery and collected into capillary tubes. Subjects were marked so that pre- and post-exposure determinations could be made on the same rat. Groups of rats were removed from the chamber after 42, 48 and 52 hours employing a one-half hour decompression. Determination was again made of the arterial oxygen and carbon dioxide tensions, pH and hematocrit after the rats had breathed room air for 30 to 90 minutes.

The changes in arterial oxygen tension are shown in Figure 52. It will be noted that the arterial oxygen tensions were fairly constant until 52 hours of exposure were reached. At this point a rapid drop in arterial pO_2 was noted in those rats in the low inert concentrations. For those subjects in the high inert gas mixtures, no fall-off was noted that was significantly different from the chamber control (made at 52 hours). For those subjects in the low inert gas mixtures, changes from pre-exposure tensions to 52-hour tensions are significant at the 0.0001 level. Figure 53 shows the change in alveolar-arterial oxygen difference between the pre- and post-exposure animals. In this case, the average for the group was not taken, but rather, use was made of the fact that each animal was coded and his A-a gradient determined at pre-exposure and either 42, 48 or 52 hours into the exposure. Again, it will be noted that there was a large increase in the A-a gradient after 52 hours in rats which were in the low inert gas series. A slight improvement after 42 hours was even observed in the high inert group.

The arterial carbon dioxide tensions are shown in Figure 54; a major change was not noted even after 52 hours of exposure for either group. Hematocrit for both groups is shown in Figure 55. There was a decrease of Hct in the group in the high inert gas mixture, but this fall was also noted in subjects serving as chamber controls. No significant change in pH was found (Figure 56).

In these experiments, maximum exposure was limited to 52 hours to prevent the death of the subjects by chronic pulmonary oxygen toxicity before the end of exposure. Only one subject died and none of the remaining subjects, independent of the gas mixture, were noted to be moribund. After the blood sampling at the end of each exposure

ARTERIAL pO_2 TENSIONS

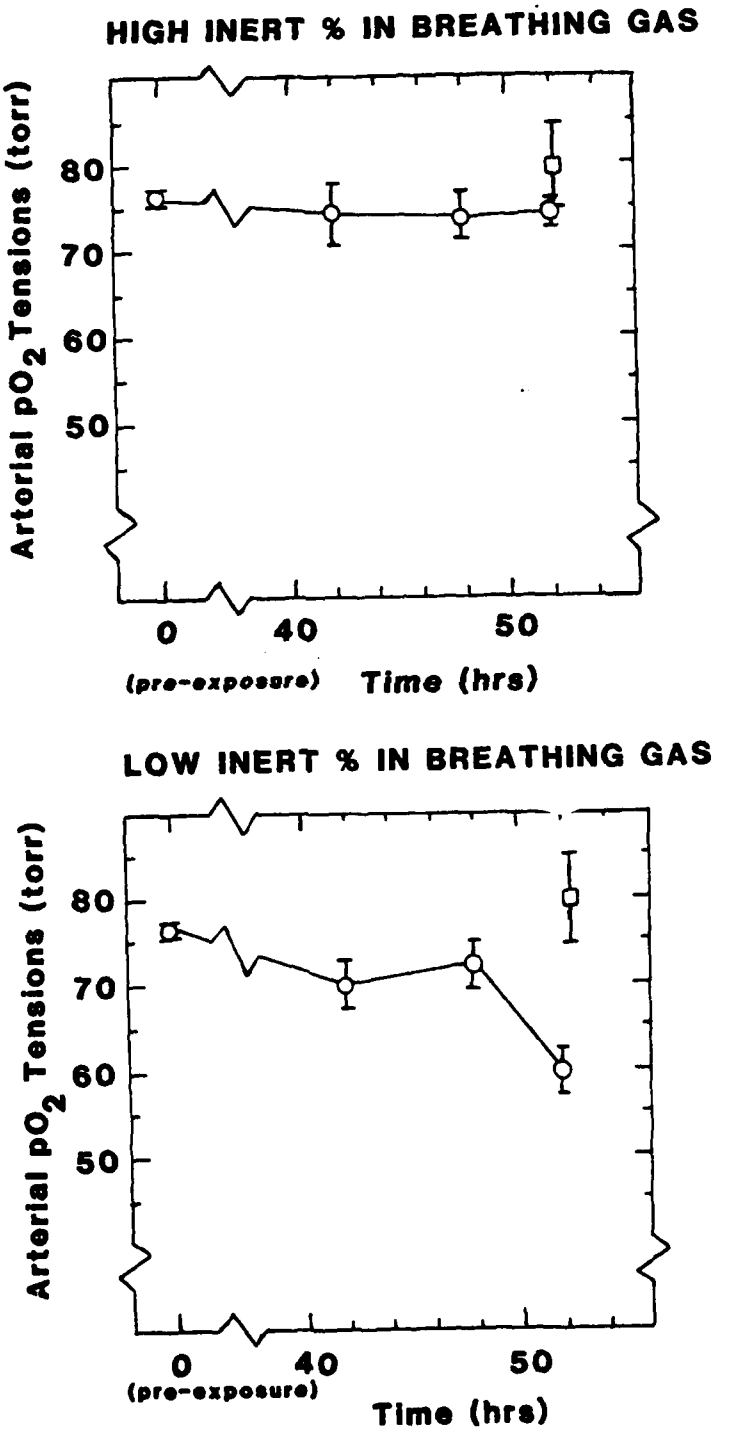

Figure 52

CHANGE IN ALVEOLAR-ARTERIAL DIFFERENCE

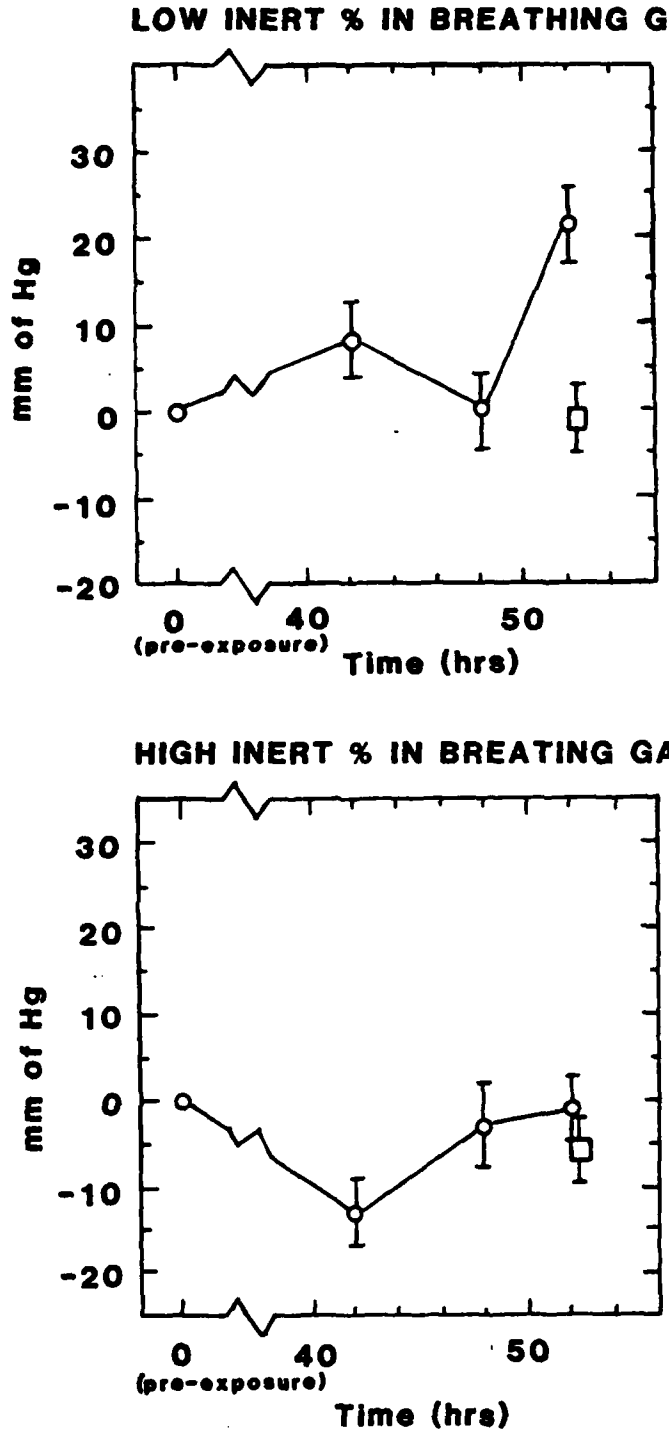

Figure 53

ARTERIAL pCO_2 TENSIONS

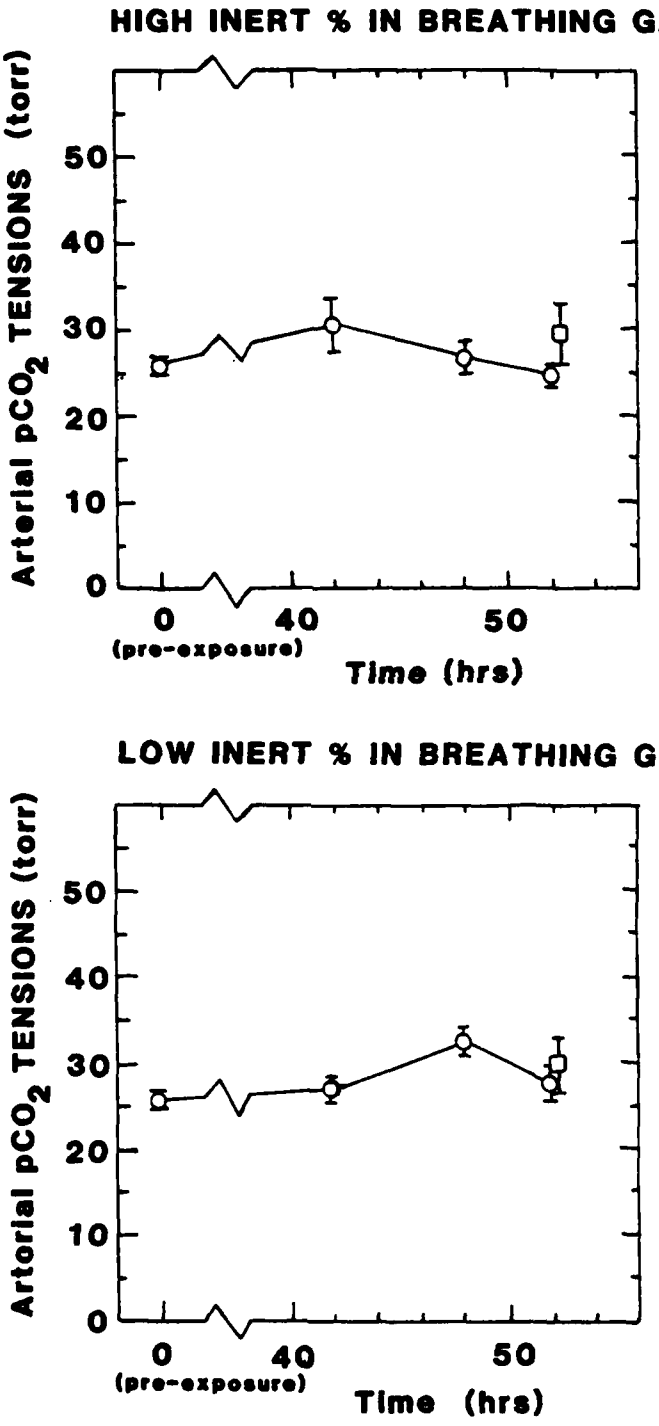

Figure 54

HEMATOCRIT

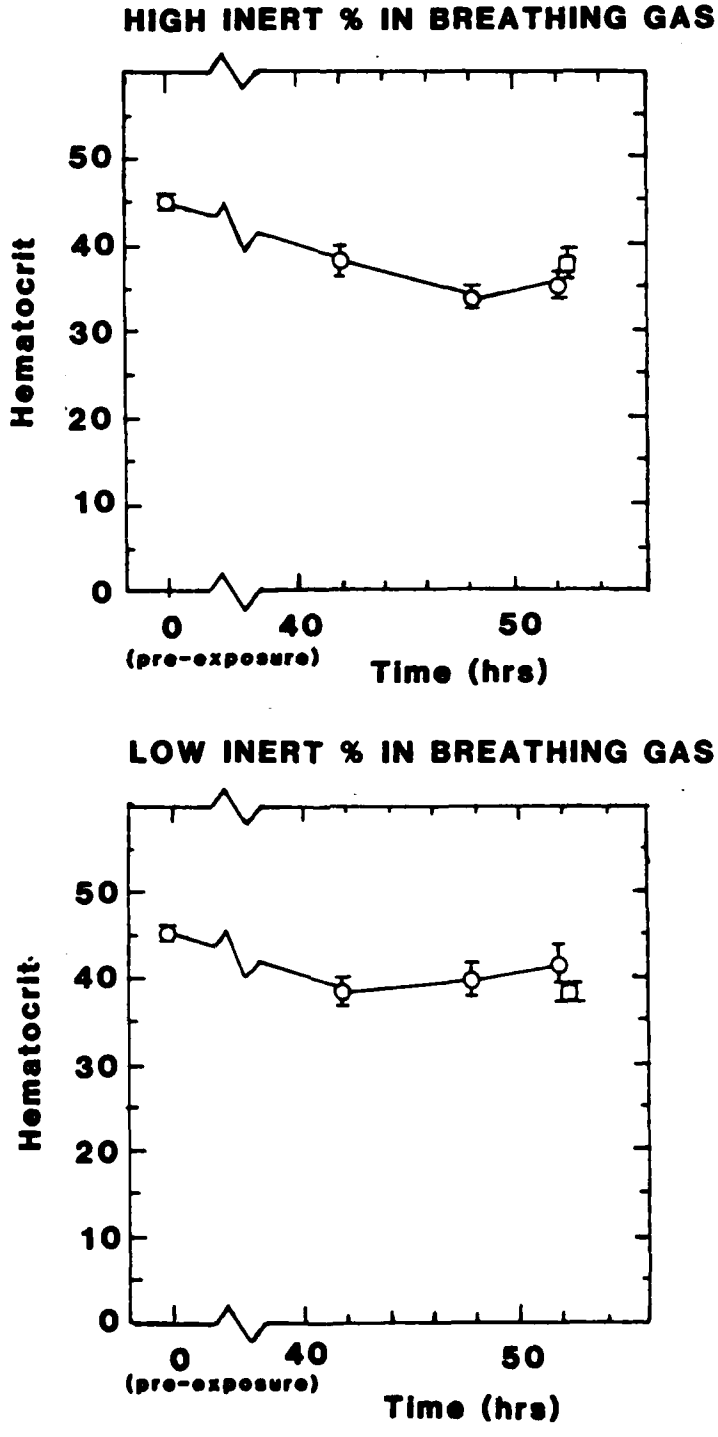

Figure 55

ARTERIAL pH

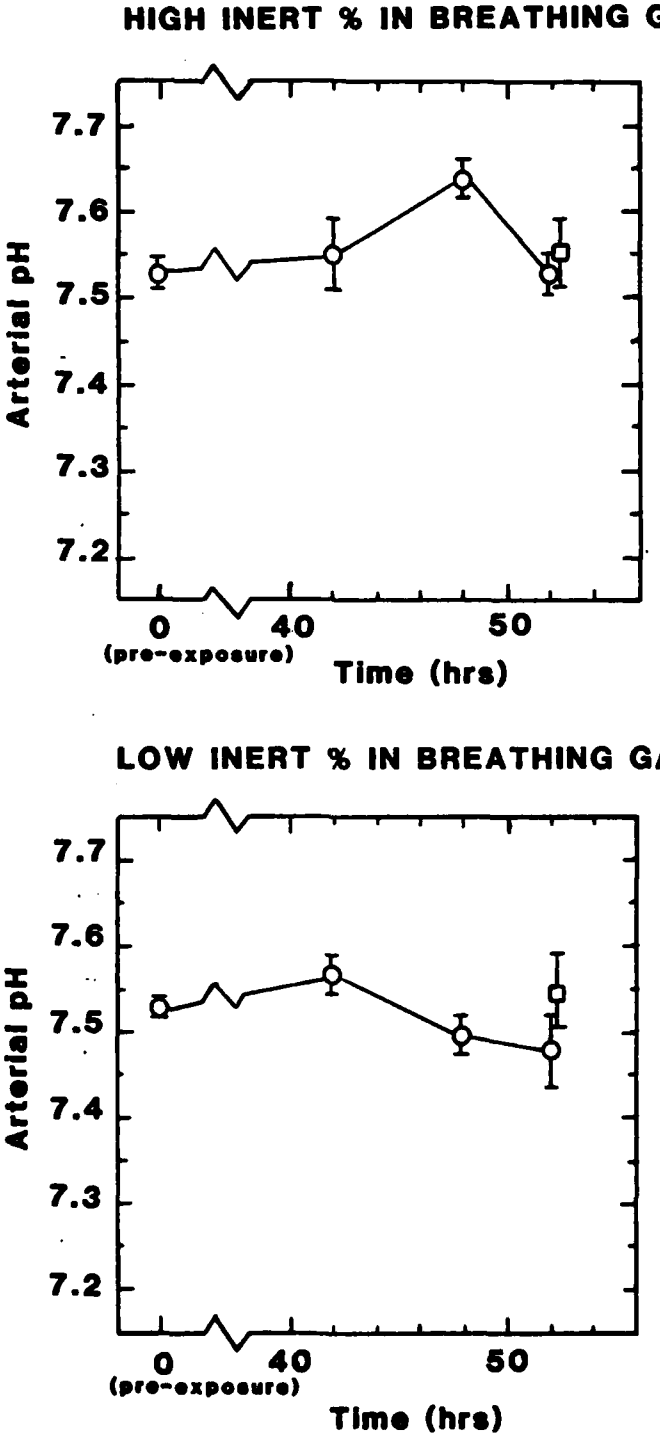

Figure 56

period, the subjects were terminated by pentobarbital injection. Lung-to-body weight ratios for both the low- and high-inert gas series were measured (Table XIV). These ratios were found to increase progressively at the 42, 48 and 52 hour periods in both groups. Lung weight ratios of those subjects in low inert gas concentrations were higher at all three times than those subjects in high inert gas dilution and, indeed, the high inert gas group had a lower lung-to-body weight ratio after 52 hours than the low inert gas group after 42 hours. At 52 hours, the low inert group lung weight ratio was 137% of chamber control; the high inert group was 110% of chamber control.

Upon autopsy, rats in neither series had lungs which displayed more than small areas of focal congestion; none displayed hepatization. Histological studies of lungs in all the groups did not reveal marked changes between the pre- and post-exposure, with the exception of perivascular edema. This was very obvious in the low inert gas series even after 42 hours, and progressed to marked edema after 52 hours. Only small degrees of perivascular edema were noted in the high inert gas series rats. Other signs of chronic pulmonary oxygen toxicity, such as cellular proliferation, interstitial edema, capillary congestion and atelectasis were not present to any marked degree in either group of rats.

In a histological study done on other rats of the same weight and age range, but which were exposed to a high and low inert fraction for 70-80 hours, toxicity signs were even more evident upon examination. We noted edema and capillary congestion being far more prominent again in the low inert series as contrasted to the high inert gas series (Figures 57 to 59).

C. SURVIVAL TIME IN CHRONIC EXPOSURE, METHODS AND RESULTS

To determine if nitrogen diluents can increase life span, when oxygen tension is kept at 1 atmosphere absolute, well below the convulsion ranges, groups of 36 mice were exposed to either:

(1) 1 atmosphere of oxygen,

(2) 1 atmosphere of oxygen and 1 atmosphere of nitrogen or,

(3) 1 atmosphere of oxygen and four atmospheres of nitrogen (compressed air).

Thirty-six Swiss-Webster male mice 4 to 5 weeks of age were exposed in each group for a total of 180 subjects. The subjects were housed in a small hyperbaric chamber, food and water were supplied as potatoes and moistened commercial rat chow. Gas was flushed through at approximately 2 liter/minute (flow rate at pressure) for a turn-over time of approximately 15 minutes. All exposures were made at room temperature (20 degrees C.). Premix gases were used to insure correct composition, and chamber pressure was recorded. The chamber exhaust was monitored and recorded with either an oxygen meter, or a Nitralizer to insure that gas mixing in the chamber had occurred.

T A B L E X I V

LUNG-BODY WEIGHT RATIOS

(X1000)

	42	48	52 hours
Low Inert			
0.8 ATA O_2 +	5.53 ± 0.28	5.77 ± 0.19	6.67 ± 0.37
0.2 ATA Inert	(8)	(12)	(15)
High Inert			
0.8 ATA O_2 +	4.33 ± 0.13	5.13 ± 0.20	5.37 ± 0.14
4.2 ATA Inert	(12)	(4)	(15)
Chamber Controls (52 hours)			4.87 ± 0.16 (9)

Average ± S.E.M.
(Number of Subjects)

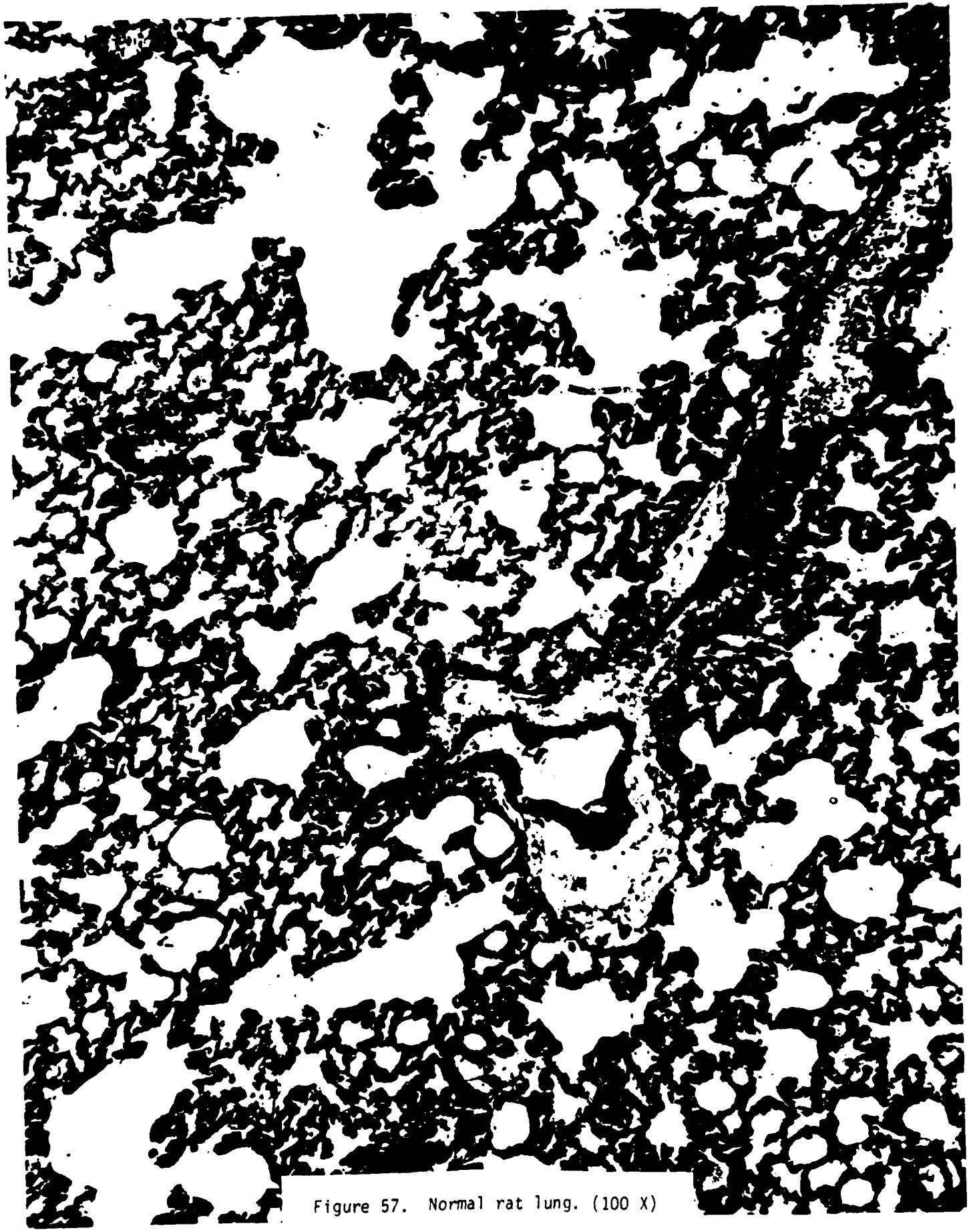

Figure 57. Normal rat lung. (100 X)

Figure 58. Exposure to 1 ATA O_2 at 1 ATA. Mostly edema present with some hemolysis. Cellular architecture fairly well preserved. Note no atelectasis.

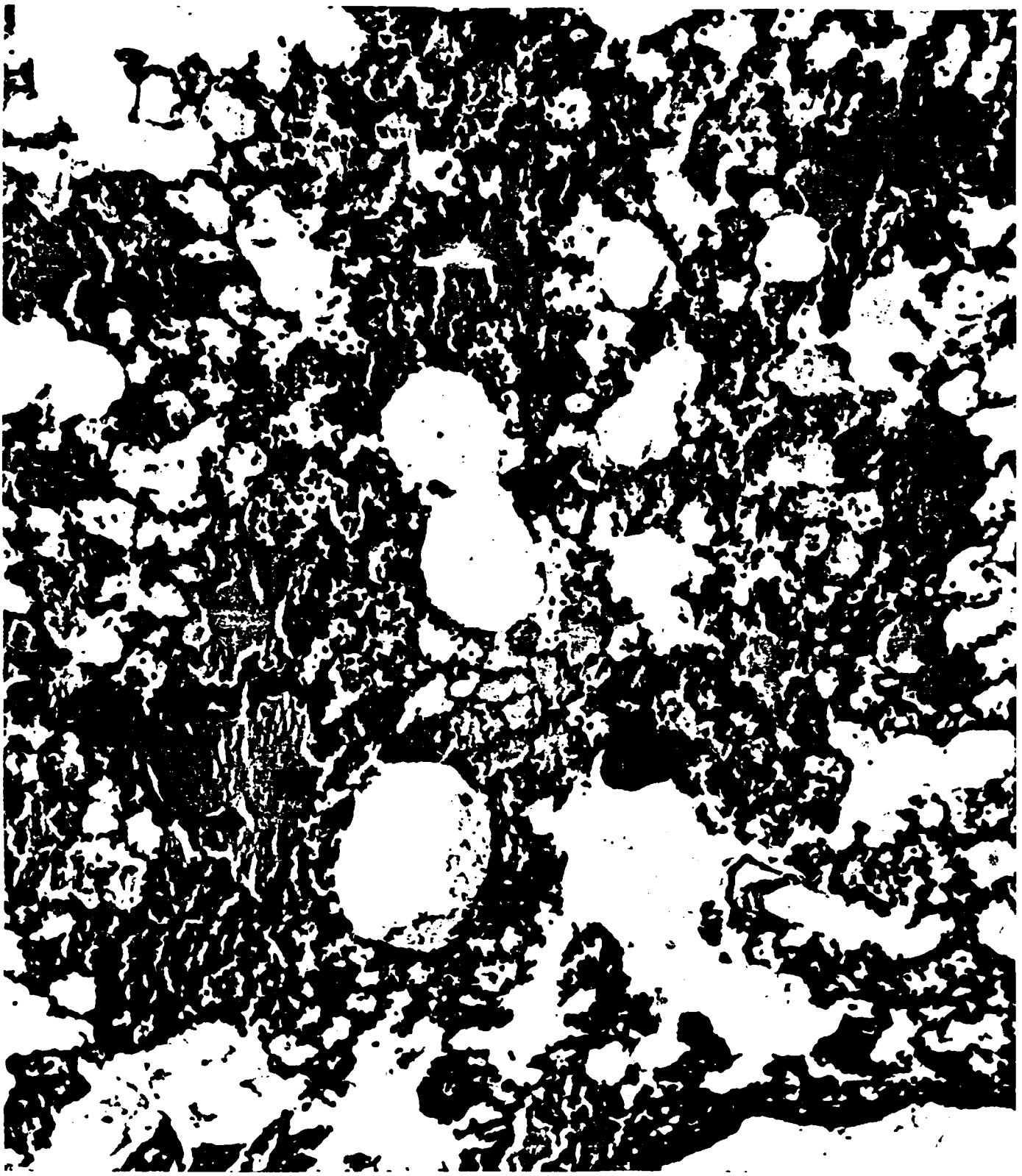

Figure 59. Lung section exposed to 1 ATA O_2 at 4.9 ATA. Note production of emphysematous tissue caused by too vigorous an inflation. Edema and hemolysis present with numerous macrophages. No atelectasis. (100 X)

To determine the number of survivors at any given time, and to clean and feed the mice, it was necessary to decompress the exposure chamber. This was done over a 30 to 40 minute period to prevent decompression sickness problems. Results are shown in Figure 60.

D. DISCUSSION

The effect of increasing the fraction of inert gas is particularly noticeable. Of further interest is the fact that, while the number of survivors decreases relatively rapidly after a given time for all types of gas mixtures, the "latency period" is longest with the highest amount of nitrogen. Measurements by Smith, Lehan and Monks (1963) in dogs indicated that blood gas contents and cardiovascular parameters were maintained constant throughout the greatest part of oxygen exposure. Only at the final 10 to 15% of their lifetime in elevated oxygen were changes such as arterial oxygen saturation greatly changed; it fell but slightly during the initial 85 to 90% of their exposure time; PCO_2 was never found to change significantly. Their dogs finally succumbed of respiratory failure after an average of 55 hours; again, the major changes occurred in the final 2 to 3 hours before death.

An interpretation given to both our blood gas and survival time data would suggest that the inert gas diluents function to increase the latency time before serious toxic effects of oxygen are manifest. The amelioration appears to be one of time and not that of overall effect as the final outcome of death is the same in the presence or absence of inert gases. Whether the same protective mechanism inherent in dilution applies to other mitigating methods, such as air breathing cycles during hyperbaric oxygen inhalation as is practiced in diving, is not clear at present.

If a protection does occur to lengthen the latency period, increased oxygen tension in the presence of inert gas diluents could find a potential use in such differing areas as shallow air habitats, clinical hyperbaric oxygen therapy, and increased oxygen tension in the breathing mixtures of deep sea divers.

(M.R. Powell)

CHRONIC PULMONARY OXYGEN TOXICITY

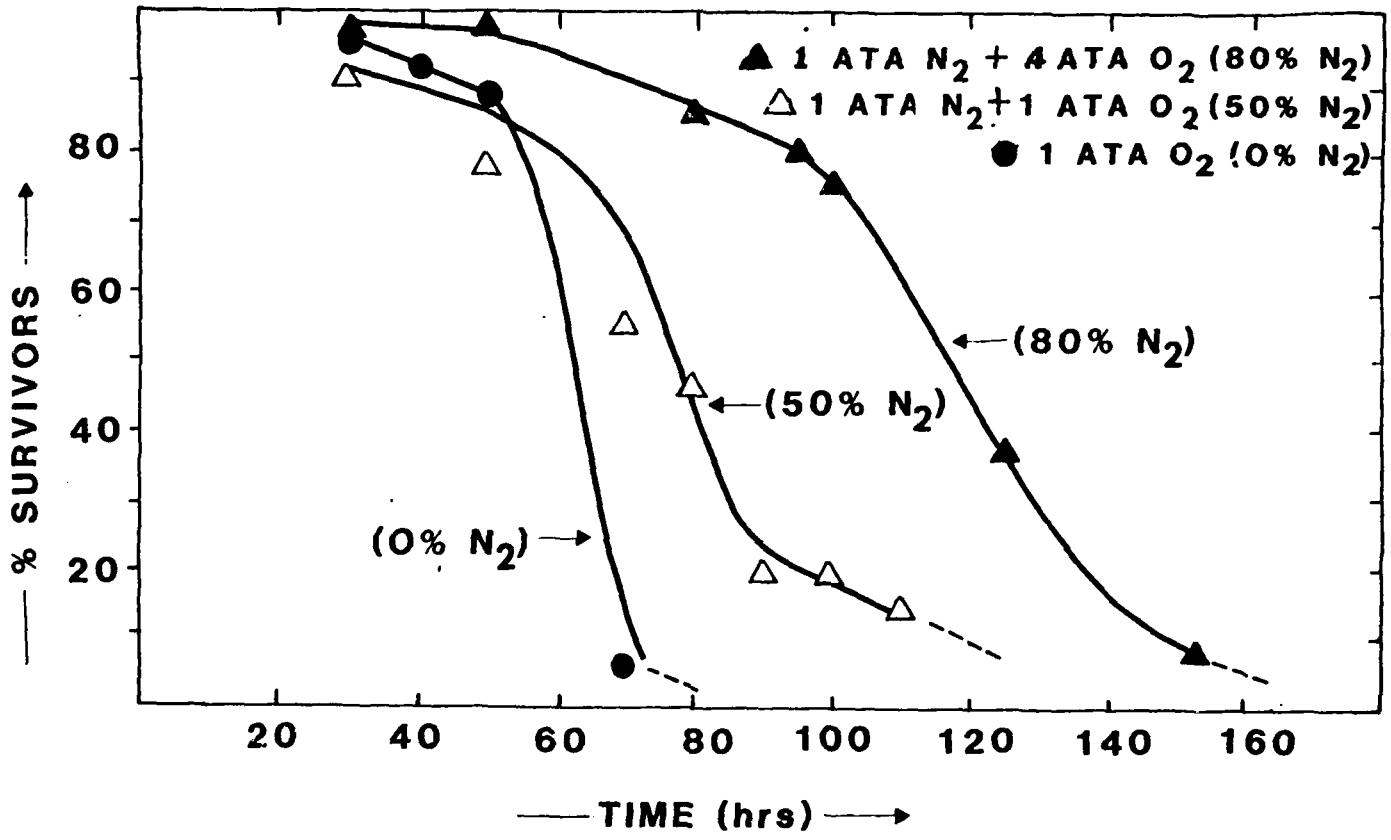

Figure 60. Percent survivors as a function of time. Swiss-Webster mice were exposed to 1 ATA of oxygen gas containing varying percents of nitrogen (0, 50 or 80%) in a hyperbaric chamber. While the partial pressure of O_2 was a constant, the total pressure changed.

VIII. REFERENCES

Ackles, K.N., D.E. Holness and C.A. Scott (1972) Measurement of the *in vivo* uptake and elimination of nitrogen in tissue. Abstracts, 5th Symposium on Underwater Physiol., p. 50.

Almqvist, H., M. Arborelius, Jr., P.O. Barr, B. Jansson, and L. Kaijser (1969) Oxygen toxicity in nitrogen mixtures. Acta. Physiol. Scandia. 75:64-68.

Barthelemy, L., (1963) Blood coagulation and chemistry during experimental dives and the treatment of diving accidents with Heparin. Proc. Second Symposium on Underwater Physiology, National Academy of Sciences National Research Council, Washington, D.C., p. 46.

Behnke, A.R., Jr. (1942) Investigation concerned with problems of high altitude flying and deep diving; application of certain findings pertaining to physical fitness to the general military service. The Military Surgeon, 90:9-28.

Behnke, A.R., (1951) Decompression sickness following exposure to high pressures. Decompression Sickness, J.F. Fulton (ed.), W.B. Saunders, Philadelphia, Chapter III.

Behnke, A.R. (1969) Some early studies of decompression. The Physiology and Medicine of Diving. R.B. Bennett and D.H. Elliott (eds.), Williams and Williams, Baltimore.

Berglund, E. and S. Josephson (1970) Pulmonary air embolization in the dog. 1. Hemodynamic changes on repeated embolizations. Scand. J. Clin. Lab. Invest., 26:97-103.

Bert, P. (1943) Barometric Pressure Researches in Experimental Physiology. M.A. Hitchcock and F.A. Hitchcock, (trans.), College Book Company, Columbus.

Blinks, L.R., V.C. Twitty and P.M. Whiteker (1951) Part II. Bubble formation in frogs and rats. Decompression Sickness, J.F. Fulton (ed.), W.B. Saunders, Co., Philadelphia, p. 145.

Bondi, K.R. (1975) The *in vitro* properties of mass spectrometer catheters as a funciton of pressure. Workshop: Problems and Solutions in the Use of Mass Spectrometer in Hyperbaric Environments, DCIEM, Ontario.

Bove, A.A., J.M. Hallenbeck and D.H. Elliott (1974) Circulatory responses to venous air embolism and decompression sickness in dogs. Undersea Biomed. Res., 1:207.

Boycott, A.E., G.C.C. Damant and J.S. Haldane (1908) The prevention of compressed air illness. J. Hyg. Long., 8:342.

Boyle, R. (1670) New pneumatical experiments about respiration. Philos. Trans., 5:2011.

Brechner, V.L. and R.W.M. Bethune (1971) Recent advances in monitoring pulmonary air embolism. Anesth. and Analg., 50:255-261.

Buckles, R.G. (1968) The physics of bubble formation and growth. Aerospace Med., 39:1062.

Buckles, R.G. and C. Knox (1969) In vivo bubble detection by acoustic-optical imaging techniques. Nature, 222:771.

Burns, J.D. (1972) Concentration-Dependent attenuation of hyperbaric oxygen toxicity. Aerospace Med. 43(9):989-992.

Chase, W.H. (1934) Anatomical and experimental observations on air embolism. Surg. Gync. and Obst., 59:569.

Cockett, A.T.K., J.C. Saunders and S.M. Pouley (1968) Treatment of experimental decompression sickness by Heparin alone. Aerospace Med. Assoc., Annual Mtg., San Francisco, CA.

Deal, C.W., B.P. Fielden and I. Monk (1971) Hemodynamic effects of pulmonary air embolism. J. Surg. Res., 11:533-538.

Devin, C. (1959) Survey of thermal, radiation and viscous damping of pulsating air bubbles in water. J. Acoust. Soc. Amer., 31:1654.

Dolen, J.E., F.W. Haynes, F.G. Hoppen, Jr., G.L. Evans, P. Bhardwaj and L. Dexter (1967) Cardiovascular responses to experimental pulmonary embolism. Amer. J. Cardiol., 20:3-9.

Dunn, F., P. D. Edmonds and W. J. Fry, (1969). Absorption and dispersion of ultrasound in biological media. Chap. 3, In: Biological Engineering, Vol. 9, H. P. Schwan (ed.), McGraw-Hill, New York.

Durant, T.M., J. Long and M.J. Oppenheimer (1947) Pulmonary (venous) air embolism. Amer. Heart J., 38:481-500.

Emerson, L.V., A.V. Hempleman and R.G. Lentel (1967) The passage of gaseous emboli through the pulmonary circulation. Resp. Physiol., 3:219.

End, E. (1938) The use of new equipment and helium gas in a world record dive. J. Indus. Hyg., 20:511.

Evans, A. and D.M. Walder (1969) Significance of gas micronuclei in the aetiology of decompression sickness. Nature, 222:251.

Evans, A. and D.N. Walder (1970) Detection of circulating bubbles in the intact mammal. Ultrasonics, 3:216-217.

Evans, A., E.E.P. Barnard and D.N. Walder (1972) Detection of gas bubbles in man at decompression. Aerospace Med., Oct., p. 1095-1096.

Ferris. E.B. and G. Engel (1951) The clinical nature of high altitude decompression sickness. Decompression Sickness, J.F. Fulton (ed.), W.B. Saunders Co., Philadelphia, p. 4.

Franklin, D.E., W.A. Schlegel and R.F. Rushmer (1961) Blood flow measured by Doppler frequency shift of back-scattered ultrasound. Science, 134:564.

Fry, W. J. and F. Dunn, (1962). Ultrasound: Analysis and experimental methods in biological research. Chap. 6, In: Physical Techniques in Biological Research, Vol. 4, W. L. Nastuk (ed.), Academic Press Inc., New York.

Gersch, I. and H. Catchpole (1951) Decompression Sickness: physical factors and pathologic consequences. Decompression Sickness, J.F. Fulton (ed.), W.B. Saunders Co., Philadelphia, p. 165.

Gersch, I., G.E. Hawkinson, and E.H. Jenney (1945) Comparison of vascular and extravascular bubbles following decompression from high pressure atmospheres of oxygen, helium-oxygen and argon-oxygen and air. J. Cell. Comp. Physiol. 26:63-74.

Gillis, M.F. (1971) Research on deep submergence diving physiology and decompression technology utilizing swine. Final Report to Office of Naval Research on Contract No. N00014-69-C-0350.

Gillis, M.F., M.T. Karagianes and P.L. Peterson (1968a) Bends: Detection of circulating gas emboli with external sensor. Science, 161:579.

Gillis, M.F., P.L. Peterson and M.T. Karagianes (1968b) In vivo detection of circulating gas emboli associated with decompression sickness using the Doppler flowmeter. Nature, 217:965.

Gooberman, G.L. (1968) Ultrasonics, Theory and Application. Hart, New York.

Greenbaum, L.J. and E.C. Hoff (1966) A bibliographical sourcebook of compressed air, diving and submarine medicime, Vol. III, Office of Naval Research and Bureau of Medicine and Surgery, Department of the Navy, Washington, D.C.

Guillerm, R., G. Masurel, C. Guillaud and J.L. Manjaret (1975) Detection ultrasonore par effet Doppler des bulles intravasculaires chez l' animal apres exposition hyperbare. Lyon Mediterranee Med., XI:1301.

Guillerm, R., G. Masurel, J.-C. LePechon, C. Guillaud and J.-M Ocana de Santuary (1977). Detection ultrasonore (effet Doppler) de bulles circulantes chez l'homme pendant la phase de decompression d'une plongee simulee a 300 metres a saturation en atmosphere oxygene-helium. Lyon Mediterranee Medical, Vol. XIII, No. 1.

Hamilton, R.W., Jr., D.J. Kenyon, M.Freitag, T. Schmidt, and M.R. Powell (1974) "Access", Technical Report, Ocean Systems, Inc.

Harkins, H.N. and P.H. Harson (1934) Embolism by air and oxygen: comparative studies. Proc. Exp. Biol. Med., 32:178.

Hartveit, F., H. Lystad and A. Minken (1968) The pathology of venous air embolism. Brit. J. Exptl. Pathol., 49:81-86.

Harvey, E.N. (1951a) Physical factors in bubble formation. Decompression Sickness. J.F. Fulton (ed.), W.B. Saunders Co., Philadelphia, p. 90.

Harvey, E.N. (1951b) Part I. Bubble formation in cats. Decompression Sickness. J.F. Fulton (ed.), W.B. Saunders Co., Philadelphia, p. 115.

Hueter, T.F. and R.F. Bold (1955) Sonics. Wiley and Sons, Publ, New York, pg. 230.

Hempleman, H.V. (1963) Tissue inert gas exchange and decompression sickness. Proc. Second Symposium on Underwater Physiology, National Academy of Sciences - National Research Council. Washington, D.C., p. 6.

Hills, B.A. (1966) A thermodynamic and kinetic approach to decompression sickeness. Library Board of South Australia, Adelaide.

Hills, B.A. and D.C. Grulke (1975) Evaluation of ultrasonic bubble detectors in vitro using calibrated micro-bubbles at selected velocities. Ultrasonics, 13:181.

Hoff, E.C. (1948, 1954) A bibliographical sourcebook of compressed air, diving and submarine medicine, Vol. I, II, Office of Naval Research and Bureau of Medicine and Surgery, Department of the Navy, Washington, D.C.

Hutchins, R.W. (1964a) Application of ultrasonics to the aetiology of decompression sickness - A feasibility study - Part I. Research and Development Division, Huntec, Ltd., Toronto, 1 January.

Hutchins, R.W. (1964b) Application of ultrasonics to the aetiology of decompression sickness - A feasibility study - Part II. Research and Development Division, Huntec, Ltd., Toronto, 15 January.

Hutchins, R.W. (1965) Application of ultrasonics to the diagnosis and prevention of decompression sickness. Huntec, Ltd. DIR Project E-38, Special Report, 28 February.

Hutchins, R.W. (1966) Application of ultrasonics to the diagnosis and prevention of decompression sickness. Huntec, Ltd. DIR Project E-38, Final Report, 24 February.

Mackay, R.S. (1963) Proc. of Second Symposium on Underwater Physiology. NAS/NRC, Publication 1171, p. 41 (discussion comment).

Mackay, R.S. and G.J. Robissow (1971) Detection of bubbles in tissues and blood. Fourth Symposium on Underwater Physiology, Philadelphia, 1969, Academic Press.

Malette, W.G., J.B. Fitzgerald and A.T.K. Cockett (1972) Dysbarism: A review with suggestions for theraphy. Aerospace Med., 33:1132.

Manley, D.M. (1969) Ultrasonic detection of gas bubbles in blood. Ultrasonics, 102, April.

Maroon, J.C., J.M. Goodman, T.G. Horner and R.L. Campbell (1968) Detection of Mminute venous air emboli with ultrasound. Surgery, Gyn. and Obst., December.

Maroon, J.C., J. Edmonds-Seal and R.L. Campbell (1969) An ultrasonic method for detecting air embolism. J. of Neurosurg., 31:196-201.

Martin, F.E., J.E. Hudgens and J.W. Wonn (1973) Manned hyperbaric demonstration of incipient bubble detection using non-linear ultrasonic propagation. Westinghouse Electric Corp. Ocean res. Eng. Cent., Rep. OER-73-16.

Minnert, E.G. (1933) On musical air-bubbles and the sound of running water. Phil. Mag., 16:235.

Monjaret, J.L., R. Guillerm and G. Masurel (1975) Detector of bubbles moving through blood vessels with Doppler signal. Colloque International sur les Capteurs Bio-Medicaux, Biocapt, Paris.

Moss, G., P. Dworkin, and A.A. Stein (1976) The centrineurogenic etiology of the respiratory distress syndrome. J. Thoracic and Cardiovascular Surg. 71:614-616.

Moulinier, H. and G. Masurel (1977) The detection of bubbles in blood vessels and the evaluation of their flow. Report on research financed by the "Direction des Recherches et Moyens d'Essais" on contract #73-34-760-00-480-75-01.

Mustard, J.F. and M.A. Pokeham (1969) Platelet function and myocardial infarction. Circ. Res. 4:20-28.

Nashimoto, I. and Y. Gotoh (1975) Relationships between precordial Doppler ultrasound records and decompression sickness. 6th symposium on Underwater Physiology, July, 1975). F.A.S.E.B., Bethesda, Maryland.

Nelson, D., L. Ostrander, F. Ernst and W. Baetz (1973) Flow limited properties of Teflon and silicon diffusing membranes. Adv. Exp. Med. Biol. 38:121.

Neuman, T.S., D.A. Hall and P.G. Linaweaver (1976) Gas phase separation during decompression in man: ultrasound monitoring. Undersea Biomed. Res., 3:121-130.

Niden, A.H. and D.M. Aviado (1956) Effects of pulmonary embolism on the pulmonary circulation with special reference to arteriovenous shunts in the lung. Cir. Res., 4:67-73.

Nims, L.F. (1951) A physical theory of decompression sickness. Decompression Sickness, J.F. Fulton (ed.), W.B. Saunders Co., Philadelphia, P. 192.

Nishi, R.Y. (1972) Ultrasonic detection of bubbles with Doppler flow transducers. Ultrasonics, 10:173.

Nishi, R.Y. (1975) The scattering and absorption of sound waves by a gas bubble in a viscous liquid. Acoustica, 33:65.

Nishi, R.Y. (1975) Mathematical correction of data for the lag-response of Teflon catheters used in mass spectrometry. Proc.: workshop on problems and solutions in the use of mass spectrometry in hyperbaric environments. D.C.I.E.M., Toronto.

Nishi, R.Y. and S.D. Livingstone (1973) Intravascular changes associated with hyperbaric decompression: theoretical considerations using ultrasound. Aerospace Med., 44:179.

Norman, J.N., M. MacIntyre, R.R. Ross, and G.S. Smith (1971) Etiological studies of pulmonary oxygen poisioning. Am. J. Physiol.

Penrod, K.E. (1956) Effect of intermittent nitrogen exposures on tolerance tooxygen at high pressures. Am J. Physiol. 186:149-151.

Philip, R.B. and G.W. Gowdey (1964) Experimental analysis of the relation between body fat and susceptibility to decompression sickness. Aerospace Med., 35:351.

Philp, R.B., C.W. Gowdey, and M. Prasall (1967) Changes in blood lipid concentration and cell counts following decompression sickness in rats and the influence of dietary lipid. Can J. Physiol. Pharm., 45:1047.

Philip, R.B. (1974) A review of blood changes associated with compression-decompression: relationship to decompression. Undersea Biomed. Res., 1:117-150.

Pilmanis, A.A. (1974) Intravenous gas emboli in man after selected open ocean air scuba dives. Abstract 5.1 Undersea Medical Society, Annual Scientific Mtg., May 10-12.

Pilmanis, A.A. (1975) Intravenous gas emboli in man after compressed air ocean diving. Technical Report, ONR N00014-67-A-0269-0026.

Powell, M.R. (1971) Detection of gas-liquid phase separation in tissues by through-transmission ultrasound. Abstracts. Biophysical Society, 15th Annual Mtg., New Orleans, 1971.

Powell, M.R. (1971) Mechanism and detection of decompression sickness. Tech. Mem. UCRI-673. Ocean Systems, Inc., Tarrytown, NY.

Powell, M.R. (1972) Gas phase separation following decompression in asymptomatic rats: visual and ultrasound monitoring. Aerospace Med., 43:1240.

Powell, M.R. (1972) Leg pain ang gas bubbles in the rat following decompression from pressure: monitoring by ultrasound. Aerospace Med., 43:168.

Powell, M.R. (1973) Tissue gas uptake at elevated pressures determined in vivo by mass spectrometry. Aerospace Medical Assoc. 44th Annual Mtg., Las Vegas, 1973.

Powell, M.R. (1974) Doppler ultrasound monitoring of venous gas bubbles in pigs following decompression from helium, neon and air. Aerospace Med., 45:505.

Powell, M.R. (1975) In vivo bubble growth following decompression. Abstract #376. The Physiologist, August.

Powell, M.R. (1977) Physiological significance of Doppler detected bubbles in decompression sickness. Undersea Medical Society, Workshop on Early Detection of Decompression Sickness, Toronto, U.M.S. Report 7-30-77.

Powell, M.R. and D.C. Johanson (1978) Ultrasound monitoring and decompression sickness. Sixth Symposium on Underwater Physiology, (1975) San Diego, F.A.S.E.B., Bethesda, Maryland.

Powell, M.R. and M.P. Spencer (1976a) Pulmonary Gas Embolization Following Decompression. Proceedings of the Third Annual Meeting of the North Pacific Chapter of the Undersea Medical Society.

Powell, M.R. and M.P. Spencer (1976b) Doppler-shifted ultrasound monitoring of Gas bubbles following decompression. Biophysical J., 16:62a.

Powell, M.R. and M.P. Spencer (1977) Pulmonary gas embolization following decompression. Fed. Proc., 36:534.

Powell, M.R. and K.J. Weydig (1974) In vivo bubble growth studies following decompression. Union Carbide Tech. Mem. CRL-T-798, Tarrytown, NY.

Reid, J.M., D.L. Davis, H.J. Ricketts and M.P. Spencer (1973) A new doppler flowmeter system and its operation with catheter mounted transducers. Cardiovascular applications of ultrasound. North Holland and Am. Elsevier Publ. Cos (R. Reneman, ed.), p. 32.

Richardson, H.F., B.C. Coles, and G.E. Hall (1937) Experimental gas embolism: I. Intravenous air embolism Canad. Med. Ass. J., 36:584-588.

Rokitha, M.A. and H. Rahn (1977) Effects of O_2 and N_2-O_2 pressures on the physical performance of deer mice: preliminary studies. Aviat. Space Environ. Med. 48(4):323-326.

Rubissow, G.J. and R.S. Mackay (1971) Ultrasonic imaging of in vivo bubbles in decompression sickness. Ultrasonics, Oct. 1971, 225.

Satomura, S. (1957) Ultrasonic Doppler method for the inspection of cardiac functions. J. Acous. Soc. Am. 29:1181-1185.

Smith, C.W., P.H. Lehan, and J.J. Monks (1963) Cardiopulmonary manifestiations with high O_2 tensions at atmosphere. J. Appl. Physiol. 18(5):849-853.

Smith, F.D. (1935) On the destructive mechanical effects of the gas bubbles liberated by the passage of intense sound through a liquid. Phil. Mag., 19:1147.

Smith, G., I.M. Ledingham and A.T. Sandison (1970) Pulmonary oxygen toxicity - pathophysiology and effects of N_2 mixture. Clinical Science of London, 38:12.

Smith, K.H. and D.C. Johanson (1970) Hyperbaric decompression by means of bubble detection. Tech. Report to ONR, Contract #N00014-69-C-040.

Smith, K.H. and M.P. Spencer (1970) Doppler indices of decompression sickness: their evaluation and use. Aerospace Med., 42(12):1396.

Spencer, M.P. (1976) Decompression limits for compressed air determined by ultrasonically detected blood bubbles. J. Appl. Physiol., 40:229-235.

Spencer, M.P. (1977) Doppler VGE and history of ultrasound detection in: Early diagnosis of decompression sickness. Undersea Medical Society. Report #7-30-77.

Spencer, M.P. and S.D. Campbell (1968) Development of bubbles in venous and arterial blood during hyperbaric decompression. Bull. of the Mason Clinic, 22(1):26-32.

Spencer, M.P., S.D. Campbell, J.L. Sealey, F.C. Henry and J. Lindbergh (1969) Experiments on decompression bubbles in circulation using ultrasonic and electromagnetic flowmeters. J. Occup. Med., 11(5):238.

Spencer, M.P. and S.D. Campbell (1972) Decompression venous gas emboli. Abstract from 5th Symposium on Underwater on Underwater Physiology, August.

Spencer, M.P. and J.F. Clark (1972) Precordial monitoring of pulmonary gas embolism and decompression bubbles. Aerospace Med., 43:762.

Spencer, M.P., S.K. Hong and R.H. Strauss (1974) Venous gas embolism (VGE) in Hawaiian divers. Undersea Biomed. Res., 1:(1).

Spencer, M.P. and D.C. Johanson (1974) Investigations of new principles for human decompression schedules using the Doppler ultrasonic blood bubble detector. Technical Report, IAPM, Seattle, WA.

Spencer, M.P., D.C. Johanson and S.D. Campbell (1972) Safe decompression with the Doppler ultrasonic blood bubble detector. Underwater Physiol. V., Proceedings of the 5th Symposium on Underwater Physiology, p. 311-325.

Spencer, M.P., D.C. Johanson, S.D. Campbell and W.F. Postles (1974) Clinical use of blood bubble detection in diagnosis, prevention and treatment of decompression sickness. *Proceedings of 5th International* Hyperbaric Congress, 2:589.

Spencer, M.P., G.H. Lawrence, G.I. Thomas and L.R. Sauvage (1969) The use of ultrasonics in the determination of arterial aeroembolism during open-heart surgery. Annals of Thoracic Surg., 8:489-497.

Spencer, M.P. and H. Okino (1972) Venous gas emboli following repeated breath-hold dives. Fed. Proc., April.

Spencer, M.P. and Y. Oyama (1971) Pulmonary capacity for dissipation of venous gas emboli. Aerospace Med., 42:822.

Spencer, M.P. and M.R. Powell (1976) Gas phase formation in "Fast" perfusion limited tissues. Proceedings of the 3rd Annual Meeting of the North Pacific Chapter of the Undersea Medical Society.

Spencer, M.P. and M.R. Powell (1977) The etiology of convulsions after hyperbaric exposures. Abstract Undersea Medical Society, Toronto.

Spencer, M.P., N. Simmons and H.F. Clarke (1971) A precordial transcutaneous cardiac output and aeroembolism monitor. Fed Proc., 30:703.

Sutphen, J.H. (1968) The feasibility of using pulsed ultrasound to detect the presence of in vivo tissue gas bubbles. Report #508, U.S. Naval Submarine Center, February 27, 1968.

Trucker, D.G. and V.G. Welsby (1968) Ultrasonic monitoring of decompression. Lancet, June, p. 1253.

Walder, D.N., A. Evans and H.V. Hempleman (1968) Ultrasonic monitoring of decompression. Lancet, 897, 27 April.

Wells, P.N.T. (1969) Physical principles of ultrasonic diagnosis. London, Academic Press, p. 282.

Workman, R.D. (1969) American decompression theory and practice. The Physiology and Medicine of Diving and Compressed Air Work, P.B. Bennett and D.H. Elliott (eds.), Williams and Wilkins, Baltimore, Chapter 12.

IX. CONCLUSIONS

These conclusions follow from research done under the contract from 1974-1978.

1. Bubble formation occurs in virtually every decompression. The assessment of local gas phase formation at the tissue levels can often be determined from the precordial bubble grade. The higher this grade, the greater the probability of decompression sickness (limb-bends).

2. Decompression by means of ultrasonic bubble detection allows an assessment of tissue outgassing with concomitant bubble (gas phase) formation. In some instances, it can be used on-line as a real time monitor of the decompression status of divers.

3. Zero crossing meters can process the audio output of Doppler flowmeters to give a semi-quantitive indication of the numbers of gas bubbles passing through the ultrasonic beam.

4. Gas injected into the central venous return evokes a rise in right ventricular systolic pressure. This rise is a function of the rate of injection (rate of pulmonary gas embolization).

5. Following decompression, the right ventricular systolic pressure can be raised by pulmonary gas embolization. From this rise the rate of decompression--induced embolization can be deduced.

6. In sheep, the rate of gas pulmonary embolization following decompressions producing Grade III precordial bubbles is about 0.02 cc/kg./min. A similar embolization rate in rats will cause death in 50% of the subjects.

7. During pulmonary embolization by air injection, bubbles were never detected in the systemic arterial system (Doppler probe on carotid artery) at any of the elevated RVSP attained (up to 60% of control). This was true of both rats and sheep.

8. In sheep, a Grade IV precordial signal will result in a rise of RVSP of approximately 15-20% above pre-dive control values. The amount of dissolved tissue gas appearing in the venous return and embolizing the pulmonary vasculature is approximately 5-10% for this grade. This represents conditions for a moderately severe decompression.

9. While bilateral hind leg problems are noted in sheep following decompression resulting in RVSP increase of 50% above control, the rise is neither a necessary nor sufficient condition.

10. Limb-bend decompression sickness could not be exacerbated by augmented (air injected per catheter, 0.03 cc/kg./min.) pulmonary embolization. Thus, high precordial grades per se do not influence d.c.s. ("chokes" excluded). An actual reduction in severity of

problems was noted; femoral vein bubble grades in sheep were also reduced. This was seen in titration decompressions involving three sheep making a total of 60 dives.

11. Carotid artery bubbles can be detected in approximately 7% of subjects with Grade IV and 50% with Grade V precordial signals (sheep as subjects). Pulmonary artery pressure plays an important role (c.f. Niden and Aviado, 1965).

12. Elevation of pulmonary artery pressures to 150% (or greater) of control by injection of micro bubbles ($r = 200\mu$) does not result in arterialization of this gas load. Therefore the bubble size must also play an important role.

13. Highly perfused tissues such as brain and kidney do not produce a gas phase following decompression. Problems associated with these organs, such as neurologic decompression sickness, are the result of gas embolism. (In vestibular and cord difficulties, autochthonous bubble formation may play the major role.)

14. Gas bubbles do not originate in the systemic arterial system. When they can be detected, it is only following the appearance of numerous gas embolie in the pulmonary vasculature.

15. In the presence of a precordial Grade IV (and possibly Grade III), the carotid artery of human divers should be monitored for the presence of arterialized gas bubbles.

16. Neurologic decompression sickness does not always follow the detection of even numerous systemic arterial gas bubbles (in animal subjects).

17. Recompression of (animal) subjects with a high precordial bubble grade does not promote arterialization of venous gas phase.

18. Gas tensions measured in muscle tissue by mass spectrometry and in situ probes are 90% of the expected value. Transudative fluid acts, therefore, as a stirred fluid with respect to Teflon-covered probes.

19. Chronic pulmonary oxygen toxicity is ameliorated by the addition of inert gas. The time to reach LD_{50} is a function of the inert gas fraction (at a given fixed oxygen partial pressure).

X. SCIENTIFIC COMMUNICATIONS, 1974-1978
Supported in Whole or in Part by Contract N00014-73-C-0094

Spencer, M.P., D.C. Johanson, S.D. Campbell and W.F. Postles (1974). Clinical use of blood bubble detection in diagnosis, prevention and treatment of decompression sickness. Proceedings of 5th International Hyperbaric Congress, 2:589.

Spencer, M.P., S.K. Hong and R.H. Strauss (1974). Venous gas embolism (VGE) in Hawaiian divers. Undersea Biomed. Res., 1:(1).

Spencer, M.P. and D. C. Johanson (1974). Investigations of new principles for human decompression schedules using the Doppler ultrasonic blood bubble detector. Technical Report, IAPM, Seattle, WA.

Powell, M.R. and D.C. Johanson (1975). Ultrasound monitoring and decompression sickness. Sixth Symposium on Underwater Physiology, San Diego, F.A.S.E.B., Bethesda, Maryland.

Powell, M.R. (1975). Helium, oxygen, and nitrogen tissue uptake at normal and hyperbaric pressures determined in vivo by mass spectrometry, in Proceedings: Problems, Solutions in the Use of Mass Spectrometry in Hyperbaric Environments. DEIEM, Toronto.

Powell, M.R. (1975). In vivo bubble growth following decompression. The Physiologist, August, 1975.

Spencer, M.P. (1976). Decompression limits for compressed air determined by ultrasonically detected blood bubbles. J. Appl. Physiol., 40:229-235.

Powell, M.R. and M.P. Spencer (1976). Doppler-shifted ultrasound monitoring of gas bubbles following decompression. Biophysical J. 16:62a.

Powell, M.R. and M.P. Spencer (1976). Pulmonary gas embolization following decompression. Proceedings of the Third Annual Meeting, North Pacific Chapter/Undersea Medical Society.

Powell, M.R. and M.P. Spencer (1977). Pulmonary gas embolization following decompression. Fed. Proc., 36:534.

Powell, M.R. (1977). Physiological significance of Doppler detected bubbles in decompression sickness. Workshop on Early Detection of Decompression Sickness, U.M.S. Report 7-30-77, also U.M.S., 12th Annual Meeting, (Toronto), Abst. 26.

Spencer, M.P. (1977) Doppler VGE and history of ultrasound detection. Early Detection of Decompression Sickness. Undersea Medical Society. Report #7-30-77.

Belizi, P.J. and M.R. Powell (1977) Amelioration of chronic pulmonary oxygen toxicity by inert gas dilution. Aerospace Medical Assoc., 48th Annual Meeting.

Spencer, M.P. and M.R. Powell (1977) The etiology of convulsions after hyperbaric exposures. Undersea Biomed. Res, 4, Abst. 22.

Powell, M.R., M.P. Spencer and H. Domanie (1977) Effects of augmented pulmonary gas embolization on short-term decompression stress. Undersea Medical Society/North Pacific Chapter, Seattle.

Spencer, M.P. (1978). A method for development of safe decompression schedules using Doppler ultrasonic bubble detection. Undersea Biomed. Res., 5, Supplement, Abst. 32.

Spencer, M.P. and W.J. Aggenbach (1978) A laboratory method to screen divers for susceptibility to bends, oxygen toxicity and nitrogen narcosis. Undersea Biomed. Res., 5, Supplement. Abst. 35.

Spencer, M.P. and M.T. Smith (1978). Determining the longest limiting decompression tissue half-time using Doppler detected venous gas emboli. Program and Abstracts. Undersea Medical Society/North Pacific Chapter, San Antonio.

XI. ACKNOWLEDGEMENTS

We would like to acknowledge the financial assistance of the Office of Naval Research for grant N00014-73-C-0094, made possible with funds provided by the Naval Medical Research and Development Command.

Additionally, we would like to acknowledge the technical assistance of David C. Johanson, Holly Domenie, Michael Turnsen and Lou Granado.

UNCLASSIFIED

SECURITY CLASSIFICATION OF THIS PAGE (When Data Entered)

REPORT DOCUMENTATION PAGE

READ INSTRUCTIONS BEFORE COMPLETING FORM

1. REPORT NUMBER: 4	2. GOVT ACCESSION NO.: AD A093485
3. RECIPIENT'S CATALOG NUMBER:	
4. TITLE (and Subtitle): The Pathophysiology of Decompression Sickness and the effects of Doppler Detectable Bubbles,	5. TYPE OF REPORT & PERIOD COVERED: Sept. no. 4, Technical 1974-1978,
	6. PERFORMING ORG. REPORT NUMBER:
7. AUTHOR(s): Michael R. Powell, Merrill P. Spencer	8. CONTRACT OR GRANT NUMBER(s): N00014-73-C-0094
9. PERFORMING ORGANIZATION NAME AND ADDRESS: Institute of Applied Physiology and Medicine, 701 - 16th Avenue, Seattle, WA 98122	10. PROGRAM ELEMENT, PROJECT, TASK AREA & WORK UNIT NUMBERS:
11. CONTROLLING OFFICE NAME AND ADDRESS: Capt. R.C. Bornman, M.D., USN, Submarine Diving Medicine/Research Division, Dept. of the Navy, Washington, D.C. 20390	12. REPORT DATE: 18 Dec 80
	13. NUMBER OF PAGES: 165
14. MONITORING AGENCY NAME & ADDRESS (if different from Controlling Office): Defense Contract Administration Services Dist. Building 5-D Naval Support Activity, Sand Point, Seattle, WA 98115	15. SECURITY CLASS. (of this report): Unclassified
	15a. DECLASSIFICATION/DOWNGRADING SCHEDULE:

16. DISTRIBUTION STATEMENT (of this Report)

Distribution of this Document is Unlimited.

17. DISTRIBUTION STATEMENT (of the abstract entered in Block 20, if different from Report)

Distribution of this Abstract is Unlimited.

18. SUPPLEMENTARY NOTES

19. KEY WORDS (Continue on reverse side if necessary and identify by block number)

decompression sickness
pathophysiology
gas phase formation
oxygen toxicity
Doppler ultrasound blood bubble detection

20. ABSTRACT (Continue on reverse side if necessary and identify by block number)

The pathophysiology of decompression sickness is elucidated from data obtained through the employment of Doppler ultrasonic bubble detectors. The effects of gas reaching the pulmonary vasculature is studied as well as gas phase formation in highly perfused organs (kidney, brain). The amelioration of chronic pulmonary oxygen toxicity by inert gas dilution is described.

DD FORM 1 JAN 73 1473 EDITION OF 1 NOV 65 IS OBSOLETE

3410

UNCLASSIFIED

SECURITY CLASSIFICATION OF THIS PAGE (When Data Entered)


DAT
FILM